IMPROVING THE MANUFACTURABILITY OF EXTENDED CUT-OUT RIB-TO-FLOOR BEAM CONNECTIONS FOR ORTHOTROPIC STEEL DECKS

Final Report

by

Ian Hodgson
Principal Investigator
ATLSS Engineering Research Center

Richard Sause
Co-Principal Investigator
ATLSS Engineering Research Center

Brian Kozy
Project Consultant
Michael Baker International, Inc

ATLSS Report No. 24-01
Project: BAA - *HIBS10-SB-002-Lehigh_EC_RFB - Contract 693JJ321C000037*
with the
Federal Highway Administration (FHWA), Washington D.C.
December 2024

ATLSS is a National Center for Engineering Research on Advanced Technology for Large Structural Systems

117 ATLSS Drive
Bethlehem, PA 18015-4729

Phone: (610)758-3525

www.atlss.lehigh.edu
Email: inatl@lehigh.edu

TECHNICAL REPORT DOCUMENTATION PAGE

1. Report No. 24-01	2. Government Accession No.	3. Recipient's Catalog No.
4. Title and Subtitle Improving the Manufacturability of Extended Cut-Out Rib-to-Floor Beam Connections for Orthotropic Steel Decks		5. Report Date December 2024 6. Performing Organization Code:
7. Author(s) I. Hodgson, https://orcid.org/0009-0005-2309-0197 R. Sause, https://orcid.org/0000-0002-6143-4385 B. Kozy		8. Performing Organization Report No.
9. Performing Organization Name and Address ATLSS Center Lehigh University 117 ATLSS Drive Bethlehem, PA, 18015		10. Work Unit No. 11. Contract or Grant No. 693JJ321C00037
12. Sponsoring Agency Name and Address Office of Infrastructure – Bridges and Structures Federal Highway Administration 6300 Georgetown Pike McLean, VA 22101-2296		13. Type of Report and Period Covered Final Report 14. Sponsoring Agency Code HIBS-10
15. Supplementary Notes		

16. Abstract

During a full-scale fatigue test program at Lehigh University performed in 2018, the fatigue performance of a prototype orthotropic steel deck (OSD) with extended cut-out (EC) rib-to-floor beam (RFB) connections with partial joint penetration (PJP) welds and reinforcing fillet welds which wrap-around at the weld termination was investigated. The full-scale prototype OSD test specimen featured EC RFB connections without internal stiffeners which greatly improves the overall manufacturability of the OSD. The full-scale prototype OSD test specimen was subjected to 8 million cycles of fatigue limit state loading for OSDs. No fatigue cracks were observed at the RFB connections demonstrating that the deck could achieve its intended 100-year service life. This promising result shows that OSDs with simplified EC RFB connection details can exhibit adequate fatigue performance.

This research explored the conditions under which adequate fatigue performance using this cost-effective EC RFB connection can be expected when used for typical bridge redecking applications. This was accomplished by assessing the sensitivity of the magnitude of critical stresses to a range of global and local parameters using 3D finite element analysis (FEA). A FEA model of the successful full-scale prototype OSD test specimen served as the basis for validation of the results. The FEA model was calibrated using the data measured during static load tests. This calibrated 3D model was then used to assess the sensitivity to various OSD parameters, including deck plate thickness, transverse support stiffness, rib shape, cut-out shape, and cut-out depth.

The results of the study indicate that this cost-effective EC RFB connection detail is a promising candidate for future redecking OSD applications. A deck plate thickness of 3/4 inch is suggested. Ribs with a trapezoidal cross-section appear to exhibit better performance than ribs with a round bottom. Adequate fatigue performance can be expected with various cut-out shapes. The design engineer may consider this prototype OSD as the basis for a Level 1 OSD design approach for a replacement bridge deck if: (1) the global and local details are similar to the tested prototype OSD; (2) the fabrication workmanship meets or exceeds that of the tested OSD; and (3) the wrap-around fillet weld at the cut-out has weld face angles greater than or equal to that of the tested OSD. The favorable results of full-scale testing and sensitivity studies presented in this report suggest a reduced need for a Level 3 OSD design. Use of these simplified OSD RFB connection details can increase the manufacturability of the deck and promote the use of OSD in the United States.

17. Key Words orthotropic steel decks, rib-to-floor beam connections, extended cut-out, fatigue, finite element analysis, laboratory fatigue testing, local structural stress, fatigue cracking, fatigue performance	18. Distribution Statement No restrictions. This document is available to the public through the National Technical Information Service, Springfield, VA 22161. http://www.ntis.gov

19. Security Classif. (of this report) Unclassified	20. Security Classif. (of this page) Unclassified	21. No. of Pages 124	22. Price N/A

Form DOT F 1700.7 (8-72) Reproduction of completed page authorized.

ACKNOWLEDGEMENTS

The authors are grateful to Dayi Wang of FHWA for providing oversight of the work. Additional thanks are given to the review panel of Justin Ocel, Ryan Slein, Derek Soden, Tuonglinh Warren, and Calvin Chong of FHWA for insightful comments and review throughout the research. Additional thanks are due to the industry experts who provided feedback on current industry practice, including John W. Fisher (professor emeritus, Lehigh University), Karl Frank (professor emeritus, University of Texas at Austin), Terry Logan (Atema), Justin Dahlberg (Iowa State University), and Ronnie Medlock (High Steel Structures).

TABLE OF CONTENTS

LIST OF FIGURES

LIST OF TABLES

LIST OF ABBREVIATIONS AND SYMBOLS

AASHTO	American Association of State Highway and Transportation Officials
ADTT	Average Daily Truck Traffic
ASTM	(formerly American Society for Testing and Materials)
ATLSS	Center for Advanced Technology for Large Structural Systems
AWS	American Welding Society
BDS	Bridge Design Specifications
CAFT	Constant-Amplitude Fatigue Threshold
CJP	Complete Joint Penetration
Cobot	Collaborative Welding Robot
DOF	Degree of Freedom
EC	Extended Cut-out
EC3	Eurocode 3
FB	Floor Beam
FCAW	Flux Core Arc Welding
FEA	Finite Element Analysis
FHWA	Federal Highway Administration
GMAW	Gas Metal Arc Welding
IIW	International Institute of Welding
ksi	Kips Per Square Inch
LOF	Lack-of-Fusion
LRFD	Load-and-Resistance Factor Design
LSS	Local Structural Stress
MA	Model A, Finite Element Model
OSD	Orthotropic Steel Deck
PJP	Partial Joint Penetration
RDP	Rib-to-Deck Plate

RFB	Rib-to-Floor Beam
SAW	Submerged Arc Welding
SMB	Submodel B, Finite Element Submodel
SMC	Submodel C, Finite Element Submodel
2D	Two-dimensional
3D	Three-dimensional

EXECUTIVE SUMMARY

A full-scale fatigue test program at Lehigh University was conducted in 2018 to investigate the fatigue performance of a prototype orthotropic steel deck (OSD) with an extended cut-out (EC) rib-to-floor beam (RFB) connection with partial joint penetration (PJP) welds and reinforcing fillet welds which wrap around the cut-out. This full-scale prototype OSD test specimen was of interest because the EC RFB connection detail did not feature bulkheads or stiffeners inside the ribs which greatly improves the overall manufacturability of the OSD. The full-scale prototype OSD test specimen comprising three floor beams and 14 ribs was subjected to 8 million cycles of AASHTO LRFD BDS[1] fatigue limit state loading for OSD. No fatigue cracks were observed at the RFB connections demonstrating that the deck could achieve its intended 100-year service life, based on the average daily truck traffic on a suspension bridge in a dense urban environment. The promising results for this successful full-scale prototype OSD test specimen shows that OSDs with details that improve manufacturability can be successfully used on bridges with heavy traffic volumes and exhibit long service lives.

The goal of this study is to explore the conditions under which adequate fatigue performance using this cost-effective EC RFB connection detail can be expected when used for common bridge redecking applications. The use of OSD with this EC RFB connection detail in other applications (such as new bridge construction) may need further study. This goal was accomplished by assessing the sensitivity of the magnitude of critical stresses to a range of global and local parameters using 3D finite element analysis (FEA). A FEA model of the successful full-scale prototype OSD test specimen served as the basis for validation of the results.

A literature review was performed to establish the range of OSD geometries and details that have been implemented on bridges in both the USA and abroad. Results of past OSD fatigue test programs described in the literature was also reviewed. Additionally, industry leaders were engaged to assess the current state of OSD design, fabrication, and maintenance.

A detailed 3D FEA model of the full-scale prototype OSD test specimen was prepared. The FEA model was calibrated using the data measured during static load tests. This calibrated 3D model was then used to assess the sensitivity to various OSD parameters, including deck plate thickness, transverse support stiffness, rib shape, cut-out shape, and cut-out depth.

The susceptibility of the EC RFB connection welds to weld throat cracking was explored using the FEA results, under both fillet-welded and PJP-welded conditions. Additionally, detailed FE models were prepared to assess the sensitivity of notch stresses at the EC RFB connection wrap-around weld toe to the weld profile, specifically the weld face angle.

The results of the study indicate that this cost-effective EC RFB connection detail is a promising candidate for future redecking OSD applications. A deck plate thickness of 3/4 inch is suggested. This cost-effective EC RFB connection detail exhibits better fatigue performance when the ribs have a trapezoidal cross-section compared to ribs with a round bottom. Adequate fatigue performance can be expected for various cut-out shapes. Use of this cost-effective EC RFB

connection detail will improve the manufacturability of the OSD and promote the use of OSD in the United States.

A design engineer may consider using the cost-effective EC RFB connection detail of the full-scale prototype OSD test specimen with a Level 1 OSD design approach per the AASHTO LRFD BDS[1] if: (1) the global and local details are similar to those of the successful full-scale prototype OSD test specimen; (2) the fabrication workmanship meets or exceeds that of the prototype OSD test specimen, and meets the welding and tolerance requirements of AASHTO LRFD BDS[1] and AASHTO/AWS D1.5[6]; and (3) the wrap-around weld toes have toe angles greater than or equal to that of the tested OSD. The design engineer would need to develop project notes and specifications to ensure that the desired weld profile at the wrap-around weld at the cut-out termination is produced consistently during production of the OSD. The weld profile should have a concave shape and a radius transition at the toe. Such specifications could include the use of custom weld profile gauges in production, and qualification of the welding procedure using mock-ups that demonstrate the desired weld profile will be achieved consistently. Additionally, the use collaborative welding robots (cobots) in fabrication could improve the consistency of these critical welds. The favorable results of full-scale testing and sensitivity studies presented in this report suggests a reduced need for a Level 3 ODS design.

CHAPTER 1. LITERATURE REVIEW

BACKGROUND

A literature search was performed to identify and characterize details related to orthotropic steel decks (OSDs) with extended-cut-out (EC) rib-to-floor beam (RFB) connections. Publications from domestic and foreign sources were reviewed and summarized. Specifics on the range of OSD geometries, including the rib (profile, wall thickness, depth, span), floor beam (depth, web thickness), cut-out geometry, and connection details (weld process, weld size, preparation, and internal stiffening) were documented.

Examples of new bridges constructed with OSD with EC RFB connections were identified in the literature. Also, examples of existing bridges that have been redecked with OSD featuring EC RFB connections were identified. Where available, documentation of the observed fatigue performance of these orthotopic decks has also been noted.

This chapter highlights the key findings from the relevant literature. These key findings complement the results of the full-scale large-size OSD fatigue test program completed at the ATLSS Center of Lehigh University in 2018. This full-scale prototype test was focused on an economical EC RFB connection which employed a closed trapezoidal rib with a cut-out in the floor beam web beneath the rib. The RFB connection had partial joint penetration (PJP) rib-to-floor beam welds with reinforcing fillet welds that wrap around the termination of the floor beam cut-out on the rib wall.

The key findings from the relevant literature, especially the range of OSD characteristics, were used in planning of a sensitivity study to assess the conditions under which adequate fatigue performance can be expected for OSDs with EC RFB connections.

LITERATURE REVIEW RESULTS

Publications on OSDs from domestic and foreign sources were reviewed, with a focus on OSDs with EC RFB connections. The relevant literature was reviewed and summarized.

Details of the OSDs with EC RFB connections identified in the literature were compiled. Specifically, these details included critical dimensions of the ribs (e.g., depth, thickness, and span) and floor beam (e.g., web thickness and depth), as well as other details of the OSDs such as rib shape, cut-out shape, deck plate thickness, RFB connection weld details, and internal stiffening. The range of OSD geometries and details were considered in the development of the FEA sensitivity study.

Table 1 and Table 2 present details of existing OSDs with EC RFB connections on bridges in North America. Details of existing OSDs with EC RFB connections on bridges outside of North America are presented in Table 3 and Table 4.

Table 1. Details of North American OSDs with EC RFB connections (Part 1)

Bridge	Span Type	Location	Year Opened	Rib Spacing (in)	Rib Thickness (in)	Rib Top Width (in)	Rib Bot. Width (in)
Williamsburg	Suspension	NYC	1998	28.5	0.37	14.0	6.5
Bronx-Whitestone	Suspension	NYC	2005	26.0	0.31	13.0	5.0
New Tacoma Narrows	Suspension	WA	2007	*	0.31	*	*
Alfred Zampa	Suspension	CA	2003	26-28.6	0.31	14.0	6.5
SFOBB	Suspension	SF	2012	23.6	0.47	11.8	*
NYC1	Suspension	NYC	2017	28.5	0.31	14.0	6.5
NYC2	Suspension	NYC	2022	27.0	0.31	12.0	6.3
NYC3	Suspension	NYC	2001	20.625	0.44	11.0	6.0
Champlain Bridge	Truss	Montreal	1993	25.75	0.3125	13	8
Maritime Off-Ramp	Girder	CA	1997	26	*	14	*
Danziger	Girder	New Orleans	1984	26	0.3125	12.75	6.5

*Information not available

Table 2. Details of North American OSDs with EC RFB connections (Part 2)

Bridge	Rib Depth (in)	FB Web Thick. (in)	FB Depth (in)	FB Spacing (ft)	DP Thickness (in)	Cut-Out Type	Bulkhead or Internal Rib Stiffener?
Williamsburg	11.0	0.31	*	10.0	0.63	3	Bulkhead
Bronx-Whitestone	13.5	0.75	*	9.9	0.63	2	Stiffener
New Tacoma Narrows	12.0	0.35	66.5	20.0	0.63	*	*
Alfred Zampa	12.0	1.02	118.1	20.3	0.63	2	Bulkhead
SFOBB	13.6	*	53.9	16.4	0.55	2	No
NYC1	12.0	0.50	23.0	16.5	0.63	2	Bulkhead
NYC2	14.0	0.63	23.3	19.8	0.75	2	No
NYC3	7.4	0.75	22.0	17.0	0.63	3	Bulkhead
Champlain Bridge	15	*	*	32.0	0.625	1, 2	*
Maritime Off-Ramp	*	0.75	88.75	*	0.625	3	No
Danziger	10	0.4375	*	*	0.5	3	No

*Information not available

Table 3. Details of worldwide (outside North America) OSDs with EC RFB connections (Part 1)

Bridge	Type	Location	Year Opened	Rib Spacing (in)	Rib Thickness (in)	Rib Top Width (in)	Rib Bot. Width (in)
New Little Belt	Suspension	Denmark	1970	23.5	0.24	11.3	5.7
Faroe Bridges	Cable Stayed	Denmark	1985	24.4	0.24	11.3	5.8
Pont De Normandie	Girder	France	1994	23.8	0.28-0.31	11.5	7.6
Hoga Kusten	Cable Stayed	Sweden	1996	23.6	0.24	11.3	5.9
Great Belt East	Suspension	Denmark	1998	23.6	0.24	11.3	5.9
Great Belt East	Suspension	Denmark	1998	23.6	0.24	11.3	5.9
Sutong	Girder	China	2008	23.6	0.31	11.2	6.5
Stonecutters	Cable Stayed	Hong Kong	2009	23.6	0.35	11.7	5.9
Megyeri	Cable Stayed	Hungary	2008	23.6	0.31	11.2	7.2
Millau Viaduct	Cable Stayed	France	2004	23.6	0.28	11.8	7.9
Incheon Second	Cable Stayed	Korea	2009	23.6	0.31	12.0	7.4
Irtysh River	Suspension	Kazakhstan	2002	24.7	0.31	12.8	8.2
Maihama	Suspension	Japan	1978	24.4	0.3	12.2	7.1
Tokyo Gate	Girder	Japan	2012	*	0.3	15.7	7.4
Fochen West	Girder	China	2013	22.4	0.3	11.2	6.7
Grot-Rowecki	Girder	Poland	1981	23.6	0.3	13.4	7.5
*	Girder	Japan	*	25.2	0.2	12.6	8.5
Jiangyin	Girder	China	1997	23.6	0.2	11.8	6.7

*Information not available

Table 4. Details of worldwide (outside North America) OSDs with EC RFB connections (Part 2)

Bridge	Rib Depth (in)	FB Web Thick. (in)	FB Depth (in)	FB Spacing (ft)	DP Thickness (in)	Cut-Out Type	Bulkhead or Internal Rib Stiffener?
New Little Belt	9.6	0.31	118.1	9.8	0.47	*	*
Faroe	11.6	0.39	128.0	13.1	0.47	*	*
Pont De Normandie	11.6	0.63	118.1	12.9	0.5-0.55	*	*
Hoga Kusten	11.6	0.39	157.5	13.1	0.47	*	*
Great Belt East	11.6	0.47	31.5	13.1	0.47	*	*
Great Belt East	11.6	0.55	35.4	13.2	0.47	*	*
Sutong	11.5	0.79	157.5	13.1	0.55	*	*
Stonecutters	13.3	0.47	varies	12.5	0.71	*	*
Megyeri	11.5	0.47	66.8	13.1	0.55	*	*
Millau Viaduct	11.8	0.79	23.6	-	-	*	*
Incheon Second	10.2	0.43	118.1	12.3	0.55	*	*
Irtysh River	10.3	*	*	13.1	0.55	*	*
Maihama	9.1	*	33.5	9.0	0.5	3	*
Tokyo Gate	13.5	*	*	13.1	0.6	1	Stiffener
Fochen West	11.0	0.5	24.4	8.2	0.6	3	*
Grot-Rowecki	7.0	0.5	33.5	8.2	0.5	3	*
*	9.4	0.4	19.7	9.5	0.5	3	*
Jiangyin	11.0	*	*	10.5	*	3	*

*Information not available

Most of the early orthotropic deck bridges in North America, built from the 1960s to mid-1970s, incorporated fitted (without an extended cut-out) RFB connections with ribs passing continuously through tight-fitting cut-outs in the floor beam webs. Early applications of OSDs on bridges featured fitted RFB connections, such as the Port Mann Bridge in British Columbia, Canada (built in 1964) (Smylie, 1966), the Concordia Bridge in Montreal, Canada (built in 1967) (Gill & Dozzi, 1966), and the Mission Bridge in British Columbia, Canada (built in 1969) (Manniche & Ward-Hall, 1975).

After the mid-1970s, some OSDs were detailed with EC RFB connections. This change in the RFB connection design may have originated in Europe on railroad bridges (Haibach & Plasil, 1983) (Lehrke, 1990) due to significant cracking experienced at fitted RFB connections that employed discontinuous ribs fillet-welded to the floor beams (Nunn, 1974a) (Nunn, 1974b) (Cuninghame, 1987). The extended cut-out in the floor beam web is intended to increase the flexibility of the connection under out-of-plane loading induced by strong-axis end rotation of the ribs from vehicle loads within their span, thereby reducing the out-of-plane bending stresses in the floor beam web at the RFB connection weld toes. Extensive background on the development of the EC RFB connection is provided in the FHWA OSD Manual (Connor et al., 2012).

In the last 20 years in the United States, OSDs with EC RFB connections in major bridge redecking applications were detailed with internal rib bulkhead plates or stiffeners. Due to the fact that internal stiffener or bulkhead welds are not inspectable, the possibility of poor alignment with the floor beam web, and the added cost, the use of internal bulkheads is typically discouraged if possible. For new construction, internal stiffeners should be avoided (Connor et al., 2012). Bulkheads were also noted to behave as flexural elements in double curvature due to the lack of a connection to the deck plate and bottom of the rib, which introduced high stresses perpendicular to the rib wall leading to weld throat cracks. In addition, there is also a risk of fabrication shrinkage cracking of in-rib welds, due to high heat input and constraint, which is difficult to detect from outside of the rib by NDE.

In the United States, OSDs have been commonly used for re-decking of existing long-span bridges to reduce dead load on the suspension cables. In these applications, the existing RC deck and stringers are removed and the new OSD is connected to the existing stiff bridge superstructure. Accordingly, the depth of the OSD floor beam is typically limited to maintain the existing roadway elevation. As a result, there is a high degree of restraint to strong-axis end rotation of the OSD ribs where they pass through the shallow floor beam supported on the relatively stiff existing floor beam (or floor truss) of the existing bridge which can produce high stresses at the floor beam web weld toes. The use of EC RFB connections provides flexibility at the floor beam to reduce the floor beam web stresses produced by end rotation of the ribs when vehicle loads are within the rib span.

Many of the major suspension bridge in New York City have been redecked with OSD within the past 20 years. These bridges include the Williamsburg, Bronx-Whitestone, Robert F. Kennedy, and Verrazano Narrows Bridges. On the west coast, major bridges such as the new San Francisco-Oakland Bay Bridge and the Alfred Zampa Memorial Bridge in the California Bay Area feature OSDs. Though good performance has been observed so far, the RFB connections often are detailed with internal stiffeners (such as the Bronx-Whitestone Bridge) or bulkheads (such as the Williamsburg and Verrazano Narrows Bridges). These details reduce the overall manufacturability of the OSD. The fatigue performance of new OSDs for the Williamsburg, Verrazano, and Bronx-Whitestone bridges were evaluated using full-scale large-size fatigue testing at the ATLSS Center at Lehigh University. (Tsakopoulos & Fisher, 2003) (Tsakopoulos & Fisher, 2005).

The EC RFB connection is recognized in the AASHTO LRFD Bridge Design Specifications (BDS), 9th Edition[1] (AASHTO, 2020) and Eurocode 3[2] (European Committee for Standardisation, 2006). The various fatigue cracking modes are identified in these design provisions along with the associated design stress indices and fatigue resistances curves.

Based on the details of existing OSDs with EC RFB connections summarized in Table 1 through Table 4, the various geometries of the cut-out in the floor beam web were categorized into three general types (Types 1, 2, and 3) as shown in Figures 1 through 3. Each detail is shown with a trapezoidal rib without any internal stiffening. The details highlight the three most common cut-out variations observed in the literature. Each detail can be implemented with varied rib-to-floor beam weld details, with varied cutout shape (i.e., a flat bottom edge as shown or a radiused bottom edge), and with or without internal stiffeners or bulkheads. This study is focused on the use of EC RFB connections without internal stiffeners or bulkheads, and without the need for manual grinding.

The Type 1 extended cut-out (Figure 1) features a bottom cut-out edge that is flat with radiused transitions to sloped sides. On either side of the rib at the top of the cut-out, there are radiused transitions to the rib wall which feature tangential terminations of the cut-out edge at the rib wall and a small stay-in-place PJP weld receiving tab that is locally perpendicular to the rib web. There are either double-sided fillet welds or fillet-reinforced PJP welds; both weld types have a wrap-around fillet weld at the cut-out termination.

The Type 2 extended cut-out (Figure 2) is the same as the Type 1 connection but with a fillet-reinforced complete joint penetration (CJP) weld which is ground smooth at the termination. In Eurocode 3[2], the suggested EC RFB connection for railroad bridges can be characterized as either a Type 1 or a Type 2 connection. The EC RFB connection shown in the AASHTO LRFD BDS[1] can also be characterized as either a Type 1 or a Type 2 connection, depending on the weld detail.

Finally, the Type 3 extended cut-out (Figure 3) has a shallow, oblong shaped extended cut-out with flat bottom edge and radiused edges at each side. A perpendicular termination of the cut-out edge at the rib wall is shown. Examples of OSDs featuring this connection are the Maritime Off-Ramp Bridge in Oakland CA and Danziger Bridge in New Orleans (Dahlberg, et al., 2022). The replacement deck for the Williamsburg Bridge (Kaczinski et al. 1997, Tsakopoulos and Fisher 2003) features an extended cut-out with the same shape, but with a CJP weld ground smooth at the termination (instead of a fillet or PJP welds. The suggested EC RFB connection for highway bridges in Eurocode 3[2] is also a Type 3 connection.

[1] FHWA approved the use of the AASHTO LRFD Bridge Design Specifications, 9th Edition, although its use is not required (see Memorandum dated April 11, 2022 at https://www.fhwa.dot.gov/bridge/structures/04112022.pdf).

[2] Eurocode 3: Design of steel structures is not a Federal requirement.

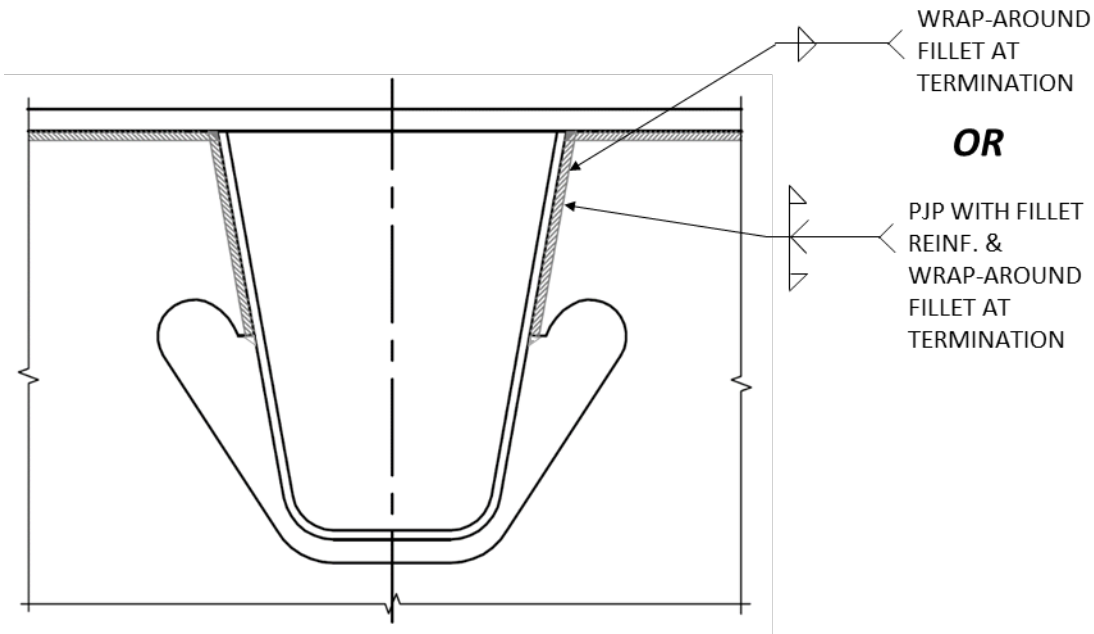

Figure 1. Type 1 extended cut-out

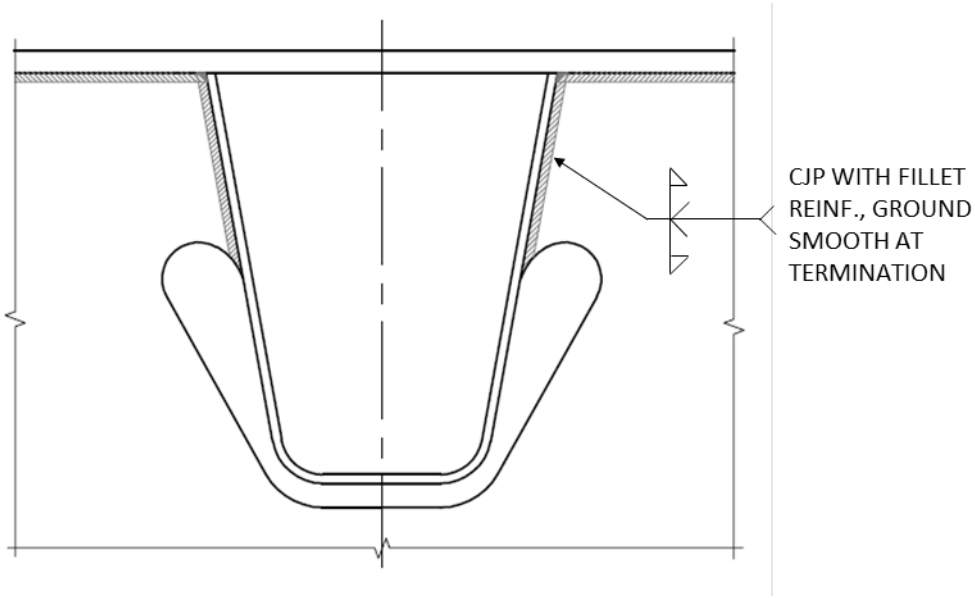

Figure 2. Type 2 extended cut-out

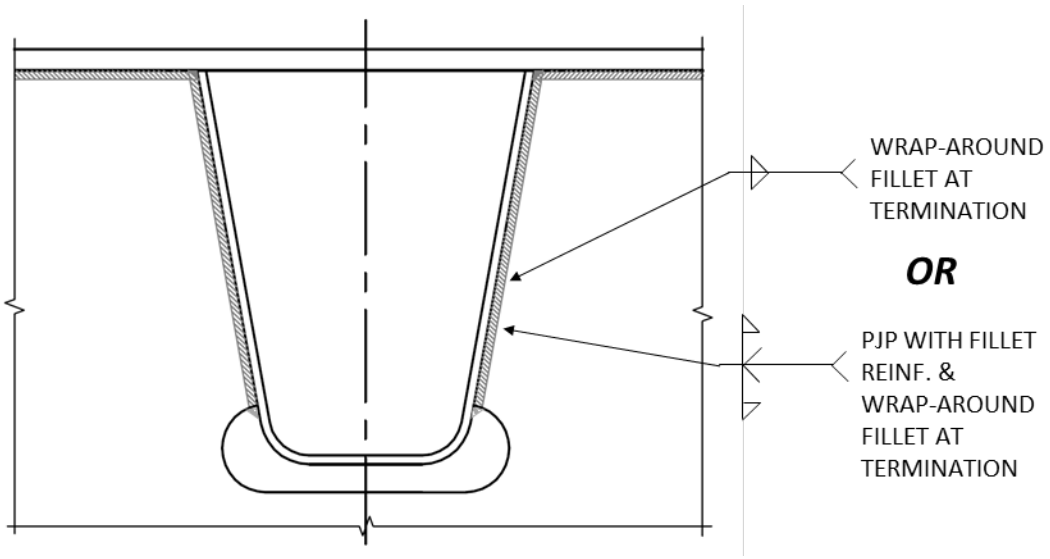

Figure 3. Type 3 extended cut-out

When an extended cut-out below the rib with tangential termination on the rib wall is employed, some OSDs have employed details with a CJP weld transitioning to fillet or PJP welds. This detail was developed based on extensive full-scale laboratory fatigue tests for the Williamsburg Bridge replacement orthotropic deck (Tsakopoulos and Fisher 2003). This extended cut-out often involves complex geometry and needs significant grinding. The weld details are labor intensive and unfit for automated manufacturing due to the need for joint preparation and non-destructive inspections. Alternatively, a simpler cut-out geometry without the ground-smooth tangential termination on the rib wall and employing fillet welds or PJP welds wrapped around the termination could provide adequate for fatigue performance (as demonstrated by the full-scale fatigue testing at Lehigh University) and could improve manufacturability.

Detailed technical documentation on domestic full-size laboratory fatigue testing of EC RFB connections is available (Tsakopoulos and Fisher 2003, Tsakopoulos and Fisher 2005). In all cases, the ribs were continuous through the floor beam, and an extended cut-out was provided in the floor beam under the rib. A fillet or PJP weld transitioning to a CJP weld at the cut-out termination on the rib wall was used in these RFB connections. A bulkhead or an internal stiffener was provided inside the rib at the RFB connections. The addition of these internal details significantly increases the fabrication cost of the OSD. The perceived need for these details was driven by the high stresses in the rib wall at the termination of the cut-out.

Details of selected documents in the literature are provided in the following references:

(AASHTO, 2020)

The AASHTO LRFD BDS[1] outlines the design and detailing of OSDs for bridges. For OSDs featuring closed-ribs, two RFB connection details are suggested in Section 9.8.3.6.4, namely (1) a fitted RFB connection (with a continuous rib passing through matching tight-fit cut-out in the floor beam web and welded all around); and (2) an EC RFB connection. These details are shown

in Figure 4. It is noted that the detail features a Type 1 or a Type 2 EC RFB connection, depending on the weld detail.

At the EC RFB connection detail, AASHTO LRFD BDS[1] prohibits web snipes in the floor beam web at the rib-to-deck weld. In addition, the edges of the extended cut-out should be ground smooth. It is also noted that PJP or CJP welds may be needed in cases where either (1) the fillet welds meeting the fatigue design considerations on their own are excessive; or (2) a ground smooth weld termination is implied (as drawn in the detail of Figure 4). A vertical distance, *c*, from the bottom of the rib to the weld termination of at least of *h*/3 is specified, where *h* is the rib depth. This avoids excessive out-of-plane stresses which may result from the relatively large stiffness associated with a small cut-out depth.

The commentary notes that the EC RFB connection is preferable since it limits the restraint of rib end rotation which produced large stresses in the floor beam web and RFB connection welds. The specification of a minimum cut-out depth, *c*, is intended to limit the restraint to rib end rotation. The fitted RFB connection is noted as a viable option for OSDs with deep and flexible floor beams.

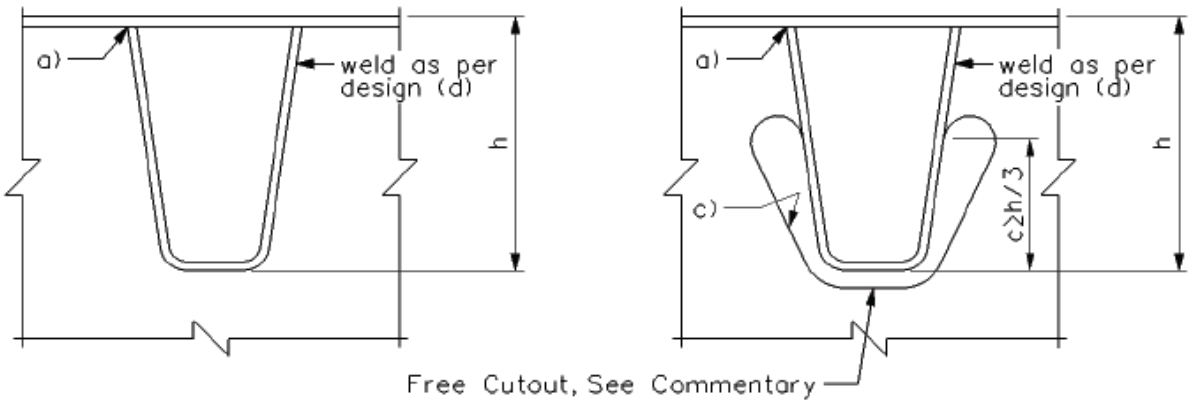

Figure 4. Fitted (left) and EC RFB (right) connection details from AASHTO LRFD BDS[1] (AASHTO, 2020)

(Eurocode 3, 2006)

Eurocode 3[2] provides details for EC RFB connections in Annex C of EN 1993-2. The standard detail for highway bridges is shown in Figure 5. This detail features a Type 3 extended cut-out (see Figure 3). Eurocode 3[2] also provides details for OSDs for railway bridges.

The standard EC RFB connection for railway bridges from Eurocode 3[2] is shown in Figure 6. This detail features a Type 1 extended cut-out (see Figure 1). Note that the detail indicates the grinding of the wrap-around weld toe is called for "when necessary". Grinding is not noted on the standard highway bridge EC RFB connection.

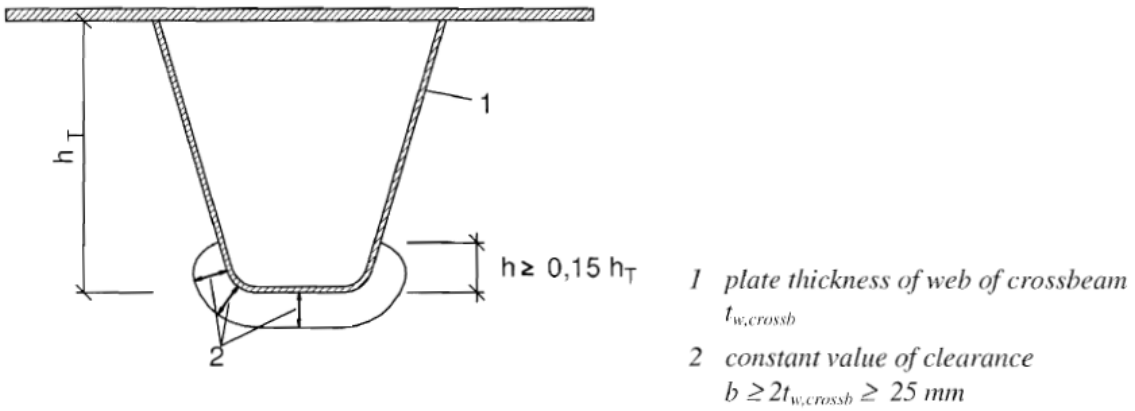

Figure 5. EC RFB connection detail for highway bridges from Eurocode 3[2] (European Committee for Standardisation, 2006)

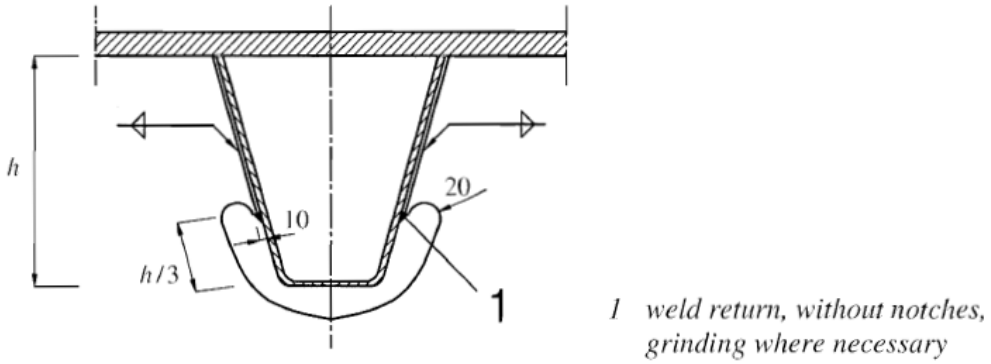

Figure 6. EC RFB connection detail for railway bridges from Eurocode 3[2] (European Committee for Standardisation, 2006)

(Connor, 2002), (Connor, 2004)

A parametric study was performed on an OSD with EC RFB connections using finite element analysis. The OSD was used in a redecking application for an existing suspension bridge. The sensitivity of stresses at various critical details in the RFB connection to changing cut-out geometries was evaluated. These geometries included the clearance between the rib and cut-out edge, and the total cut-out height.

The study considered three characteristic cut-out geometries with varying levels of out-of-plane stiffness. Separate loading conditions were applied with produced stress conditions in the floor beam web that maximized in-plane response, maximized out-of-plane response, and a stress condition with a combination of both in-plane and out-of-plane response.

It was found that the fatigue response of the floor beam web was dominated by in-plane components of stress. Variation in the deck plate thickness had little effect (less than 10%) on the stresses in the cut-out region of the RFB connection.

Ribs closest to the connection between the floor beam and longitudinal element experience the highest stresses. Furthermore, the stresses at the cut-out were very sensitive to floor beam web thickness, regardless of cut-out geometry. Increased floor beam web thickness resulted in a higher proportion of out-of-plane stresses, due to the increased out-of-plane stiffness. Increasing the floor beam web thickness was found to be the most efficient way to decrease stresses in at the EC RFB connection. The cut-out geometry was also shown to have a significant effect on the stress magnitudes at the cut-out edge.

The study found that increasing the gap between the cut-out edge and the bottom of the rib increases the in-plane stresses and decreases the out-of-plane stresses in the floor beam web. Increasing the total depth of the cut-out (vertical distance from the underside of the deck plate to the lowest point of the cut-out edge) also increases the in-plane stresses and decreases the out-of-plane stresses in the floor beam web. For the OSD proportions studied, increasing the depth of the cut-out generally increased the total stress range, regardless of floor beam thickness.

The sensitivity to bulkhead plate thickness, as well as misalignment of the bulkhead plate with respect to the floor beam web, was assessed. The results indicated that misalignment of the bulkhead plate can have a significant effect on the stresses in the bulkhead plate and floor beam web.

Connor (Connor, 2002) also compared the analytical results for the OSD with and without internal bulkhead plates. The results showed that removing the bulkhead plate reduced the normal stresses in the floor beam web perpendicular to the rib wall. However, the stresses at the cut-out edge and vertical weld toe stresses in the rib wall at the cut-out were increased considerably. It should be noted that the OSD used for the study was for a bridge with cantilevered floor beams which generally increased the in-plane live load tensile stress demands on the bulkhead plate.

(Connor et al., 2012)

FHWA developed a comprehensive manual to OSD design entitled “Manual for Design, Construction, and Maintenance of Orthotropic Steel Deck Bridges” (Connor et al., 2012). For the RFB connections of OSDs, the manual summarizes two RFB connections that can be used, namely the EC RFB connection and the fitted RFB connection. It is noted that the fitted RFB connection is better suited to OSDs with deep floor beams that are relatively flexible under out-of-plane loading.

Furthermore, the EC RFB connection, with its stress relieving cut-out in the floor beam web, has demonstrated good performance when the geometry is carefully detailed. Early OSD designs with EC RFB connection featuring shallow cut-outs exhibited poor fatigue performance and led to the addition of a design criterion for a minimum height of the cut-out above the bottom of the

rib of one third of the rib depth in the AASHTO LRFD BDS, 5th Edition[3] (AASHTO, 2010). The EC RFB connection detail in the 2010 5th Edition of AASHTO LRFD BDS[3] included bulkhead plates and a perpendicular cut-out termination at the rib wall with a wrap-around weld.

The manual also notes that results of full-scale testing demonstrated the bulkhead plates introduced additional stress concentrations, fabrication problems, and increased cost. Furthermore, since accurate alignment of bulkhead plates is not guaranteed, additional secondary stresses are possibly introduced. Finally, bulkhead plates cannot be inspected. Therefore, the manual discourages the use of bulkhead plates.

The test results also showed that increasing the floor beam web thickness decreases the in-plane connection stresses much more than the increase in out-of-plane stresses resulting from the increased stiffness of a thicker web.

The manual also provides a number of examples of OSD bridges in service with EC RFB connections. Examples of both domestic and international bridges are provided along with critical details of the OSDs such as rib geometry, rib spacing, floor beam spacing, and member thicknesses. Applicable examples have been incorporated in the summaries provided in Table 1 through Table 4.

Finally, the manual provides a summary of limits for critical OSD dimensions, including rib spacing, floor beam spacing, rib-to-floor beam depth ratio, extended cut-out to rib depth ratio, and member plate thicknesses (see Table 5). These ranges served as an important reference during the planning of the FEA sensitivity study.

Table 5. Limits for OSD geometries in (Connor et al., 2012)

Dimension	Suggested Range
Deck Plate Thickness, t_d	$t_d > 5/8$ inch
Rib Thickness, t_r	1/4 inch $< t_r <$ 1/2 inch
Rib Spacing, s (ribs with direct wheel load)	24 inches $< s <$ 30 inches
Rib Spacing, s (ribs without direct wheel load)	24 inches $< s <$ 40 inches
Floor Beam Spacing, L	L < 20 feet
Ratio of Rib Depth to Floor Beam Depth, h_{rib}/h_{FB}	$h_{rib}/h_{FB} < 0.4$
Floor Beam Web Thickness, t_{FB}	3/8 inch $< t_{FB} <$ 3/4 inch
Ratio of Cut-Out Depth to Rib Depth, h_{cutout}/h_{rib}	$h_{cutout}/h_{rib} > 0.33$

(Haibach & Plasil, 1983)

Fatigue testing of railway bridge OSD subassemblies with different RFB connection details was performed in the early 1980s at the Fraunhofer Institute for Structural Durability in Darmstadt,

[3] Previous editions of AASHTO LRFD Bridge Design Specifications (1st to 7th Editions) are not a Federal requirement.

Germany and funded by the Federal Ministry of Transport and the German Research Foundation. The test program included four test series (A, B, C, D), though the paper was focused on Test Series C. During Test Series A, a single rib-to-floor beam connection under bending was studied. Butt welded rib splice plate connections were tested during Test Series B. RFB connections were evaluated by Test series C, and the rib-to-deck plate connections were evaluated by Test Series D. A number of extended cut-out geometries were selected for testing based on the results of previous analyses.

The OSD test specimens had continuous trapezoidal ribs passing through cut-outs in the floor beam web. The specimens were based on a through-truss or plate girder railroad bridge supporting a single track with either top or bottom level track and ballast thickness of 15.7 inches. The trapezoidal ribs were formed from 1/4-inch, 5/16-inch, and 3/8-inch thick plate with a top width of 12 inch, rib bottom width of 5.3 inches, and a height of 10.8 inches. The ribs spacing ranged from 23.6 inches to 3 ft. 11.5 inches. The floor beam spacing was 9 ft. 10 inches with spans of 12 ft. 10 inches to 14 ft. 9 inches.

Test Series C had multiple stages of testing to evaluate the fatigue performance of two RFB connection details, namely Form I, with an extended cut-out below the rib; and Form II, without an extended cut-out below the rib (i.e., a fitted RFB connection). Two variations of Form I were evaluated. The extended cut-out of Form I.1 followed the trapezoidal shape of the rib and had upper radii of 3/8 inch and lower radii of 2 inches. The extended cut-out of Form I.2 had a rounded bottom edge with upper radii of 3/8 inch and lower radius of 4 inches. The terminations of these two EC RFB connections were perpendicular to the rib wall. The final cut-out of Form I had a rounded bottom edge with upper radii of 3/4 inch and a termination that was tangent to the rib wall with a 3/8-inch welding tab.

During the initial fatigue testing, seven tests were performed with variation of RFB connections as well as specimen geometry including floor beam span, rib spacing, and floor beam web thickness. Tests of the fitted RFB connection, Form II, were terminated early due to cracking on the edge of the welded rib. The test program continued without additional testing of Form II. The results of the initial fatigue tests led to changes in Form I.1 and I.2, resulting in the final Form I. The modifications were selected to reduce the stress concentration at the cut-out termination on the rib wall. During fatigue testing of the final Form I, the cracking which had occurred on the test specimens with Form I.1 and Form I.2 RFB connections did not occur. The final Form I RFB connection exhibited better fatigue performance in subsequent fatigue testing compared to the earlier forms.

(HNTB, 2015)

A summary of standard practice for OSD design and detailing with a focus on cost-effective details is provided. OSD design provisions and practices in the North America, Germany, Netherlands, China, and Japan are reviewed. Additionally, the report provides an overview of typical OSD fabrication practices, focusing on the two critical details: (1) rib-to-deck connection; and (2) RFB connection.

The use of EC RFB connections with internal stiffening is noted to have been developed in the United States for applications with shallow floor beams. The use of such details is noted to be

rare outside of the United States. The fabrication cost drivers of OSDs with EC RFB connections identified are (1) the fit-up between continuous ribs which pass through matching cut-outs in the floor beam web; (2) the transition detail where the cut-out meets the rib wall; (3) internal bulkhead plates; and (4) welding position (avoiding downhill welding).

The authors state that the primary purpose of the extended cut-out is to allow for increased fit-up tolerance. They note that the EC RFB connection is the standard RFB connection detail for OSDs in Japan and Germany. Attempts in Germany to change the standard RFB connection detail to a fitted RFB connection failed due to resistance from fabricators.

Tight fit-up between the continuous rib and the cut-out in the floor beam web affects the fatigue performance, though the sensitivity has not been systematically studied. Tight fit-up is difficult to achieve though it is easier with an EC RFB connection than a fitted RFB connection.

In the United States, it has been common to detail a CJP weld where the cut-out meets the rib wall. This weld is then ground smooth which results in a detail with very good fatigue performance, however, this detail is expensive and can account for 25% to 40% of the total fabrication cost of the connection. It is noted that European and Japanese practice is to use a wrap-around fillet weld (in lieu of the CJP weld) that is ground smooth at the weld toe.

Internal bulkhead plates are noted to be costly, often needing PJP welds. They are also prone to misalignment with the floor beam web and the alignment is difficult to verify. Therefore, use of bulkheads is generally discouraged when floor beam configurations permit use of alternative details. Finally, the welding of the RFB connection should be performed in the uphill direction.

(Kolstein, 2007)

This dissertation summarizes the European Coal and Steel Community (ECSC) research on OSD between 1976 and 1994 and OSD research conducted worldwide through 2006. The purpose was to provide additional test data to be used to aid the development of fatigue resistance categories for welded details in OSDs by the European Standard on Steel Structures committees. Results from a total of 147 fatigue tests were summarized. The tests were performed between 1961 and 2005 and were focused on the behavior of the RFB connection. Most of this research involved OSD details not employed in current designs such as OSDs with thin deck plates (less than 1/2 inch) and ribs that are not continuous through the floor beam webs. The results provide insight into issues related to fatigue performance of the RFB connection with and without an extended cut-out as well as the impact of fabrication parameters such as fit-up gap, joint preparation, welding processes, and degree of weld penetration. A weld throat thickness of greater than 50 percent of the floor beam web thickness is suggested.

The dissertation also describes cracks observed in the RFB connections in temporary flyover viaducts in France. Some of these bridges had extended cut-out RFB connections. In the extended cut-out RFB connections, cracks were located at the fillet weld toe at the cut-out termination. Multiple fatigue cracks were observed in the Maihama Bridge in Japan. The ribs were continuous through the floor beam web with an extended cut-out. The edge of the extended cut-out of the RFB connection featured a perpendicular termination at the rib wall with the fillet

weld wrapped around the termination. Cracks in both the floor beam web and rib wall extending from the welded termination of the cut-out were observed.

(Miki & Suganuma, 2014)

This report presents the results of inspections of bridges with OSDs in the Metropolitan Expressway in Japan performed between 2002 and 2004. Of the OSD bridges inspected with longitudinal ribs, 43 percent experienced fatigue damage. Fatigue cracking was observed at welded rib splices, rib-to-deck plate connection welds, RFB connection welds, and vertical-stiffener-to-deck-plate welds. The authors noted that the RFB connection cracks occurred due to a combination of global bending and shear forces in the floor beam and stress concentration effects at the welds.

The report also presented findings of finite element analyses and fatigue testing performed for the design of the OSD for the Tokyo Gate Bridge. This OSD included trapezoidal ribs with an EC RFB connection with a perpendicular termination at the rib wall. The termination was not ground smooth. A variety of cut-out terminations, cut-out geometries, termination tab lengths, and internal rib stiffener geometries were studied using FEA. The effect of RFB connection weld length was also studied. Three different RFB connection weld lengths were analyzed: a long connection (12 inches); a short connection (5 1/8 inches); and a medium connection (8 5/16 inches). The results of the study showed that both long and short RFB connection lengths produced smaller rib wall weld toe stresses than the medium length connection. To further reduce the rib wall weld toe stress at the RFB cut-out termination, internal stiffeners were added.

Fatigue testing of OSD specimens with four different EC RFB connections was performed. All but one EC RFB connection featured a perpendicular cut-out termination at the rib wall with a wrap-around fillet weld. Two of the EC RFB connections tested featured internal rib stiffeners, and other two had no stiffeners. Both EC RFB connections without internal stiffeners experienced fatigue cracking while cracking was not observed for the two RFB connections with internal stiffeners. The fatigue cracks were located at the welded termination of the cut-out and propagated into the rib wall.

(Kitner 2016)

Kitner performed detailed FEA of OSDs with various RFB connection details, including EC RFB connections (Kitner, 2016). The results showed that very high vertical stresses in the rib wall at the wrap-around weld toe can occur. For the EC RFB connection studied, the analysis showed a peak vertical rib wall stress of approximately 22 ksi at the weld toe is expected, far exceeding the fatigue resistance for infinite fatigue life of 10 ksi represented by Fatigue Category C in AASHTO LRFD BDS[1]. This connection detail is used only in locations of lower stress, for example interior RFB connections, away from floor beam connections to supporting longitudinal members (e.g., girders, trusses).

Kitner noted that modern OSDs in North America employ both trapezoidal and round bottom ribs, with and without internal stiffening. In the US, most OSDs have trapezoidal ribs. Canadian OSDs typically have round bottom ribs.

(Saunders et al. 2019)

This FHWA-funded research effort was focused on the RFB connections that have the potential for automated fabrication and to assess the conditions under which good fatigue performance can be expected. Extensive and detailed FEA as well as full-scale laboratory tests were performed. Analytical studies included OSDs with EC RFB connections without internal stiffening. The EC RFB connection detail featured a round bottom rib with either a Type 1 or a Type 2 extended cut-out, with corresponding fillet weld wrap-around or CJP weld ground smooth weld termination details, respectively.

A prototype two-girder bridge was considered as the supporting superstructure for the OSD. Multi-level analytical submodeling was performed to assess the very localized stresses at the wrap-around weld toe. It was found that under the AASHTO LRFD BDS[1] Fatigue I OSD tandem axle load, the vertical weld toe stresses exceeded the constant-amplitude fatigue threshold (CAFT) of 10 ksi indicating that fatigue cracking was likely for this EC RFB connection with wrap-around fillet weld terminations.

Variations of the floor beam restraint conditions, simulating differences between new bridge construction and existing bridge redecking applications, showed that for this detail and global bridge configuration, weld toe fatigue cracking at the wrap-around welds is likely. This detail was not expected to exhibit good fatigue performance and was therefore excluded from the full-scale testing program.

CHAPTER 2. INDUSTRY SURVEY

BACKGROUND

Input from industry leaders experienced in the design and fabrication of OSDs was solicited to identify the current standard practice employed in the United States for OSD with EC RFB connections.

As noted previously, a focus of this research is the results of fatigue testing of the full-scale prototype OSD test specimen performed at the ATLSS Center of Lehigh University between 2017 and 2019. A portion of the test program investigated the fatigue performance of an EC RFB connection featuring a PJP weld between the floor beam and rib wall, with a wrap-around reinforcing fillet weld, and without the use of internal stiffeners or bulkheads. No fatigue cracks were observed at the wrap-around weld toe at any of the connections, either at floor beams or intermediate diaphragms (unsupported leveling members centered between floor beams).

At the conclusion of the testing, eight of the most highly stressed connections (four at floor beams and four at intermediate diaphragms) were removed from the deck and sectioned through the mid-thickness of the floor beam (or intermediate diaphragm) web. These samples were then macro-etched to assess where fatigue crack initiation had occurred. Figure 7 shows a macro-etch through the center of the floor beam web through the wrap-around fillet reinforcing weld at one of the RFB connections from the full-scale prototype OSD test specimen after 8 million cycles at AASHTO LRFD BDS[1] Fatigue I loading for OSD. As shown, no cracking in the rib at the wrap-around fillet weld toe was observed, despite hot spot stresses at the weld toe of nearly 13 ksi which is significantly above the CAFT of 10 ksi for weld toe cracking. In fact, all eight samples were found to be free from fatigue cracks at the weld toe.

The welds were found to have a favorable profile without a sharp corner at the weld toe on the rib wall. As shown in the macro etch of one of the wrap-around fillet welds at a fatigue-sensitive location in Figure 7, there is a smooth transition between weld and base metal at the lower weld toe, where the vertical stresses in the rib wall due to in-plane loading of the floor beam (perpendicular to the weld toe) are highest and thus represent the most likely location of fatigue cracking. These cracks would be expected to be horizontal, and would propagate into the rib wall (thickness direction) and horizontally away from the floor beam (or intermediate diaphragm) web.

A key question that should be considered in this research is whether US fabricators can consistently produce fillet welds having a profile comparable to the weld shown in Figure 7. The angle of the weld face with respect to the face of the rib wall greatly impacts the magnitude of the stress concentration at the weld toe and therefore the fatigue strength, given the same global (or geometric) stresses at the connection. These geometric stresses are representative of the local structural stress (LSS), also known as the hot-spot stress. The LSS is a stress index calculated by extrapolation of the stresses at points at prescribed distances from the weld toe (Hobbacher, 2008). Through this extrapolation, the LSS inherently incorporates stresses resulting from global bridge behavior as well as the more localized geometry of the connection, but does not incorporate the very localized effects of weld profile (i.e., weld face angle and weld toe radius).

Therefore, without explicitly modeling this localized weld geometry, the results of further FEA cannot be broadly extrapolated if weld profiles vary significantly from the macro etch shown in Figure 7.

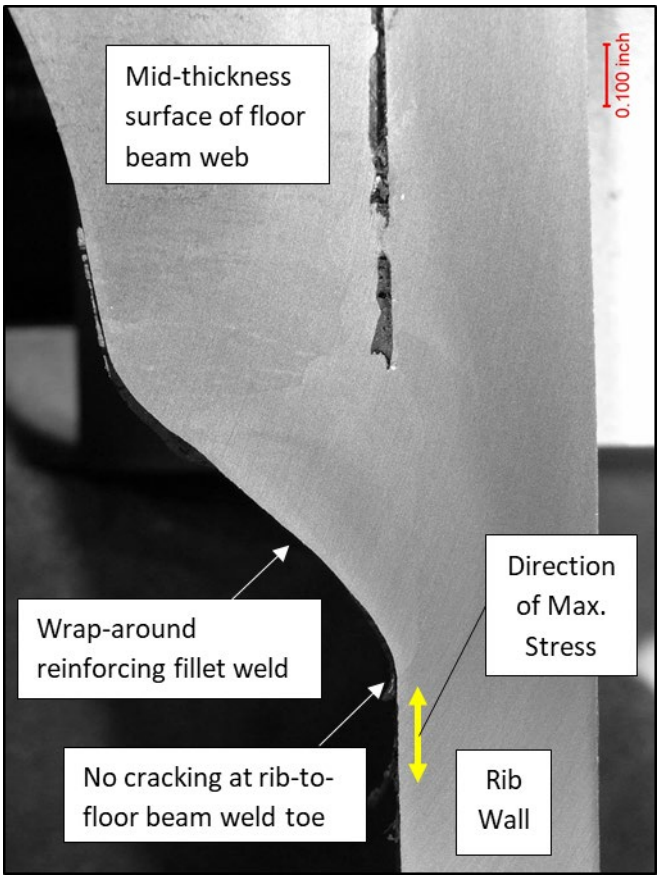

Figure 7. Macro-etch through the center of the floor beam web and the wrap-around fillet reinforcing weld at the RFB connection from the full-scale prototype OSD test specimen after 8 million cycles at AASHTO LRFD BDS[1] Fatigue I loading for OSD, showing no cracking in the rib at the wrap-around fillet weld toe

An FHWA-funded project performed by Iowa State University aimed to provide standardized design considerations for OSDs on bridges with regular characteristics (Dahlberg, et al., 2022). The research team included many industry experts in both the design and fabrication of OSDs.

The research was structured to develop standardized details of OSDs that could be applied to the Level 1 OSD design procedure prescribed in AASHTO LRFD BDS[1] (AASHTO, 2020). Two standard details are presented in the report. The first detail employs a trapezoidal closed rib. The second employs a flat plate open rib.

The proposed closed rib design features a fully fitted RFB connection, with no extended cut-out in the floor beam web. A closed-rib OSD design is easier to fabricate given the simpler welding details (two-sided fillet or PJP welds) compared to more expensive CJP welds ground smooth associated with many EC RFB connections. An OSD with fully fitted RFB connections can be fabricated using automated techniques (e.g., robotic welding), although tight fit-up of the rib within the matching cut-outs can be challenging without automated measurement/cutting.

The closed-rib RFB connection detail has been found to be optimal for new bridge construction, where the OSD is integral with the bridge superstructure (i.e., floor beam, girders). In cases of redecking of existing bridges, where the OSD is supported on existing bridge superstructure which can provide significant restraint to out-of-plane rotation of the floor beams under traffic loading, high weld toe stresses in the floor beam web can result at the fitted RFB connection, which can lead to fatigue cracking (Connor et al., 2012) (Saunders, et al., 2019).

It is envisioned that an optimized closed-rib detail with an extended cut-out could be developed in the future for redecking applications where the available depth of floor beam is limited and/or with widely spaced floor beams. The results of this research project, including the detailed sensitivity studies, could aid in developing a standardized EC RFB connection detail, and its range of applicability.

The Iowa State research team shared details of two OSDs with EC RFB connections similar to the detail studied in this research, namely (1) the Maritime Off-Ramp Bridge in Oakland, California; and (2) the Danziger Bridge in New Orleans, Louisiana (J. Dahlberg, personal communication, January 25, 2022).

The Maritime Off-Ramp Bridge is applicable to this research since the OSD features EC RFB connections without internal stiffeners or bulkheads, and with simple fillet welds (no CJP welds ground smooth). The connection is categorized as a Type 3 EC RFB connection (see Figure 3), with a perpendicular termination of the diaphragm plate at the rib wall. The bridge was constructed in 1999. To date there have been no reported fatigue issues with the OSD.

This OSD is different from many of the OSDs in redecking applications which feature EC RFB connections because this OSD was constructed integrally with the bridge (i.e., new construction application). Additionally, instead of existing transverse floor beams or floor trusses which support the new OSD and often provide significant restraint to out-of-plane rotation (i.e., plane of the floor beam web) at the RFB connection, the OSD of this bridge is integral with a box girder with full depth diaphragms (3/4 inch thick, approximately 7 ft. deep) spaced at a maximum of 18 ft. This configuration would be expected to provide less restraint to end rotation

of the ribs (the deformation which produces the out-of-plane stresses in the diaphragm), and therefore result in smaller stresses at the connection due to out-of-plane loading (vehicles positioned between diaphragms).

An interesting feature of this OSD is that the rib-to-diaphragm connection features fillet welds (3/8 inch, both sides), with no end preparation of the diaphragm plate at the rib opening. Fillet welding greatly simplifies the fabrication of the OSD. However, use of fillet welds increases the size of the unfused root between the diaphragm and rib wall which could lower the resistance to throat cracking, so care should be taken when considering the design of these welds, factoring in the diaphragm plate thickness, fillet weld size, and expected stresses.

The OSD of the Danziger Bridge is also has EC RFB connections of interest to this study. This OSD is integral with the bridge superstructure and was constructed in the mid-1980s. The bridge has a lift span comprising three box girders, spaced at 37 ft. 9 inches and with welded plate floor beams spaced at 14 ft. 7 inches which cantilever approximately 15 ft. beyond the outer box girders. As of 2018, no fatigue issues were noted at the rib-to-floor beam connection.

The RFB connection of this OSD also features a fillet-welded RFB connection without internal stiffeners or bulkheads. This detail is similar to that of the Maritime Off-Ramp and is also categorized as a Type 3 EC RFB connection with a perpendicular termination of the diaphragm plate at the rib wall. The cut-out on the Danziger Bridge is shallower than the Maritime Off-Ramp Bridge detail. The RFB connection has fillet welds (1/4 inch, both sides), with no end preparation of the 7/16 inch thick floor beam web which greatly simplifies the fabrication.

OBSERVATIONS

Additional discussions with industry experts provided the research team with valuable insight into current standard practice for OSD design and fabrication. As noted, an important question that should be considered in this research is whether the favorable profile of welds of the full-scale prototype OSD test specimen (particularly the critical wrap-around fillet weld at the top of the cut-out in the RFB connection shown in Figure 7) can be considered typical for US OSD fabricators now or in the near future. The full-scale prototype OSD test specimen was fabricated by a US fabricator.

However, the opinions of the industry experts varied. Some noted that such weld profiles can be expected from OSD fabricators. Others noted that such favorable weld profiles may be achievable but that the actual profiles may vary, and such favorable weld profiles may not even represent the typical weld profile produced by most fabricators. Detailed specifications would need to be developed to ensure that minimum weld profile parameters are met. One expert noted that development of such specifications should include feedback from fabricators to ensure the specifications are reasonable yet reliably produce welds with a favorable weld profile comparable to that of the weld in the full-scale prototype OSD test specimen. It should be noted that enforcing such specifications would include enhanced visual inspection beyond what is typically performed for fillet welds.

When asked about the use of PJP versus fillet welds for the RFB connection, one expert noted that more economical fillet welds could be used so long as the stresses are sufficiently low. However, it was noted that the use of PJP welds can make fit-up of the connections easier.

Regarding testing of OSD designs, it was noted by several experts that the use of component testing rather than large-size deck specimen testing should be encouraged. Extensive large-size deck specimen testing can be an impediment to the use of OSDs in smaller bridges.

Finally, one expert noted that the use of automated fabrication technology, such as robotic welding, would aid in consistently achieving the desired weld profile, as well as improve the cost-effectiveness of the OSDs through improved manufacturability.

Cooperative robots (commonly known as “cobots”) could be used to perform welding of OSDs with increased efficiency and reliability over fully manual processes. Use of cobot welding combines the accuracy and speed of industrial robotic welding with the flexibility of manual welding. For the welding of EC RFB connections, this technology is of interest because it could help to ensure that favorable weld profiles are consistently produced.

CHAPTER 3. SUMMARY OF 2018 FULL-SCALE LABORATORY FATIGUE TEST PROGRAM

BACKGROUND

In 2018, fatigue testing of a full-scale prototype OSD test specimen was conducted to investigate its performance in a re-decking application on an existing suspension bridge. The research was funded by a regional transportation agency and was performed at the ATLSS Center lab at Lehigh University. A key goal of the testing was to investigate the performance of a cost-effective EC RFB connection with PJP welds and reinforcing wrap-around fillet welds. The fatigue testing was performed to assess whether an OSD detailed with this cost-effective EC RFB connection would be expected to have a fatigue life that exceeds the design life of 100 years.

To make this assessment, a total of 8 million loading cycles of the Fatigue I tandem axle load for OSD specified in AASHTO LRFD BDS[1] (AASHTO, 2020) were applied to the full-scale prototype OSD test specimen. The Fatigue I tandem axle load represents the fatigue limit state load, or the tandem axle load which is expected to produce the upper bound stress range (i.e., the maximum stress range in the life of the structure), generally assumed to be the load which occurs with a frequency of 1 in 10,000. For the design of a welded bridge detail, the stress range produced by the Fatigue I loading would be compared to the CAFT for the representative fatigue detail category specified in AASHTO LRFD BDS[1]. If the stress range is less than the CAFT, infinite fatigue life would be expected (all stress cycles would be less than the CAFT).

For finite life fatigue design, the methodology of AASHTO LRFD BDS[1] is based on the concept of equivalent fatigue damage, in which the fatigue damage produced by all the cycles in the stress range spectrum is equivalent to the fatigue damage produced by the same number of cycles with a stress range equal to the effective stress. The stress range produced by the Fatigue II load case in AASHTO LRFD BDS[1] is intended to represent the effective stress range. The Fatigue II load case was developed based on weigh-in-motion (WIM) studies and presented in NCHRP 299 (Moses, et al., 1987) with the three-axle “fatigue truck” loading configuration. The effective load is calculated as the root-mean-cube (RMC) of the truck spectrum (trucks less than 20 kips are excluded).

For primary bridge components, the design truck axle loads (both single and tandem axles) are specified as single point loads for each axle. For bridge decks, including OSDs, in which the response is sensitive to the local presence of wheel loading, AASHTO LRFD BDS[1] specifies both the Fatigue I and II load cases to be applied to patch areas corresponding to single and tandem axles wheels. For the single front axle there are two patches 10-inch square spaced 6 ft. apart. For the rear tandem axle, there are four patches 10 inches long by 20 inches wide, spaced 6 ft. apart transversely, and 4 ft. longitudinally.

In AASHTO LRFD BDS, 8th Edition[4] (AASHTO, 2017), the load factors for Fatigue I and II load cases for primary bridge component were changed to 0.8 and 1.75, respectively. These factors remain the same in AASHTO LRFD BDS, 9th Edition[1]. Considering the ratio of these factors indicates that the ratio of maximum load (i.e., 1 in 10,000 frequency) is 2.19 times the effective load. These factors were updated from the factors in previous versions of AASHTO LRFD BDS[3] of 0.75 and 1.5 (with a ratio of 2.0), based on the results of WIM studies (Modjeski and Masters, Inc., 2015).

For the fatigue design of OSDs, the load factor for Fatigue II (for finite fatigue life design) is the same as for primary bridge component. However, for Fatigue I (for infinite fatigue life design) the load factor is increased to 2.275 (an increase of 30%) from the factor for primary bridge components. This results in a ratio of maximum to effective loads for OSDs equal to 2.84. In the 7th and previous versions of AASHTO LRFD[3], the Fatigue I and II factors for OSDs were 2.25 and 0.75 (a ratio of 3.0). It should be noted that the value of the fatigue limit state load (Fatigue I load) is nearly the same (2.275 vs. 2.25) as it was the stated intent in the revision to the 8th Edition[4], though the ratio is slightly less (2.84). All fatigue load cases also include a 15% dynamic amplification allowance.

The higher loads for the fatigue limit state load (Fatigue I load) for OSDs is based on field monitoring studies conducted on the OSD of Williamsburg Bridge, a suspension bridge over the East River in New York City that was redecked with an OSD with EC RFB connections in the late nineties (Connor, 2002). Measurements and counting of stress cycles at critical details of the OSD was performed over an extended period of time. It was found that the ratio of the stress cycle occurring with a frequency of 1 in 10,000 was significantly larger that the two times the effective (RMC) stress cycle, primarily due to the sensitivity of the OSD to the local presence of truck wheels. The ratio was found to vary with detail. For some OSD details it was found that the ratio of 2 used for primary bridge components would result in an unconservative design. Therefore, it was suggested to raise the ratio to 3.0 for certain details (RFB connection welds and cut-out) while the ratio could remain at 2.0 for other details (rib-to-deck, deck-to-floor beam, deck splices). Ultimately, the load factors were changed in AASHTO LRFD BDS[3] such that the ratio is 3.0 for all OSD details. As noted, in the current AASHTO LRFD BDS[1], the ratio is slightly reduced (=2.84) though the magnitude of the fatigue limit state load for OSDs is the same.

Due to the large number of cycles experienced by OSDs on major bridges in redecking applications, they are typically designed for infinite life. The full-scale prototype OSD test specimen was also designed for infinite fatigue life (using the Fatigue I load case). Theoretically, if the stresses at all critical details produced by the Fatigue I load case are less than their respective fatigue resistance (the CAFT), infinite fatigue life would be expected.

During the fatigue testing, measured vertical LSS values at the weld toes of the wrap-around fillet welds at the cut-out termination on the rib walls greater than 13 ksi, exceeding the CAFT of

[4] AASHTO LRFD Bridge Design Specifications, 8th Edition (2017) is incorporated by reference at 23 CFR 625.4(d)(1)(v)

10 ksi (for Fatigue Category C), were observed. However, no fatigue cracks were observed at the wrap-around fillet weld toes of any of the EC RFB connections.

Considering the statistics from the original NCHRP fatigue test data (Keating & Fisher, 1986) that served as the basis for Fatigue Category C, 8 million loading cycles producing a maximum vertical LSS range at the weld toe of the wrap-around fillet weld equal to 13.2 ksi (as observed during the full-scale OSD fatigue test at a cut-out termination) far exceeds the upper bound fatigue life of 3.3 million cycles (2 standard deviations above the mean, or 2.3% probability of cracking). This level of exceedance without the occurrence of cracking indicates that fatigue cracking of this detail would be highly unlikely with additional loading cycles (i.e., infinite fatigue life is expected) and also suggests that the CAFL of this detail is most likely higher than that of Fatigue Category C. Further study of the fatigue resistance of this detail should be considered.

The design of orthotropic steel decks according to AASTHO LRFD BDS[1] is performed using one of three design levels. For a Level 1 design, the engineer selects the OSD details based on previous test results which show that the OSD details have adequate fatigue resistance, with few calculations needed. Level 2 design also relies on previous test results, but simplified one- or two-dimensional analyses may be performed to validate global member sizing. A Level 3 design relies on 3D finite element analysis to quantify critical local stresses to validate the expected fatigue performance, in cases where previous fatigue test data are not available. It is noted in the commentary of AASHTO LRFD BDS[1] that Level 3 design should always be used in the case of a redecking application (for which OSDs with EC RFB connections are better suited), unless an exception is made by the bridge owner.

Appendix C of the FHWA Manual for Design, Construction, and Maintenance of Orthotropic Steel Bridges (Connor et al., 2012) provides an example of a Level 1 design. The example relies on the results of fatigue testing of the prototype OSD for the redecking of the Bronx-Whitestone Bridge in New York City, which was tested at Lehigh University. It is noted that the design of this OSD could be considered as a standard panel but that subsequent Level 1 designs relying on the associated test results are to be fabricated with the same level of workmanship.

During the 2018 full-scale prototype fatigue test program, the measured vertical local structural stresses (LSS) at the wrap-around fillet weld toes on the rib walls at the EC RFB connection exceeded the fatigue threshold stress of 10 ksi (Fatigue Category C). However, no fatigue cracks were observed at the wrap-around fillet weld toe at any of the EC RFB connections, including the RFB connections of floor beams and intermediate diaphragms (unsupported transverse leveling elements centered between floor beams).

The results of this 2018 testing program serve as the basis for the current research which aims to establish the range of applicability of this cost-effective EC RFB connection.

DESCRIPTION OF OSD FATIGUE TEST PROGRAM

Test Setup

Figure 8 and Figure 9 show the test setup in the ATLSS Center lab. The full-scale prototype OSD test specimen was approximately 29 ft. by 41 ft 6 inches in plan with 14 ribs, and was

supported on three transverse floor trusses. The transverse extent of the full-scale prototype OSD test specimen represents two outside lanes of the bridge, and longitudinal extent of the test specimen includes two rib spans. The floor trusses were supported on one end by a longitudinal truss (intended to simulate the longitudinal stiffening truss of the suspension bridge) and supported on the other end by the laboratory reaction wall. The longitudinal truss was supported at each panel point by steel stub columns supported on the laboratory strong floor.

Figure 10 shows a transverse cross-section through the OSD and indicates the rib numbering. Ribs 1 through 12 were trapezoidal closed ribs, while Ribs 13 and 14 were plate-type open ribs (not the focus of study since they were not directly loaded by wheel loads). Cyclic loading was applied in the outside lane only, over Ribs 7 through 12. Figure 11 shows a plan view of the full-scale prototype OSD test specimen with floor beam and rib spacing, and the four fixed loading positions. The intermediate diaphragms (ID1 and ID2) are not supported by the longitudinal truss or reaction wall, and serve only as transverse leveling members to better distribute concentrated wheel loads to adjacent ribs. Figure 12 shows the dimensions of the load patches at each fixed loading position. The load applied by each actuator is divided into four patches representing at tandem axle. The load patch dimensions match those specified in AASHTO LRFD BDS[1] (AASHTO, 2020).

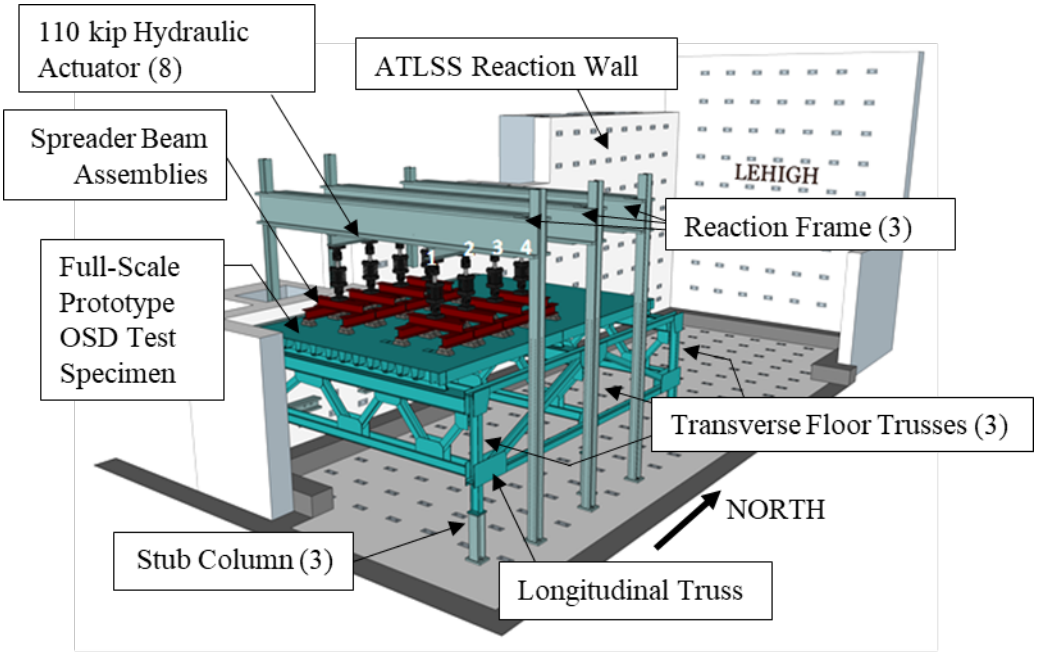

Figure 8. Schematic view of test setup in the ATLSS Center lab for fatigue testing of the full-scale prototype OSD test specimen with EC RFB connection with PJP welds and no internal stiffeners (the loading was applied by Actuators 1 through 4 in sequence)

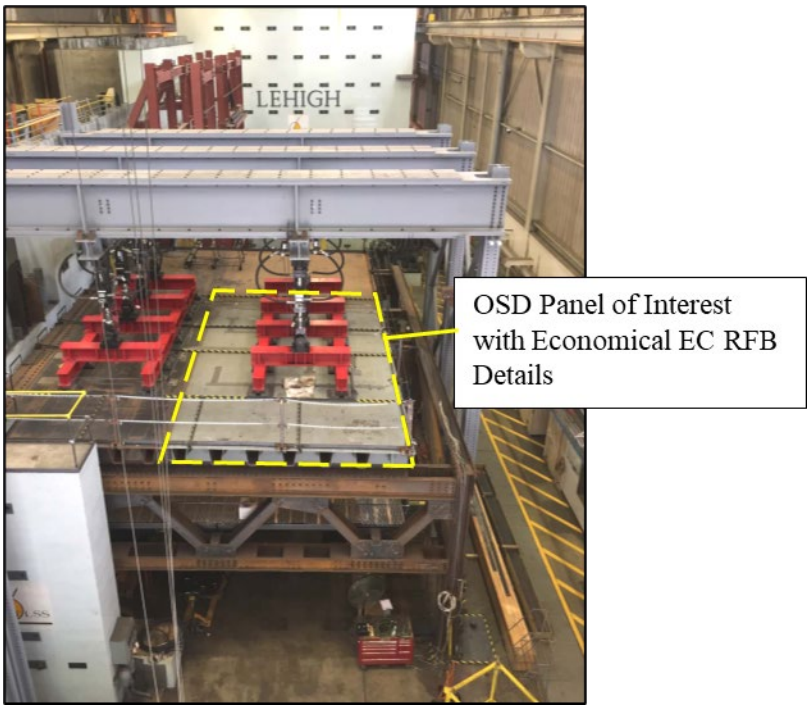

Figure 9. Setup in ATLSS Center lab for fatigue testing of the full-scale prototype OSD in 2018 (view looking north)

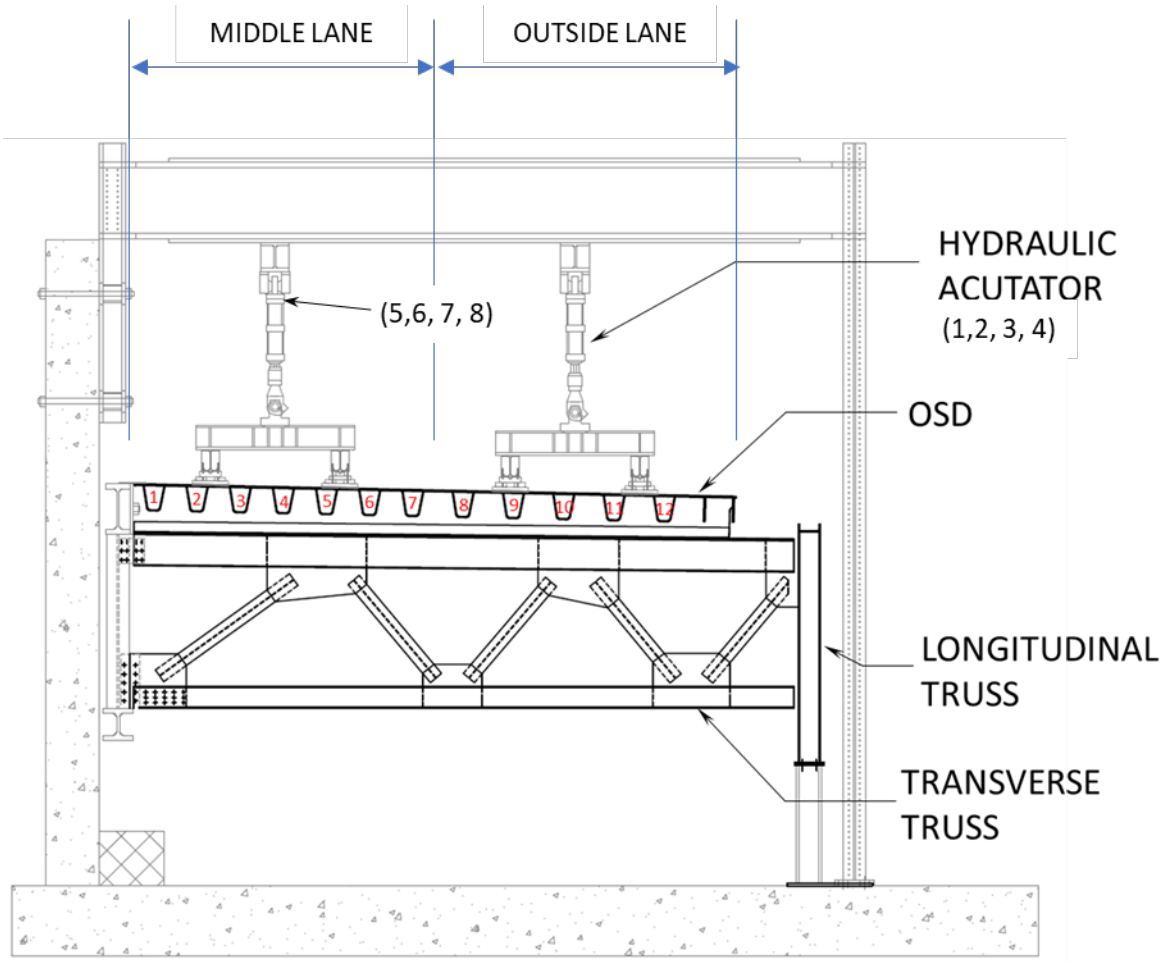

Figure 10. Section drawing of setup in ATLSS Center lab for fatigue testing of the full-scale prototype OSD in 2018 (view looking north)

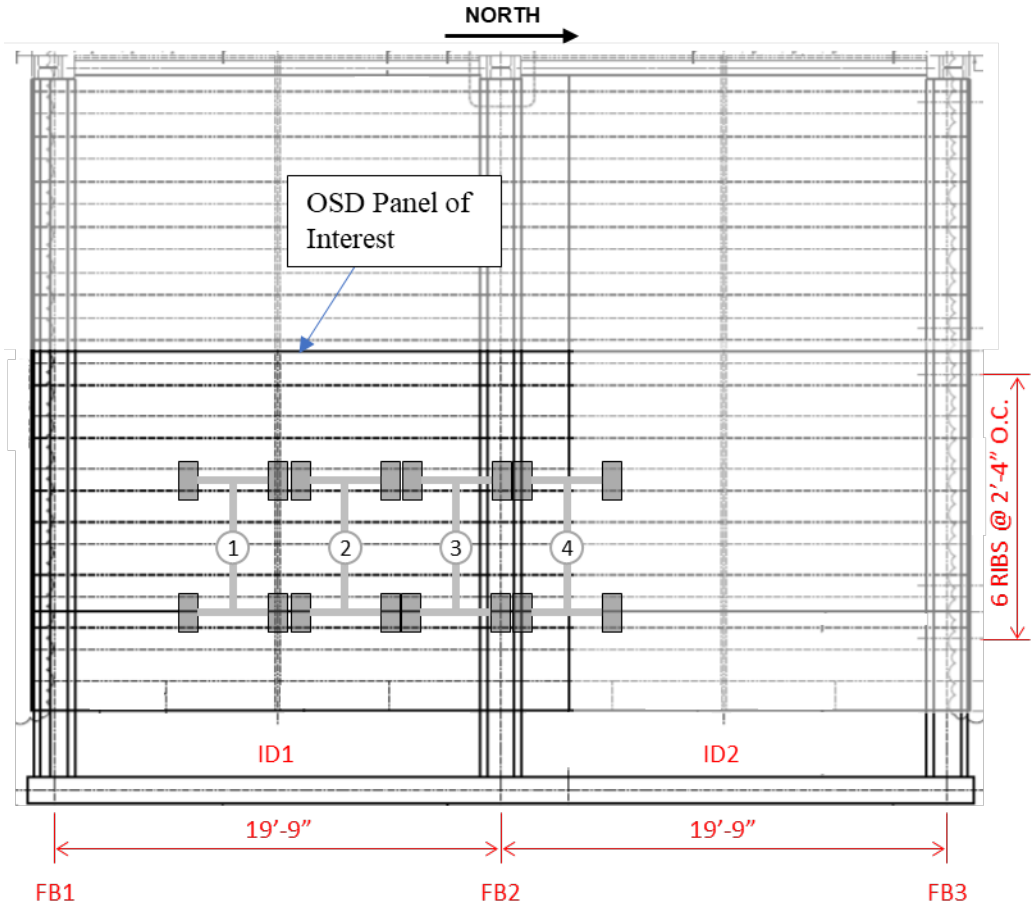

Figure 11. Plan view drawing of the full-scale prototype OSD test specimen showing loading positions (1 through 4) and extent of the OSD panel of interest

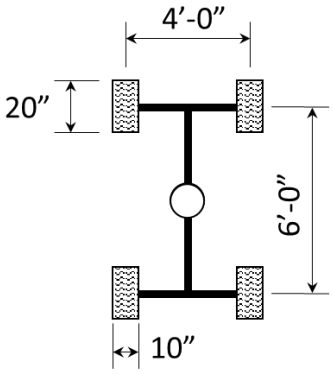

Figure 12. Overall dimensions of the tandem axle patch loading applied by each actuator

Full-Scale Prototype OSD Test Specimen

The full-scale prototype OSD test specimen was fabricated by a US fabricator and was comprised of four separate panels which were connected to make a continuous deck during erection in the laboratory. As shown in Figure 9 and Figure 11, the OSD panel of interest is the south east panel. The RFB connections of the OSD panel of interest (at Ribs 7 through 12) are the economical PJP-welded EC RFB connection without internal stiffening (the focus of this research study), and are present at Floor Beams 1 and 2 (FB1 and FB2) and Intermediate Diaphragm 1 (ID1).

The four panels and supporting transverse and longitudinal trusses were erected in the ATLSS Center lab by iron workers from the fabricator's shop. The 3/4-inch deck plate of the four panels was spliced with CJP single-V-groove welds performed using the submerged arc welding (SAW) process and the backing bars were left in place. The support fixtures and overhead loading frames were erected by ATLSS Center lab technicians.

The closed ribs were cold-bent from 5/16-inch plate. The closed-rib-to-deck connections throughout the OSD panel of interest were single-bevel PJP groove welds with 60% average penetration (50% minimum) and 1/50-inch root gap. For edge preparation, the ends of the rib at the deck were machined with a 3/32-inch land and a 50-degree bevel. The flux-core arc welding (FCAW) process was used. At the transverse joint between OSD panels, the ribs were spliced using bolted connections.

There were three transverse trusses in the full-scale prototype OSD test specimen, spaced at 19 ft. 9 inches. Each truss comprised double channel top and bottom chords (MC18x58 top chord and C12x25 bottom chord). The double-channel top chord had a continuous top flange plate that supported the double angle connection to the floor beam web of the OSD. Batten plates (3/8 inch x 17 inches) were used on the bottom flange of the top chord, and both flanges of the bottom chord. The diagonals of the truss were W12x40 members and connected with bolted gusset plates.

The longitudinal truss was comprised of two panels between the three floor trusses. Each longitudinal truss panel had a single diagonal. The diagonals, chords and verticals were all W12x40 members and were connected with bolted gusset plates.

EC RFB Connection

The EC RFB connection detail used in the OSD panel of interest of the full-scale prototype OSD test specimen tested in 2018 is shown in Figure 13. This RFB connection featured a flat-bottomed extended cut-out opening in the web of the floor beam/intermediate diaphragm through which the 5/16-inch-thick trapezoidal closed rib passed. The RFB connection weld was a PJP weld (1/4-inch penetration) with a 5/16-inch reinforcing fillet weld which wrapped around the bottom of the connection through the opening. The floor beam web plate thickness was 5/8 inch while the intermediate diaphragm web thickness was 1/2 inch (cut from a W24x94). At the 1/2-inch-thick intermediate diaphragm web, the 1/4-inch penetration of the PJP (both sides) made the RFB connection weld effectively a full penetration weld, though these welds are significantly easier to perform than CJP welds. They also do not need the same level of non-destructive evaluation (NDE) as CJP welds.

A manual FCAW process was used to produce the RFB connection welds. The welds were performed in the 3 position (vertical) with the panel inverted (deck plate down). The weld on each side of the floor beam web was performed by welding in the upward direction, with a termination at the cut-out.

The full-scale prototype OSD test specimen was detailed with this EC RFB connection to assess its fatigue resistance under the AASHTO LRFD BDS[1] Fatigue I load case for OSD. Considering that this detail does not need manual grinding, special weld procedures, special NDE, or internal stiffeners/bulkheads, and considering that it is easier to achieve a tight fit-up during fabrication (as compared to a fully-fitted RFB connection), the fabrication costs would be lower. Therefore, so long as the fatigue performance is acceptable, this detail would improve the cost-effectiveness of OSD for highway bridges, in cases where EC RFB connections are warranted (such as in redecking of existing bridges). Use of such connections in OSDs in the United States and Europe has been limited due to concerns of fatigue cracking at the weld toe on the rib wall due to high vertical stresses. This concern has been addressed in previous OSD designs through the use of CJP welds with ground-smooth terminations, as well as the use of internal stiffeners and bulkheads. However, these design details are costly. The purpose of this research effort is to establish the range of global and local variables under which acceptable fatigue performance could be expected over the full design life of the deck, using the good performance of the full-scale prototype OSD test specimen with economical EC RFB connections as a baseline for the assessment. As noted, the full-scale prototype OSD test specimen was subjected to 8 million cycles of the AASHTO LRFD BDS[1] Fatigue I tandem axle load for OSD (the fatigue limit state load for OSD) without development of fatigue cracks.

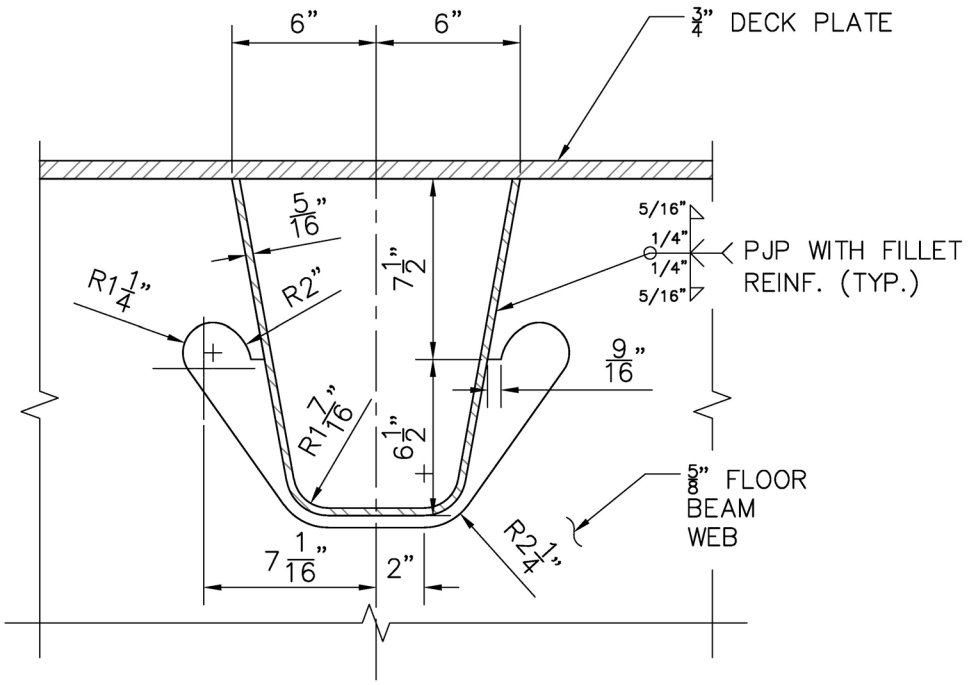

Figure 13. EC RFB connection with wrap-around reinforcing fillet welds used in laboratory testing of the full-scale prototype OSD test conducted at the ATLSS Center lab, Lehigh University in 2018

Fatigue Testing Procedure

The full-scale prototype OSD test specimen was fatigue tested by applying loads at four position in sequence (Actuators 1 through 4 in Figure 8 and Figure 11) in the outside lane. The load at each actuator position was equal to 82.8 kips, the fatigue limit state load for OSDs from the 7th edition of AASHTO LRFD BDS[3] (AASHTO, 2014) (i.e., the Fatigue I tandem axle for OSD design with 15% impact allowance). As noted previously, in the current version (9th edition) of AASHTO LRFD BDS[1] (AASHTO, 2020), the Fatigue I tandem axle load with 15% impact is essentially the same (83.7 kips vs. 82.8 kips), though the Fatigue II load with 15% impact is slightly higher (29.4 kips vs. 27.6 kips).

The test specimen was developed using FEA to ensure behavior under the simulated tandem axle loads applied according to the loading protocol would be representative of the in-situ response of the OSD (on the bridge) to truck loading. Additionally, prior to fatigue testing, crawl testing was performed using an actual truck tandem axle loaded with steel billets resulting in an applied tandem axle load of 50 kips. The axle was slowly rolled longitudinally across the deck at various transverse positions to maximize the responses at instrumented details. Good agreement between the test results and result of a global FEA of the test specimen was observed.

The loading protocol is illustrated in Figure 14. Each load cycle represented a sequence of four load applications in overlapping succession (load was removed from one actuator as load was simultaneously increased at the next actuator) at the four fixed loading positions. This loading sequence was intended to simulate a moving truck using several fixed-position time varying loads. At all actuators, including the four additional actuators (Actuators 5, 6, 7 and 8) in the adjacent OSD panels (Lane 2), a nominal level of continuous (static) load was applied to simulate the dead load of the overlay. At each fixed loading position, the load (applied by a hydraulic actuator) was spread onto four equal areas with dimensions and spacings matching the design tandem-axle load in AASHTO LRFD BDS[1] which specifies wheel patch areas of 10 inches by 20 inches, center-to-center longitudinal wheel patch spacing of 48 inches, and center-to-center transverse wheel patch spacing of 72 inches. (see Figure 12).

As shown in Figure 10, the loading actuator for the outside lane load is positioned transversely such that the right wheel patches are centered between Ribs 11 and 12 and the left wheel patches are nearly centered over Rib 9. Longitudinally, at Actuators 1 and 3, the northmost wheel patches were centered over ID1 and FB2, respectively, to maximize the response at these RFB connections. Therefore, the most highly stressed EC RFB connections are the east and west sides of Rib 9, the east side of Rib 11, and the west side of Rib 12.

As part of the test program, the full-scale OSD was extensively instrumented. A total of 342 resistance strain gages were installed on the specimen, concentrated in the OSD panel of interest with the economical EC RFB connection. Strain gages were installed at many fatigue-sensitive details including the EC RFB connection. The instrumentation plan at a highly-stressed RFB connection is shown in Figure 15. To assess the likelihood of weld toe fatigue cracking, the local structural stress (LSS) methodology was used by placing strain gages at locations 0.4 and 1.0 times the plate thickness away from the weld toe. These strain gages had a gage length of 1 mm The LSS at the weld toe was extrapolated using these two measurements. This methodology is presented in the AASHTO LRFD BDS[3] (AASHTO, 2016), the FHWA OSD manual (Connor et al., 2012), and by the International Institute of Welding (IIW) (Hobbacher, 2008). The LSS is then compared to an appropriate fatigue resistance curve to estimate the life (for example, Fatigue Category C in AASHTO LRFD BDS[1]). Strain Gages 53 and 54 in Figure 15(b) (and Strain Gages 23 and 24 on the opposite rib wall) were installed on the rib wall normal to the wrap-around fillet weld toe in a vertical orientation to estimate the LSS at the weld toe for the critical EC RFB cracking (horizontal crack in the rib wall initiating at the weld toe).

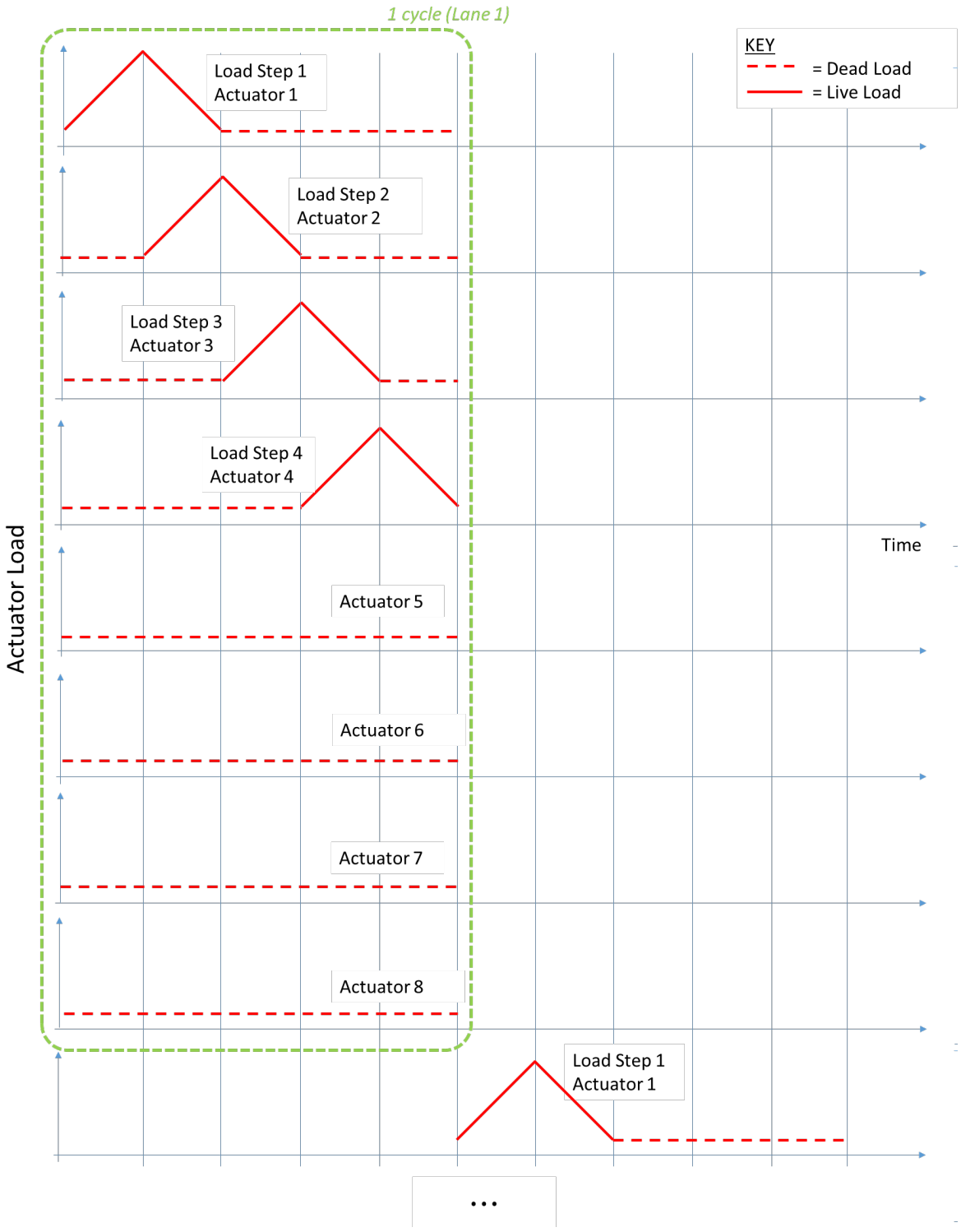

Figure 14. Loading protocol: complete sequence of actuator force application

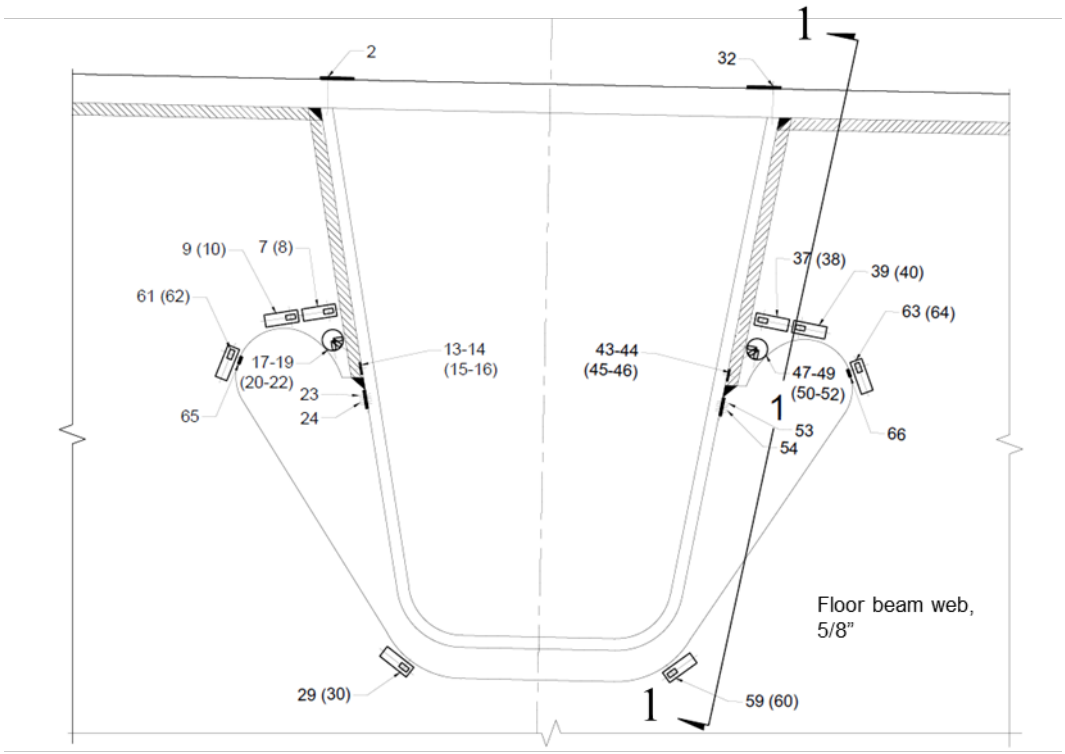

(a) Cross-section at rib

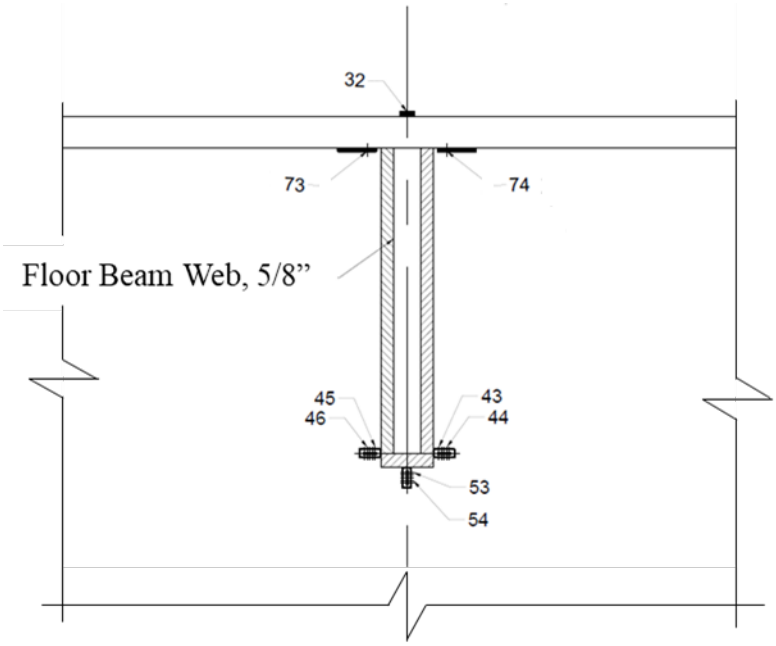

(b) Section “1”

Figure 15. Strain gage plan for a highly stressed EC RFB connection of the full-scale prototype OSD test specimen: (a) cross-section view of the rib; and (b) cross-section view of the floor beam

Fatigue testing was concluded after 8 million cycles had been applied. Hands-on visual inspection was performed approximately every 200,000 cycles throughout the test program. No horizontal weld toe fatigue cracks were observed at the bottom of the wrap-around reinforcing fillet weld of the EC RFB connection at any of the detail locations, including the most highly stressed details. Weld throat cracking was also not observed in any of the PJP welds.

TEST RESULTS

No fatigue cracks were discovered at any of EC RFB connections of the full-scale prototype OSD test specimen during the fatigue testing. As noted, a total of 8 million cycles of the AASHTO LFRD BDS[1] Fatigue I tandem axle design load for OSDs (each cycle was a sequence of load applications in successive positions on the deck) were applied to the full-scale prototype OSD test specimen.

Macro-Etch Testing

To confirm that fatigue cracks did not initiate at: (1) the wrap-around fillet weld toe; or (2) the PJP weld throat of the EC RFB connection, macro-etch testing of highly stressed OSD details in the full-scale prototype OSD test specimen was performed. Over 72 macros were prepared from various locations throughout the OSD panel. To evaluate these two cracking modes at the EC RFB connection, macro-etch specimens were taken at two location types, namely Type 1 and Type 2 as shown in Figure 16. The Type 1 macro is cut on the mid-thickness plane of the floor beam or intermediate diaphragm web, perpendicular to the wrap-around fillet weld, showing a cross-section through the wrap-around fillet weld. The Type 2 macro is cut on a plane perpendicular to the PJP weld axis (above the wrap-around), showing across-section through the PJP weld.

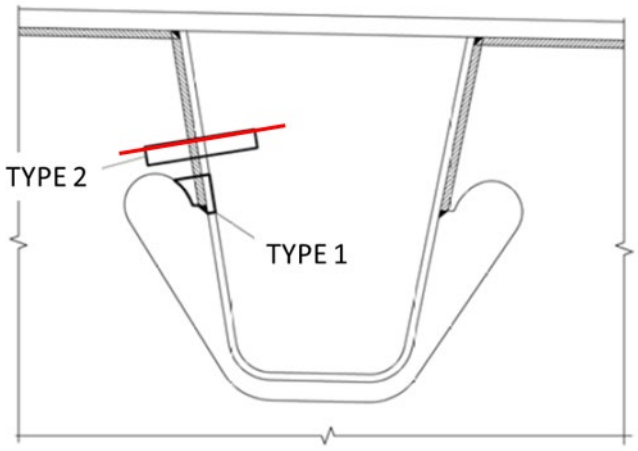

Figure 16. Locations of macro-etch specimens taken through the bottom of the wrap-around fillet weld cut on the mid-thickness plane of the floor beam web (Type 1); and on a plane perpendicular to the PJP weld axis (Type 2)

Type 1 macros were taken at the four most highly stressed connections, namely the east and west walls of Rib 9 (Rib 9E and 9W), the east wall of Rib 11 (Rib 11E), and the west wall of Rib 12 (Rib 12W), at both Intermediate Diaphragm 1 and Floor Beam 2. Therefore, a total of eight Type 1 macros were removed.

Figure 17 shows the four macro-etch specimens from Intermediate Diaphragm 1. Figure 18 shows the four macro-etch specimens from Floor Beam 2. As the figures show, no fatigue cracks were detected at the weld toe of the wrap-around reinforcing fillet weld.

As reflected in the macro-etch specimens, the welds were found to be of high quality without sharp corners at the weld toes on the rib wall. At each location, there is a smooth transition between weld and base metal at the lower weld toe, which is a location with high vertical stresses in the rib wall due to in-plane loading of the floor beam (perpendicular to the weld toe), and thus a likely location of fatigue cracks. These cracks would be expected to be horizontal, and would propagate into the rib wall (thickness direction) and horizontally away from the floor beam (or intermediate diaphragm) web.

An important question to be considered in this research is whether the weld profiles shown in Figure 17 and Figure 18 are likely to be typical of US fabrication practice. The angle of the weld face with respect to the face of the rib wall greatly affects the magnitude of the stress concentration at the weld toe and therefore the fatigue resistance, when the global (or geometric) stresses at the connection are the same. The LSS incorporates stresses resulting from global bridge behavior as well as the more localized geometry of the connection, but the LSS does not incorporate the very localized effects of weld profile (weld face angle or weld toe radius). Therefore, without explicitly modeling this localized weld geometry, the results of further FEA cannot be broadly extrapolated to weld profiles that vary significantly from the weld profiles shown in Figure 17 and Figure 18.

Figure 19 shows the Type 2 macro-etch specimens through the PJP weld at the RFB connection at Rib 9E and 12W. The welds were found to be of high quality, and without any indication of weld toe or throat fatigue cracking.

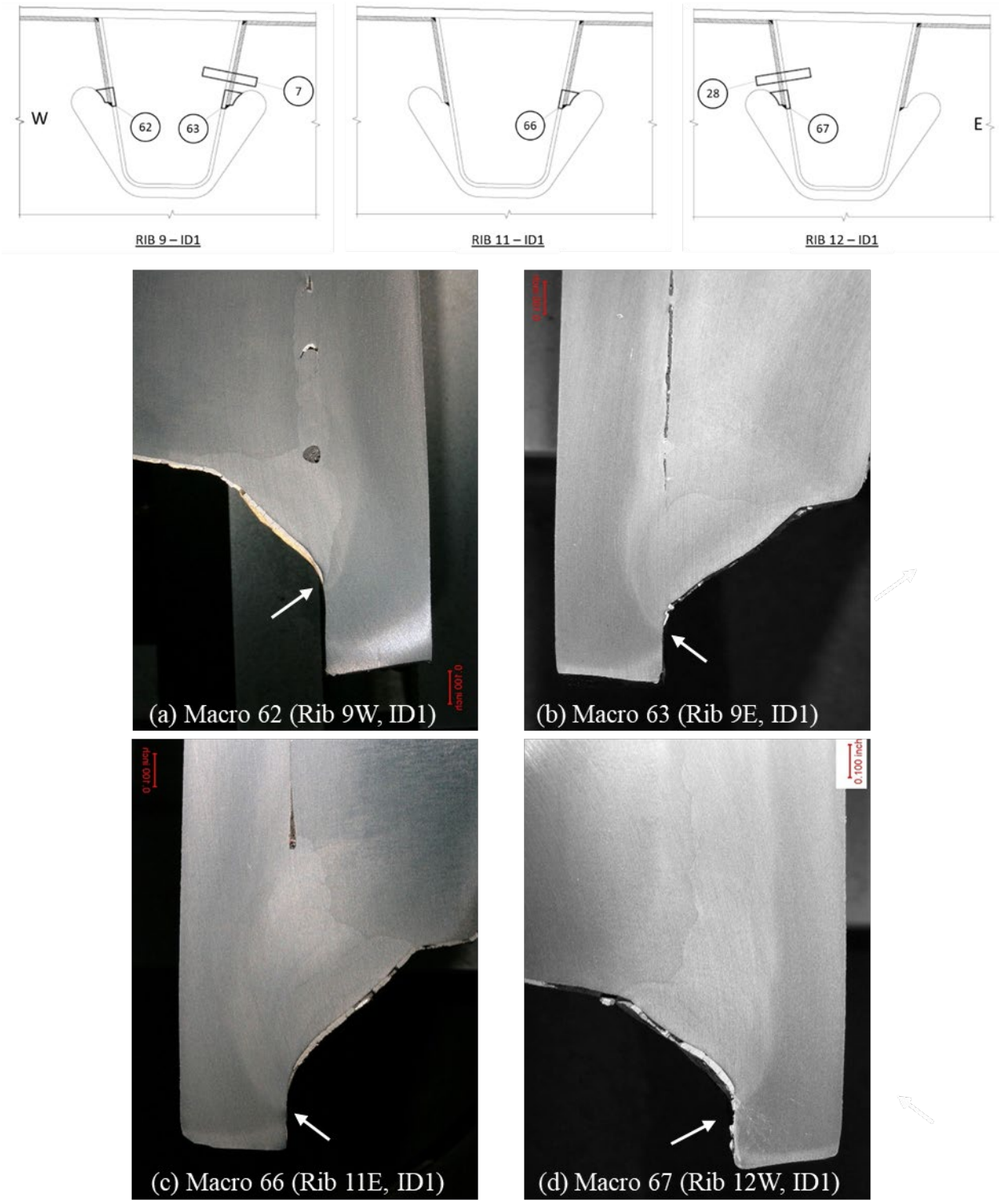

Figure 17. Type 1 macro-etch specimens at Rib 9W, 9E, 11E, and 12W (most highly stressed ribs) at Intermediate Diaphragm 1 of the full-scale prototype OSD test specimen

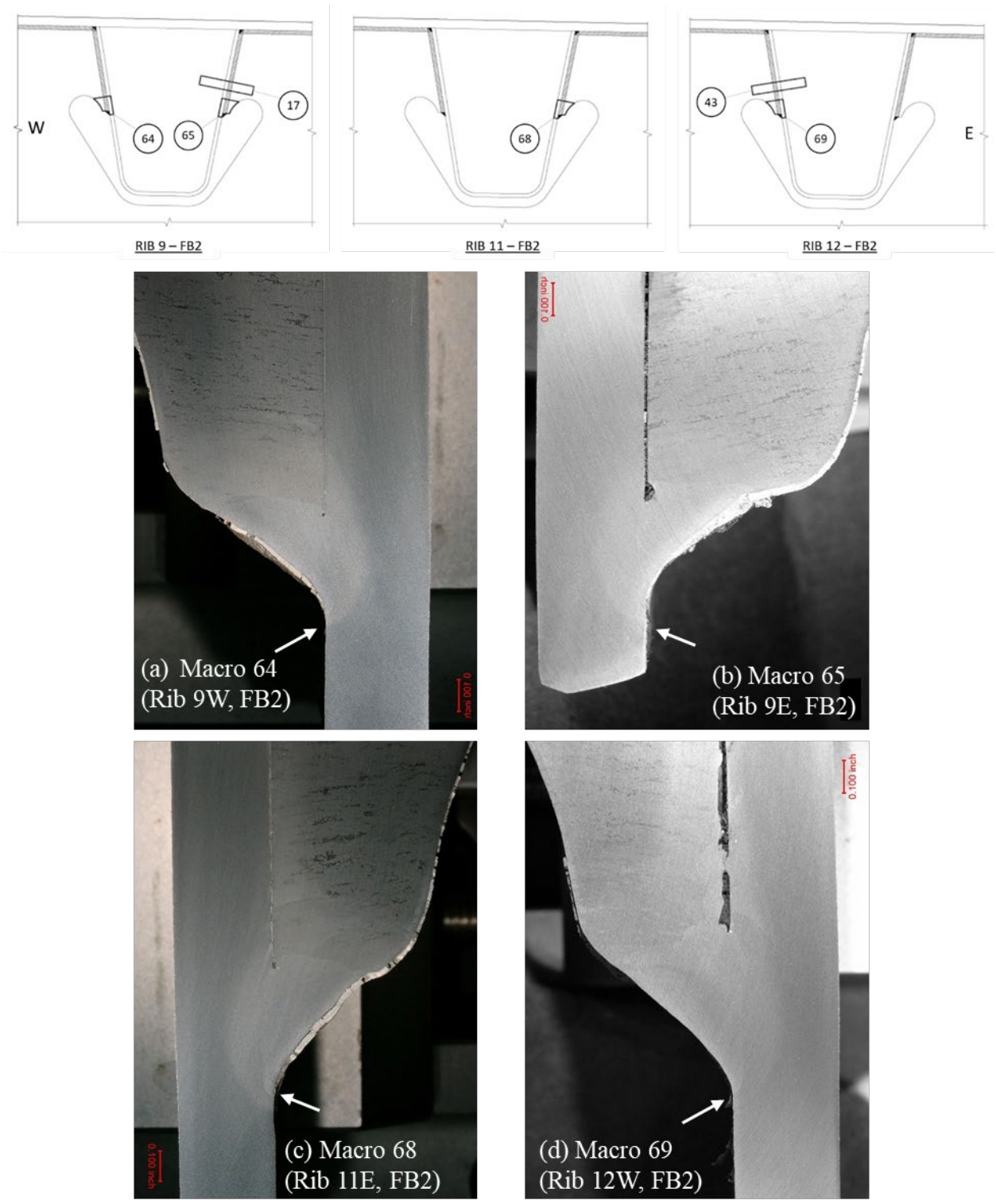

Figure 18. Type 1 macro-etch specimens at Ribs 9W, 9E, 11E, and 12W (most highly stressed ribs) at Floor Beam 2 of the full-scale prototype OSD test specimen

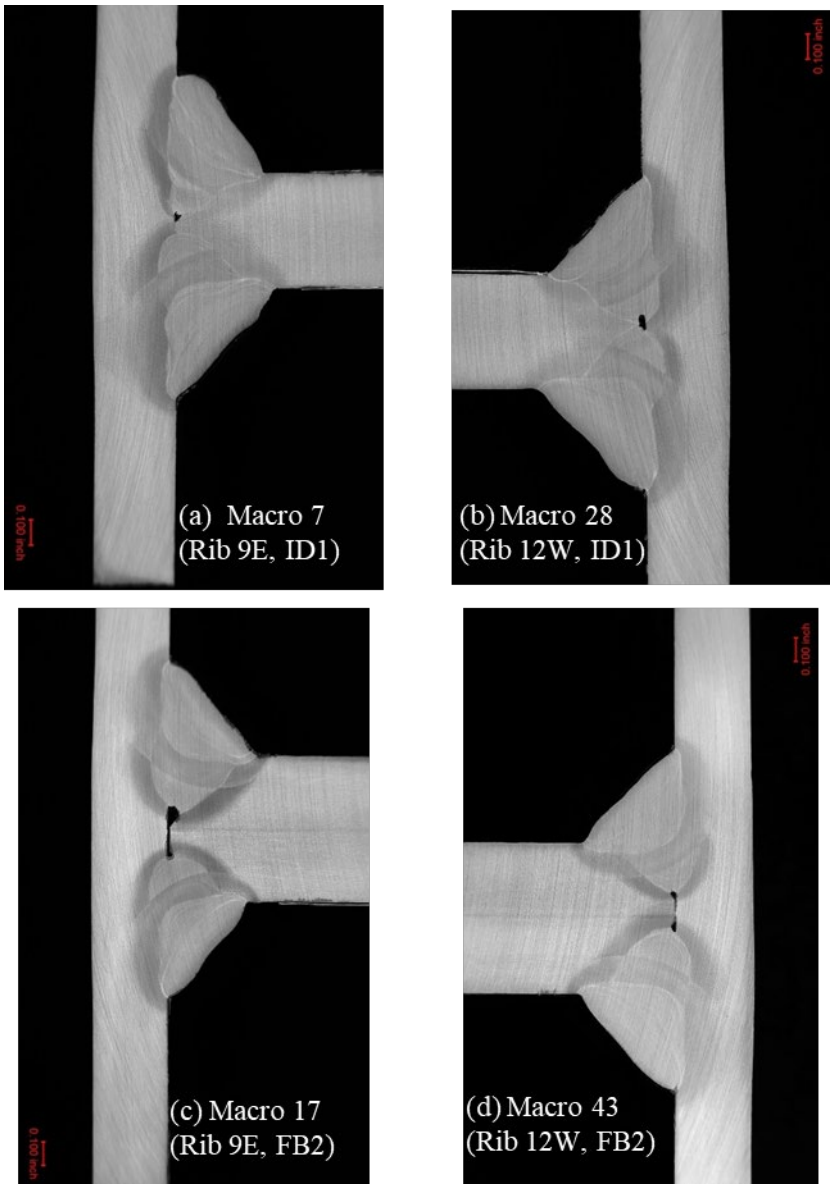

Figure 19. Type 2 macro-etch specimens at Rib 12W and 9E at Intermediate Diaphragm 1 and Floor Beam 2 of the full-scale prototype OSD test specimen

Weld Profiles

The profile of a fillet weld can have a significant effect on the weld toe fatigue strength. Characteristics of a fillet weld such as weld toe angle (weld face angle measured at the toe) and weld toe radius can affect the fatigue strength at the weld toe. Acceptable limits for weld toe angle and weld toe radius are not provided in either AWS D1.1[5] (AWS, 2015) or

[5] AWS D1.1 Structural Welding Code (2015) is incorporated by reference at 23 CFR 625.4(d)(2)(i).

AASHTO/AWS D1.5[6] (AASHTO/AWS, 2015). However, acceptable limits for weld toe angle and weld toe radius are provided in ISO 5817[7] (ISO, 2014) and ISO 6520[8] (ISO, 1998).

Table 6 shows the general limits on weld face angle at the weld toe for fillet welds. For welds subjected to fatigue stresses, limits for the toe radius are also provided, as shown in Table 7. The three quality levels shown, C63, B90, and B125, correspond to lower bound fatigue strength at 2 million cycles of 63 MPa (9.1 ksi), 90 MPa (13.1 ksi), and 125 MPa (18.1 ksi), respectively. For comparison, the lower bound fatigue strength at 2 million cycles for Fatigue Categories D, C and B in AASHTO LRFD BDS[1] are 71.2 MPa (10.3 ksi), 89.7 MPa (13.0 ksi) and 125 MPa (18.1 ksi), respectively. The fatigue strength of B90 effectively the same as AASHTO Fatigue Category C.

Note that for quality levels C63 and B90 a minimum weld toe radius is not provided. For the highest quality level, B125, a minimum weld toe radius of 4 mm (0.16 inches) is provided. The document notes that 4 mm is difficult to achieve without some form of weld toe preparation (e.g., peening or toe grinding).

Table 6. Minimum fillet weld face angle at the weld toe angle per ISO 5817[7] for various quality levels (B, C, and D)

Quality Level D	Quality Level C	Quality Level B
90 degrees	100 degrees	110 degrees

Table 7. Minimum for fillet weld toe radius and weld face angle per ISO 5817[7] for various quality levels for welds subjected to fatigue (B, C, and D)

Weld Profile Parameter	Quality Level C63	Quality Level B90	Quality Level B125
Weld Toe Radius	100 degrees	110 degrees	110 degrees
Weld Face Angle	Not defined	Not defined	4 mm

Measurement of weld face angle and weld toe radius is challenging. A methodology using weld profile data obtained from laser scanning is presented by (Renken, et al., 2021). Using this methodology, the measured profile of the weld around the toe is discretized and cubic splines are fit to the profile. The weld toe radius is determined at the point of maximum curvature. Best-fit lines on either side of the weld toe determine the weld face angle.

This approach was applied to the eight macro-etch specimens from the previous OSD fatigue testing. Digital images of the macro-etch specimens were discretized every 0.0125 inches to obtain the weld profile. Figure 20 shows the discretization of Macro 68 at Rib 11E/Floor Beam 2. Figure 21 shows a plot of the weld profile for this macro-etch specimen, the circle fit to the point of maximum curvature on the weld profile calculated using the approach developed by

[6] AASHTO/AWS D1.5 Bridge Welding Code (2015) is incorporated by reference at 23 CFR 625.4(d)(2)(iii).

[7] ISO 5817, Welding (2014) is not a Federal requirement.

[8] ISO 6520, Welding and allied processes (1998) is not a Federal requirement.

(Renken, et al., 2021). The OSD panel was coated with a primer only which is evident in the figure. The figure also shows the best-fit lines on either side of the weld toe.

This process was performed for each of the eight macro-etch specimens taken at the EC RFB connection wrap-around fillet weld. The results are summarized in Table 8. As shown, each weld meets the minimum weld toe angle of 110 degrees for quality level B125 in ISO 5817[7]. However, none of the locations meet the 4 mm minimum weld toe radius for quality level B125 (since weld toe preparation was not performed on the full-scale prototype OSD test specimen). The minimum radius was 0.04 inches (1 mm).

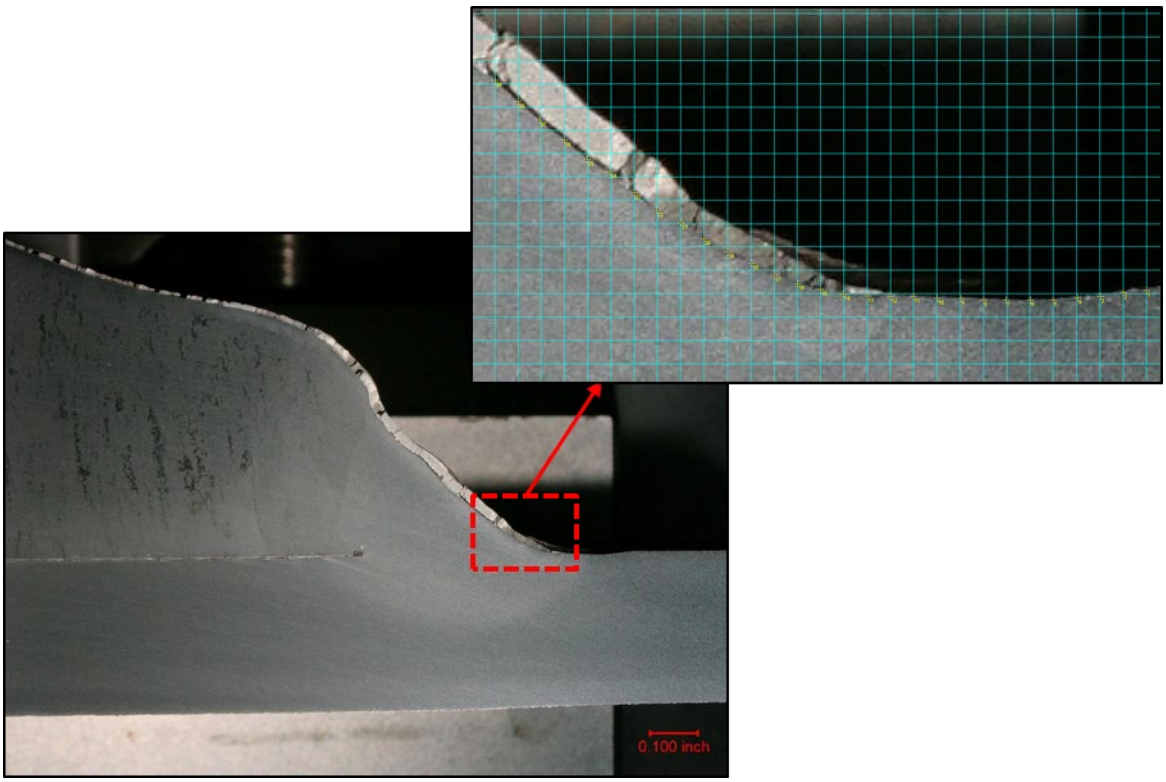

Figure 20. Macro 68 (Rib 11E, FB2) showing discretization used to measure the weld profiles of the full-scale prototype OSD test specimen

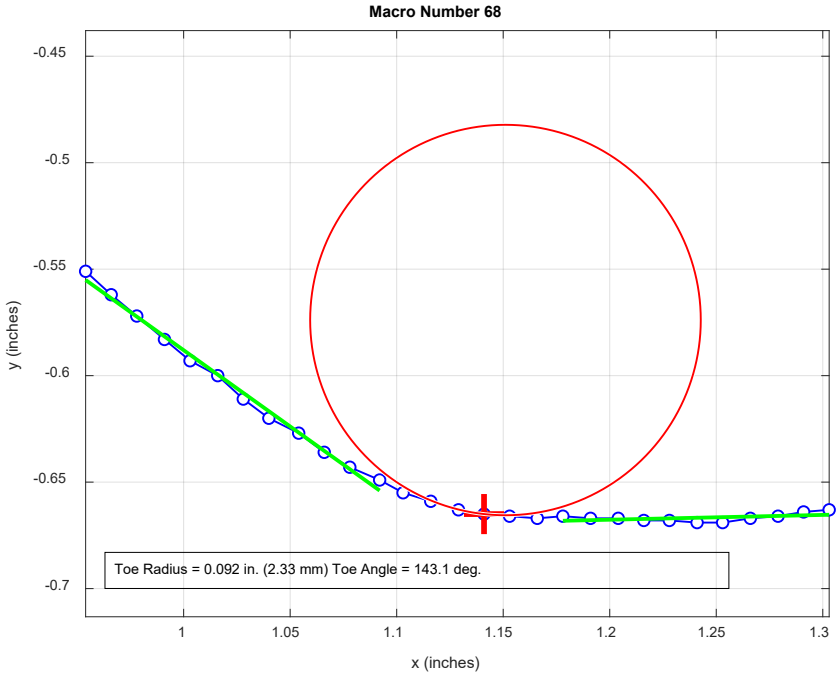

Figure 21. Macro 68 weld profile showing calculated minimum radius at the weld toe and weld toe angle

Table 8. Summary of measured weld toe radius and weld face angle from macro-etch specimens taken from the full-scale prototype OSD test specimen

Macro Number	Location	Weld Toe Radius (in)	Weld Toe Radius (mm)	Weld Face Angle (deg)
62	Rib 9W/ID1	0.0656	1.67	138
63	Rib 9E/ID1	0.0404	1.03	126
64	Rib 9W/FB2	0.0545	1.38	135
65	Rib 9E/FB2	0.0879	2.23	148
66	Rib 11E/ID1	0.1295	3.29	142
67	Rib 12W/ID1	0.0833	2.12	134
68	Rib 11E/FB2	0.0917	2.33	143
69	Rib 12W/FB2	0.0783	1.99	143

Measured Stresses

The full-scale prototype OSD test specimen was extensively instrumented to assess the behavior of the deck and to quantify the local strains that could cause fatigue crack initiation and propagation. At weld toe locations where fatigue cracking had the potential to develop, two uniaxial strain gages were installed at distances of 0.4 and 1.0 times the thickness of the plate to which the strain gage was mounted. The strain gages were oriented to measure strains perpendicular to the weld toe.

For the EC RFB connection, the critical fatigue cracking mode is weld toe cracking at the toe of the wrap-around fillet weld at the cut-out, initiated by vertical stresses in the rib wall. These cracks would be expected to initiate at the weld toe and propagate both inwards through the rib wall thickness and horizontally away from the floor beam web (or intermediate diaphragm).

At this critical location, due to the relatively small thickness of the rib wall (5/16 inches) the 0.4*t* distance is only 1/8 inch (where *t* is the thickness of the steel plate to which the gage is mounted). Accurately installing a small strain gage is challenging. Therefore, in these locations, 5-gauge co-linear strips were installed such that two of the gages could be located at the desired 0.4t and 1.0t locations. An example of a vertical strip gage installation at Rib 12E at Intermediate Diaphragm 1 is shown in Figure 22. Five strain gauges are present in the strip but only two were used.

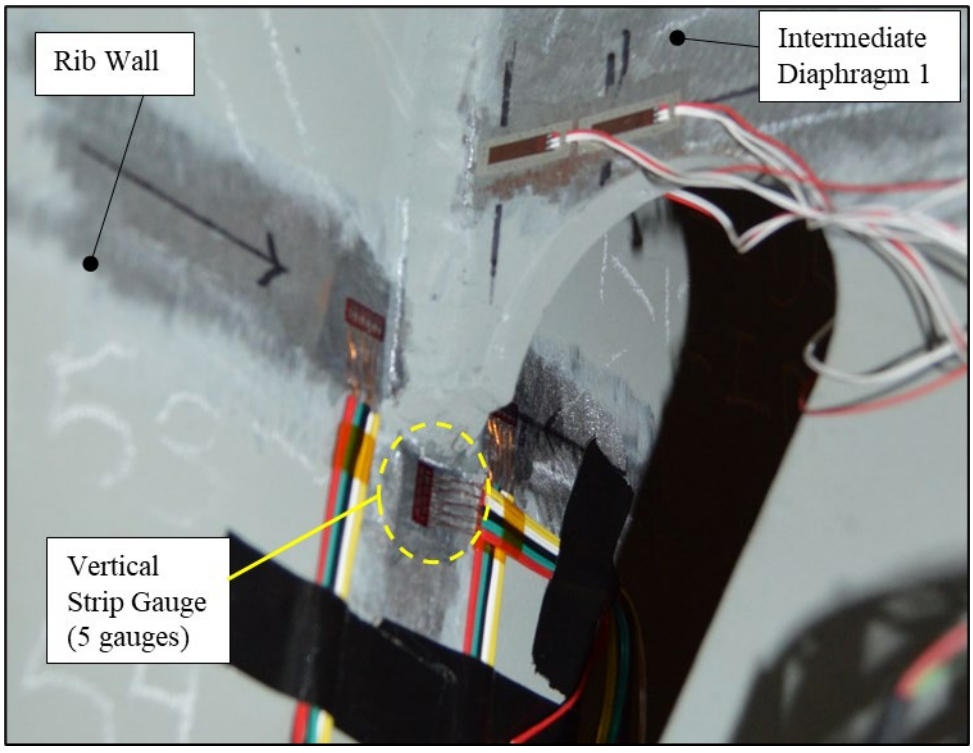

Figure 22. Vertical strain gauges (2 gauges in a strip of 5) installed at 0.4t and 1.0t from the weld toe at the wrap-around fillet weld at an EC RFB connection at Intermediate Diaphragm 1 (the same configuration was used at Floor Beam 2)

Given the measurements at the 0.4t and 1.0t locations, the LSS can be determined using linear extrapolation, as shown in Equation 1.

$$LSS = 1.67\sigma_{0.4t} - 0.67\sigma_{1.0t} \quad \text{(Eq. 1)}$$

A summary of the measurements at three highly stressed EC RFB connections at Floor Beam 2 is presented in Table 9. Strain measurements during testing were made using uniaxial strain gages normal to the weld toe. In the absence of measurements of the 2D state of strain, stresses can be estimated using the ratio of transverse to normal (to weld toe) strains, $^{\varepsilon_y}/_{\varepsilon_x}$, obtained from 3D FEA, using the following formula (Hobbacher, 2008):

$$\sigma = E\varepsilon_x \frac{1 + \nu\frac{\varepsilon_y}{\varepsilon_x}}{1 - \nu^2} \quad \text{(Eq. 2)}$$

The vertical measured strains centered on the floor beam web from static tests under loads at Actuator 3 and 4, and the corresponding ratios of strain from FEA, were used to estimate the stresses at distances of 0.4t and 1.0t from the weld toe, and the LSS. These results are shown in Table 9. As shown, the highest stresses at Ribs 9W, 11E, and 12W were produced under loading at Actuator 4. The highest LSS was 15.8 ksi at Rib 11E.

Table 9. Measured vertical rib wall stresses and LSS at the weld toe of the wrap-around fillet weld at the most highly stressed EC RFB connections at Floor Beam 2 under loads applied at Actuators 3 and 4

Rib	Actuator 3 0.4t (ksi)	Actuator 3 1.0t (ksi)	Actuator 3 LSS (ksi)	Actuator 4 0.4t (ksi)	Actuator 4 1.0t (ksi)	Actuator 4 LSS (ksi)
9W	6.22	5.12	6.94	8.78	7.12	9.89
9E	6.78	3.94	8.68	5.86	3.52	7.42
11E	4.75	2.12	6.50	11.32	4.58	15.81
12W	5.45	4.34	6.19	11.55	8.97	13.26

At Ribs 11E and 12W, the LSS measured during testing (over 13 ksi at one location) exceeded the CAFT for Fatigue Category C (equal to 10 ksi) though no cracks developed.

The stresses at Intermediate Diaphragm 1 were lower than those at Floor Beam 2. Therefore, this study is focused on the results from EC RFB connections at Floor Beam 2. It should be noted that at the four critical locations at Floor Beam 2, there was no reversal in the response during the loading sequence from Actuator 1 through 4. Therefore, the maximum stress produced by the four load applications represents the stress range for the sequence. Also, the stresses produced during the experiment at the four critical locations at Floor Beam 2 produced by Actuators 1 and 2 were always smaller than those produced by Actuators 3 and 4. Therefore the measured stresses during loading at Actuators 1 and 2 are not presented.

OBSERVATIONS

In the past, full-scale large-size fatigue testing of OSD prototypes has been used to validate the fatigue performance of a number of prototype OSDs under the fatigue limit state load (Fatigue I load case with 15% impact from AASHTO LRFD BDS[1] for OSDs). A number of these test programs were conducted at the ATLSS Center at Lehigh University. However, such testing is costly and needs a significant amount of time to plan and complete. The project schedule accounts for specimen design, fabrication, testing and assessment of the results. As a result, such test programs are only feasible for large redecking projects on major bridges for which the initial construction cost is high. Considering the enormous cost of potential fatigue cracking at details with thousands identical locations, such testing could be warranted for such bridges.

There are a number of advantages to performing such tests. First, the results of full-scale large-size fatigue test allow the fatigue resistance of proposed details to be assessed in the laboratory under realistic loading and boundary conditions. Configuration of an OSD test specimen with multiple rib spans and multiple panels better reflects the behavior of an OSD in service than small size test configurations. Furthermore, multiple detail types (e.g., RFB connection, rib-to-deck welds, deck-to-floor beam, and deck splice connections), variations in a given details (e.g., weld parameters or geometry), and multiple instances of the same detail can be evaluated in one specimen.

Second, trial fabrication of an OSD test specimen allows potential fabrication issues with proposed details to be identified. Modifications to the OSD details and/or construction specifications can be made based on the results of experience during fabrication, and/or based on the observations during fatigue testing.

With proper design, fabrication, and maintenance, OSDs are known to be capable of achieving a long service life of up to 100 years, far exceeding the typical useful life of a standard concrete bridge deck. Considering this, it would be advantageous to promote the use OSD on bridges of all sizes, and not limit their use to large span signature bridges. Clearly, full-scale large-size fatigue testing of protype decks is not feasible for most bridges. The objective of this research is to identify a range of global and local OSD characteristics within which acceptable fatigue performance could be expected, using the favorable results of fatigue testing of a single full-scale large-size OSD test specimen. These results will aid in development of robust OSDs for smaller bridges without the need for costly large-size fatigue tests.

Fatigue testing of smaller size test OSD test specimens may be warranted in cases where the fatigue resistance of certain OSD details is not well established. However, care should be taken in the development of the test specimen and setup to ensure that the stress conditions produced in the test specimen are representative of the in-situ stresses in the OSD. This can be aided through the use of FEA.

CHAPTER 4. FINITE ELEMENT ANALYSIS OF THE FULL-SCALE PROTOTYPE OSD TEST SPECIMEN

A 3D linear elastic FEA model of the full-scale prototype OSD test specimen described in Chapter 3 was developed using Abaqus, a commercially available software produced by Dassault Systèmes. This finite element model served as the base case for the sensitivity study models.

The 3D finite element mesh for each model and submodel was automatically generated by Abaqus given a target element size using a structured meshing algorithm. All models and submodels were meshed using a combination of elastic 3D continuum solid hexahedral elements and 3D shell elements. Each solid hexahedral element has twenty nodes, uses a second order interpolation function with reduced integration, and has three translational degrees of freedom (DOF) per node. This element type is identified as the C3D20R element in Abaqus. The entire OSD and the double angle connection to the supporting transverse truss were modeled using solid elements.

The remainder of the test specimen, including transverse trusses, longitudinal truss, and support columns, was modeled using shell elements. Each shell element has eight nodes, uses a second order interpolation function with reduced integration, and has 6 DOF per node. This element type is identified as the S8R element in Abaqus.

Linear elastic material properties for steel components were used. A modulus of elasticity of 29,000 ksi and Poisson's ratio of 0.3 were assumed.

The "submodeling" procedure in Abaqus was used to provide localized stresses at the RFB connections. Submodeling uses a more refined FEA model of a local region of a larger, coarser FEA model to generate more accurate localized stress results. The submodel with the more refined mesh is loaded using boundary displacements that are interpolated from the larger FEA model with the coarser mesh. The benefits of the submodeling technique are reduced modeling effort (i.e., by creating the refined mesh of only part of the larger model) and decreased computation time.

Two levels of submodeling were used in the base FEA model of the full-scale prototype OSD test specimen. The first model was the global model representing the entirety of the full-scale prototype OSD test specimen and related aspects of the test setup, and is denoted Model A (MA). MA is shown in Figure 23. The largest stresses measured during the testing occurred at Floor Beam 2. Therefore, the analyses focused on the stresses at the RFB connections of Floor Beam 2 (at Ribs 9, 11, and 12 below the wheel load patches) under loads applied separately by Actuator 3 and by Actuator 4, resulting in two load cases. The load magnitude is the fatigue limit-state tandem axle load for OSDs with 15% impact specified in AASHTO LRFD BDS[1], equal to 82.8 kips. The loading pads are shown in Figure 23. Note that load cases for Actuators 1 and 2 were not included since: (1) the measured responses at the critical EC RFB connections of Floor Beam 2 during loading by Actuators 1 and 2 were always lower than the responses during loading by Actuators 3 and 4; and (2) there was no reversal in the responses during the sequence of load applications from the four actuators. Therefore, the maximum stress produced by either Actuator

3 or 4 represents the stress range for the complete loading sequence from the four actuators (i.e., one load cycle).

For the OSD and double angle connections of MA, a target element size of 1 inch was assigned in Abaqus. The target element size for the trusses and support columns was 3 inches. The mesh of the transverse trusses, longitudinal trusses, and support columns in MA is shown in Figure 24. The gusset plates at Floor Beam 2 were included in the model. Batten plates between double channel flanges at the top and bottom chord were modeled using shell elements.

Figure 25 shows the MA mesh of the OSD and double angle connection between the OSD and top chord of the transverse truss. The ribs were spliced 2 ft. north of Floor Beam 2. As shown in Figure 25, the splice connections were included in MA as solid elements. Finally, Figure 26 shows the MA mesh of the floor beam/intermediate diaphragm web.

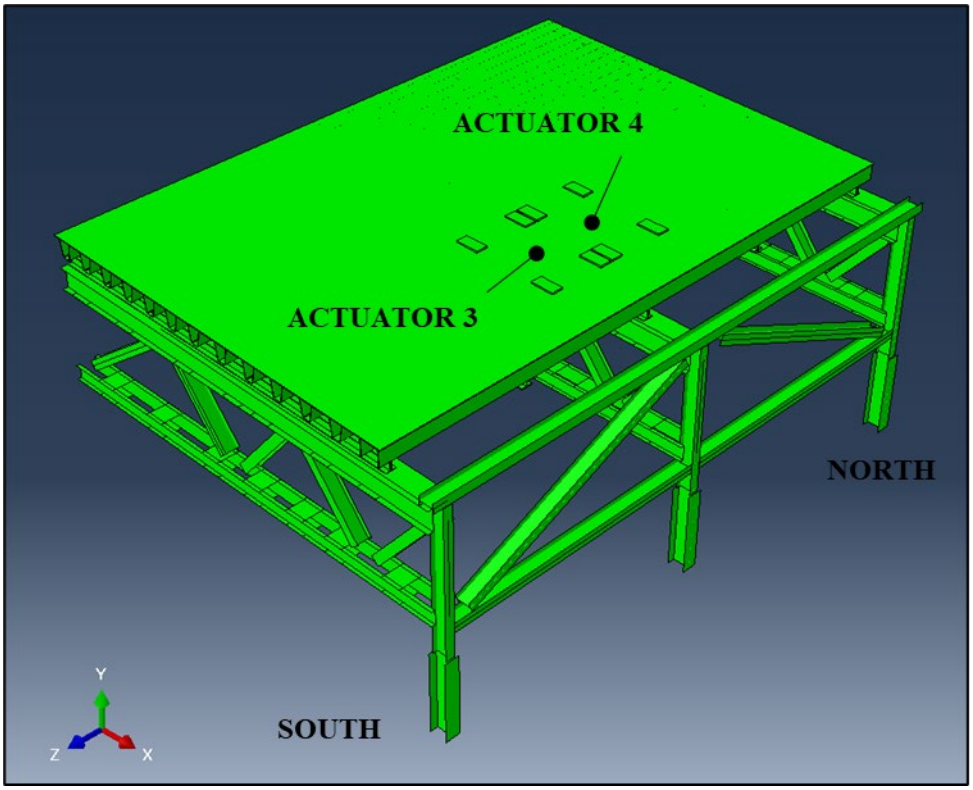

Figure 23. Model A (MA) geometry

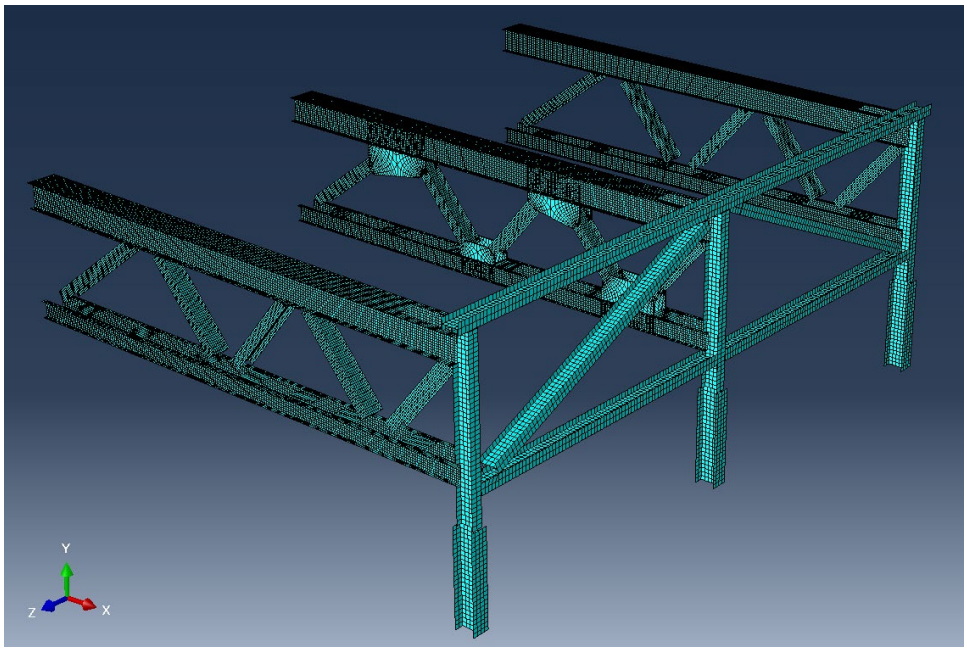

Figure 24. Model A (MA) – Shell element mesh of transverse trusses and longitudinal truss

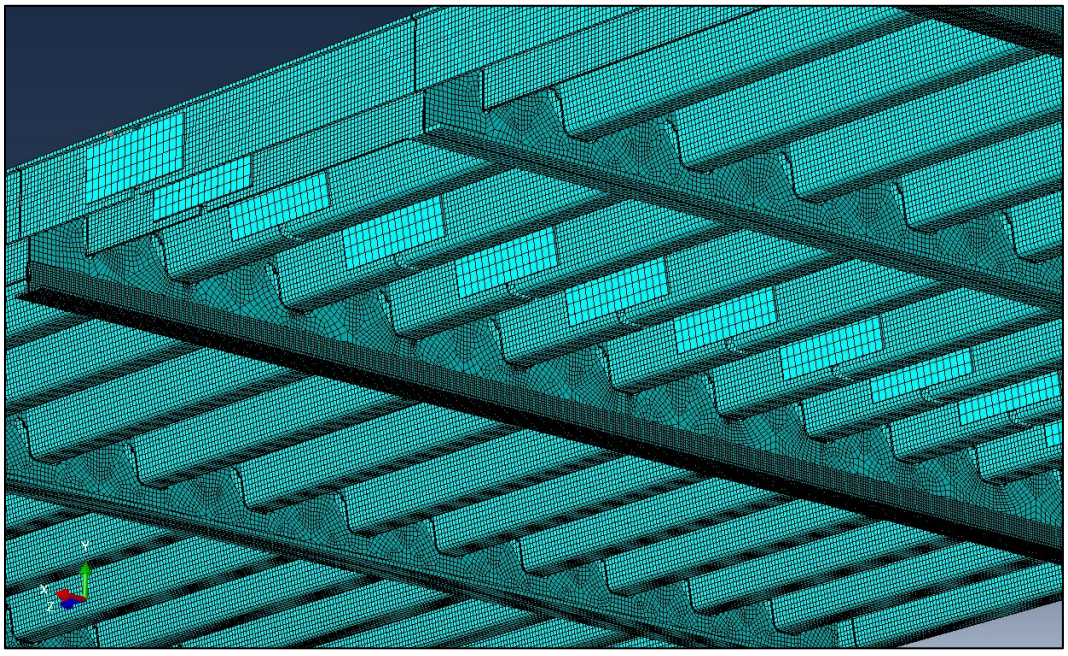

Figure 25. Model A (MA) – Solid element mesh of the OSD and the double angle connection to transverse truss

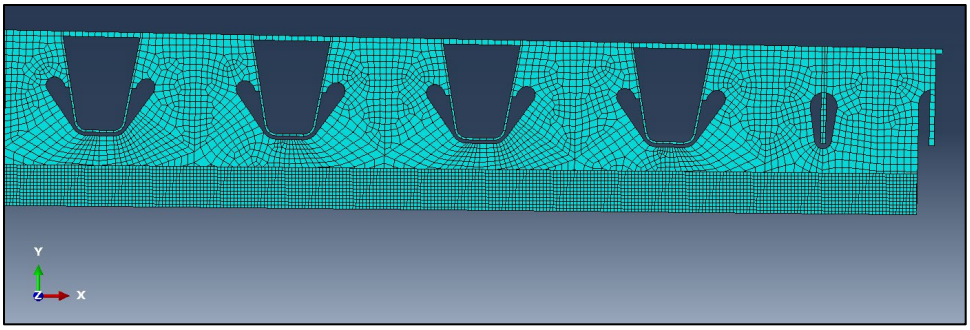

Figure 26. Model A (MA) – Solid element mesh of the floor beams/intermediate diaphragms around the EC RFB connections

A submodel of an EC RFB connection at Floor Beam 2 was prepared, termed Submodel B (SMB). The SMB mesh is shown in Figure 27. A target element size of 0.1 inches was assigned in Abaqus for regions around the RFB connection welds. Elsewhere, a target element size of 0.4 inches was used. In SMB, the rib extends 18 inches on either side of the floor beam web centerline. Transversely, SMB also includes 14 inches of floor beam web on either side of the rib centerline (half the center-to-center rib spacing of 28 inches). Vertically, the floor beam web extends below the rib to a point just above the top of the double angle connection. SMB does not include the deck plate since it is not of interest and its omission simplifies the submodel. The 5/16-inch reinforcing fillets of the RFB connection welds were explicitly modeled in SMB, including the wrap-around fillet weld at the bottom of the connection. A region of discontinuity was introduced into the mesh to represent the unfused strip between the floor beam web and rib wall. A detailed view of the SMB mesh at the wrap-around fillet and cut-out is shown in Figure 28. The boundaries of SMB that are driven by the displacements interpolated from the results of MA are modeled in Abaqus and are shown in Figure 29. The SMB model was analyzed three times. Each time the boundary displacements were interpolated from a different location within MA representing one of the EC RFB connections at three locations in Floor Beam 2, namely (1) Rib 9; (2) Rib 11; and (3) Rib 12. At each of these locations, the geometry of the EC RFB connection is identical. Therefore, the same submodel (SMB) can be used. For each of the three SMB locations, two load cases were analyzed (loading at Actuator 3 and loading at Actuator 4). The analyses focused on stresses at four critical locations, namely: (1) the west side of Rib 9 (R9W); (2) the east side of Rib 9 (R9E); the east side of Rib 11 (R11E); and the west side of Rib 12 (R12W).

Figure 30 presents a contour plot of the normal stresses in a direction in the plane of the rib wall and in a vertical plane (the 2 direction), for the RFB connection at Rib 12W under loading at Actuator 4. These stress results were obtained by transforming the stress results from global coordinates to local coordinates. In this local coordinate system, the 2 direction is normal to the wrap-around fillet weld toe and in the plane of the rib wall. The plot shows the concentration of vertical stress at the toe of the wrap-around fillet weld as expected.

Figure 31 and Figure 32 show plots of stresses normal to the wrap-around fillet weld toe versus distance to the weld toe, for loading at Actuator 3 and loading at Actuator 4, respectively. As shown, the stresses increase with decreasing distance to the weld toe.

Figure 33 and Figure 34 show the variation of the LSS along the horizontal weld toe from FEA (from south to north), for loading at Actuator 3 and at Actuator 4, respectively. As shown, with the load pad centered over the floor beam (Actuator 3), the variation is lower than with the load at Actuator 4. The stresses are slightly higher to the south end of the weld. For loading at Actuator 4, there is more variation with higher stresses to the north. Strain measurements in the laboratory were made at the centerline of the floor beam web (a distance of 0.3125 inch in Figure 33 and Figure 34).

The LSS from FEA can be calculated from these results through linear extrapolation of the stress at distances of 0.4 times the rib wall thickness (equal to 1/8 inch) and 1.0 times the rib wall thickness (equal to 5/16 inch) away from the weld toe. These results are shown in Table 10.

A comparison of the LSS from FEA with the LSS from strain measurements shows that there is reasonable agreement at Rib 12W, with an 2.6% difference (LSS Diff shown in Table 11). There is a large difference at Rib 11E which had a large value of the LSS from strain measurements, equal to 15.81 ksi (compared to the LSS from FEA equal to 13.36 ksi); however, the measured strain at 1.0t was significantly less than the strain at 0.4t, which led to a large value of the LSS (from extrapolating the corresponding stresses). This large LSS difference was not observed at the other locations. The reason for this discrepancy is not clear. However, it is believed that the FEA submodel (SMB) was sufficiently refined (with sufficiently small elements) to capture the complex stress conditions around the EC RFB connection. The FEA submodel SMB presented here was used in the sensitivity study phase of this research to identify the critical variables and qualitatively determine the range of applicability of the cost-effective EC RFB connection for OSDs.

At the other locations, the stresses were lower, but the differences between measured and FEA stresses were higher, with a maximum difference of 30% at Rib 9E. The reason for the difference is not clear. Various refinements to the global model MA were made, including addition of the rib splices, gusset plates and double-channel top chord diaphragms at Floor Beam 2. Some improvement was achieved, though discrepancy still exists. It is recognized that some of the discrepancy may be the result of variations in the physical tests setup from the configuration assumed in the analysis. Some of these discrepancies include the positioning of the loading pads, the distribution of contact stresses between the loading pads and deck plate (uniform load is applied to rubber pads in the FEA model), variations in the rib wall thickness from the thickness of 5/16 inch, unequal distribution of actuator load to the four load pads, and positioning of the strain gages at the weld toe.

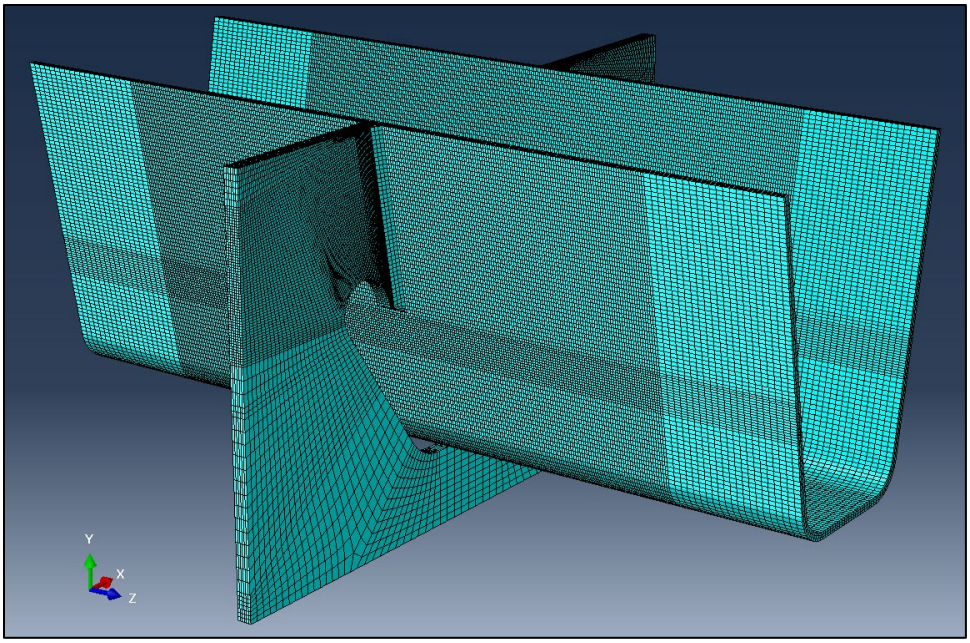

Figure 27. Submodel B (SMB) - Solid element mesh of EC RFB connection at Floor Beam 2

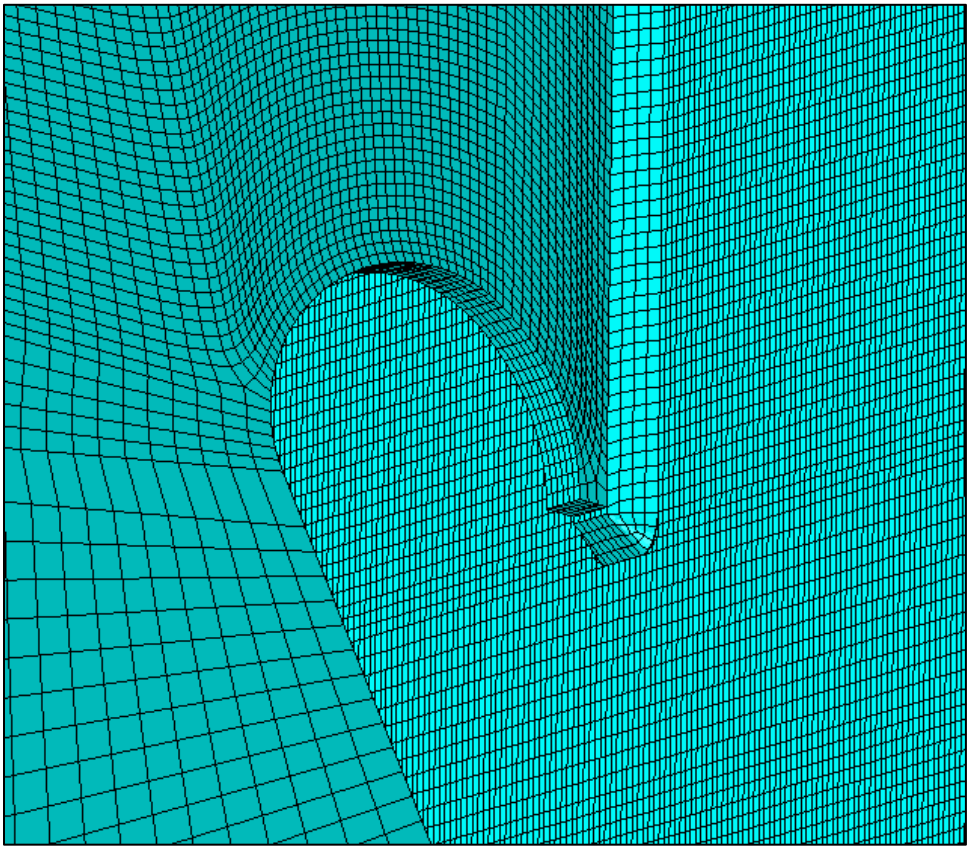

Figure 28. Submodel B (SMB) – Detail of solid element mesh at wrap-around fillet weld of EC RFB connection

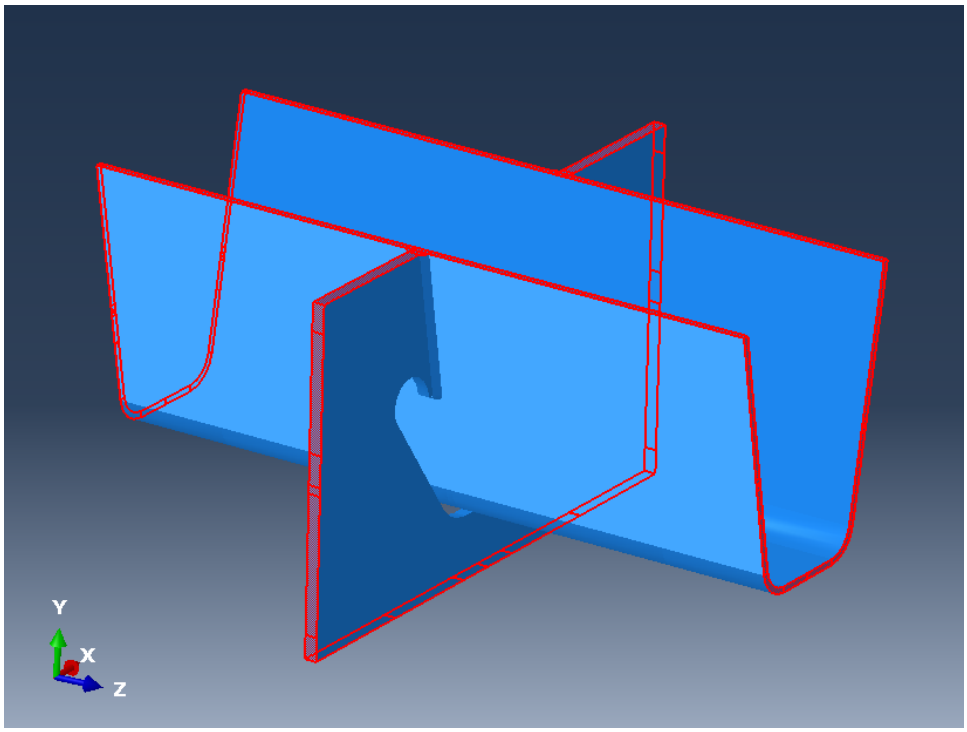

Figure 29. Submodel B (SMB) – Boundaries (highlighted in red) driven by interpolated displacements from MA analysis

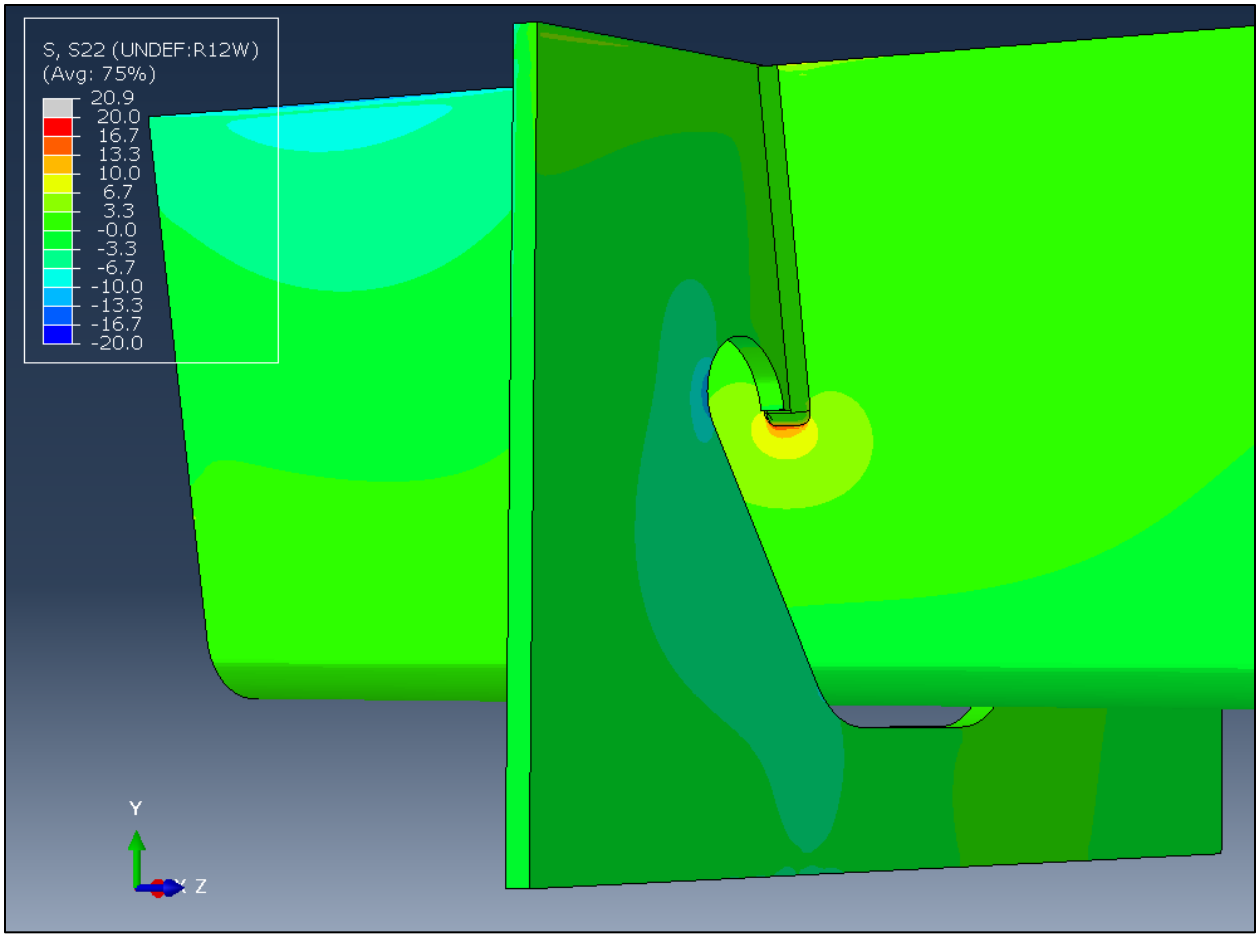

Figure 30. Submodel B (SMB) – Contour plot of normal stress, S22 (vertical on face of rib side wall, in ksi) at the west side of Rib 12 (R12W) under loading at Actuator 4

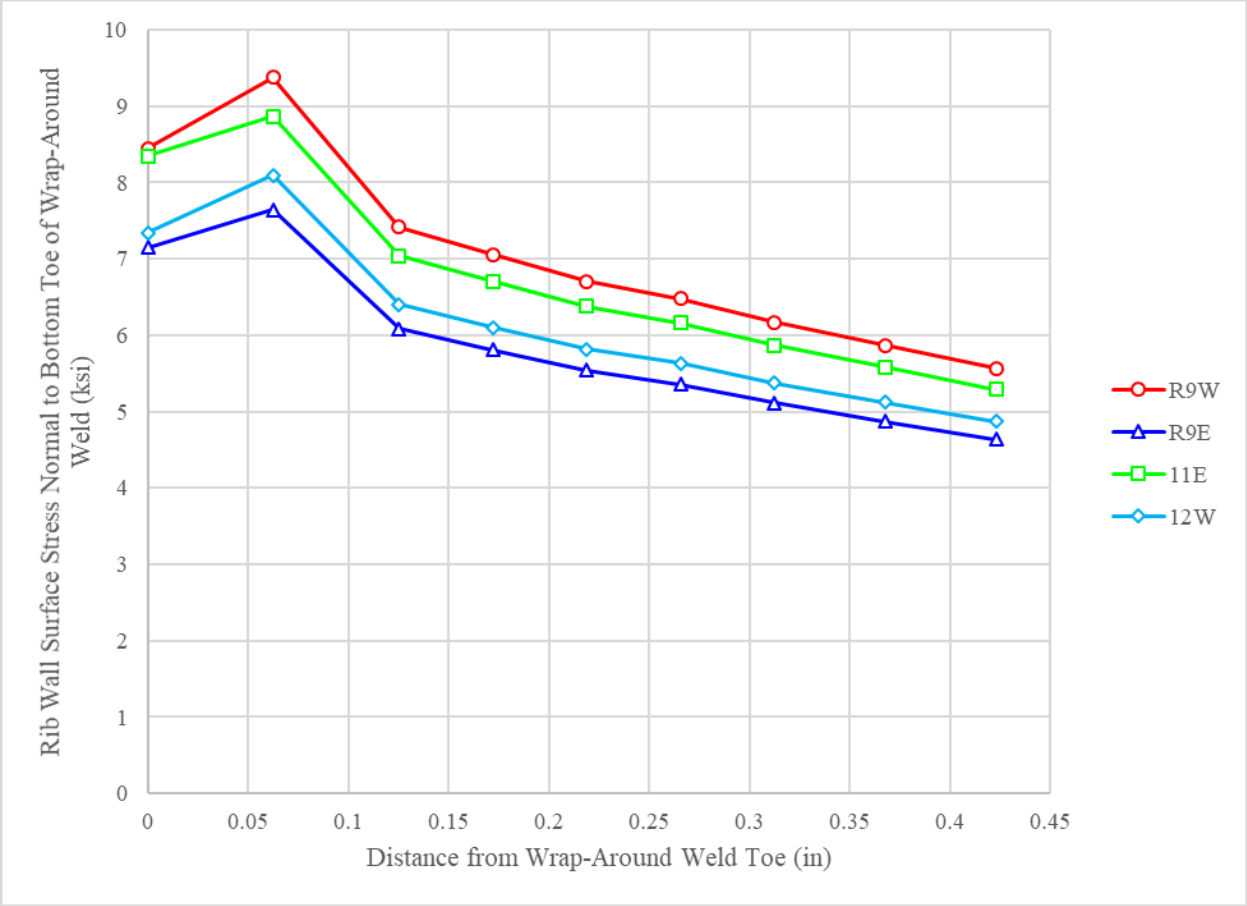

Figure 31. Plot of rib wall surface stress at center of floor beam web normal to wrap-around fillet weld toe versus normal distance from the bottom of the wrap-around fillet weld toe at four EC RFB connections under loading applied at Actuator 3

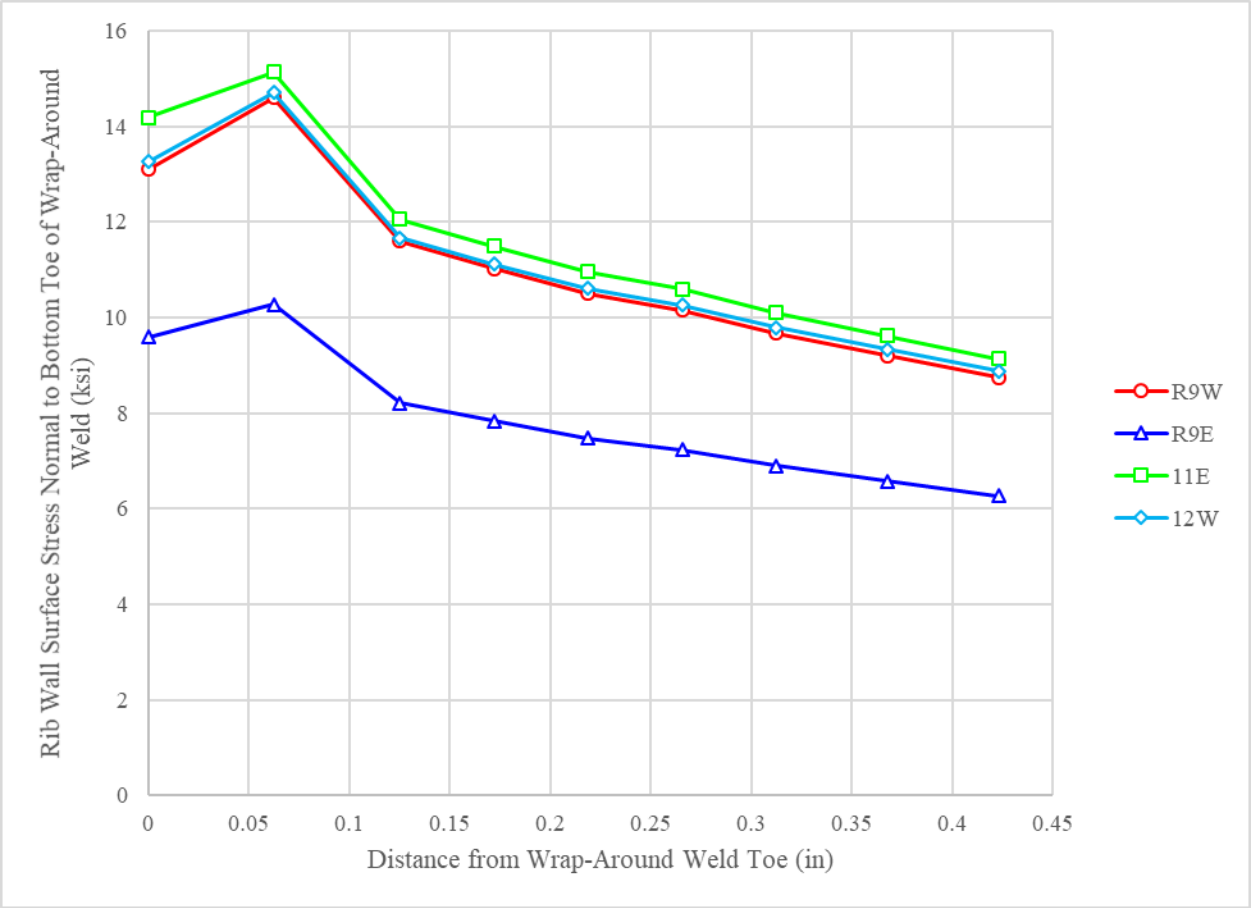

Figure 32. Plot of rib wall surface stress at center of floor beam web normal to wrap-around fillet weld toe versus normal distance from the bottom of the wrap-around fillet weld toe at four EC RFB connections under loading applied at Actuator 4

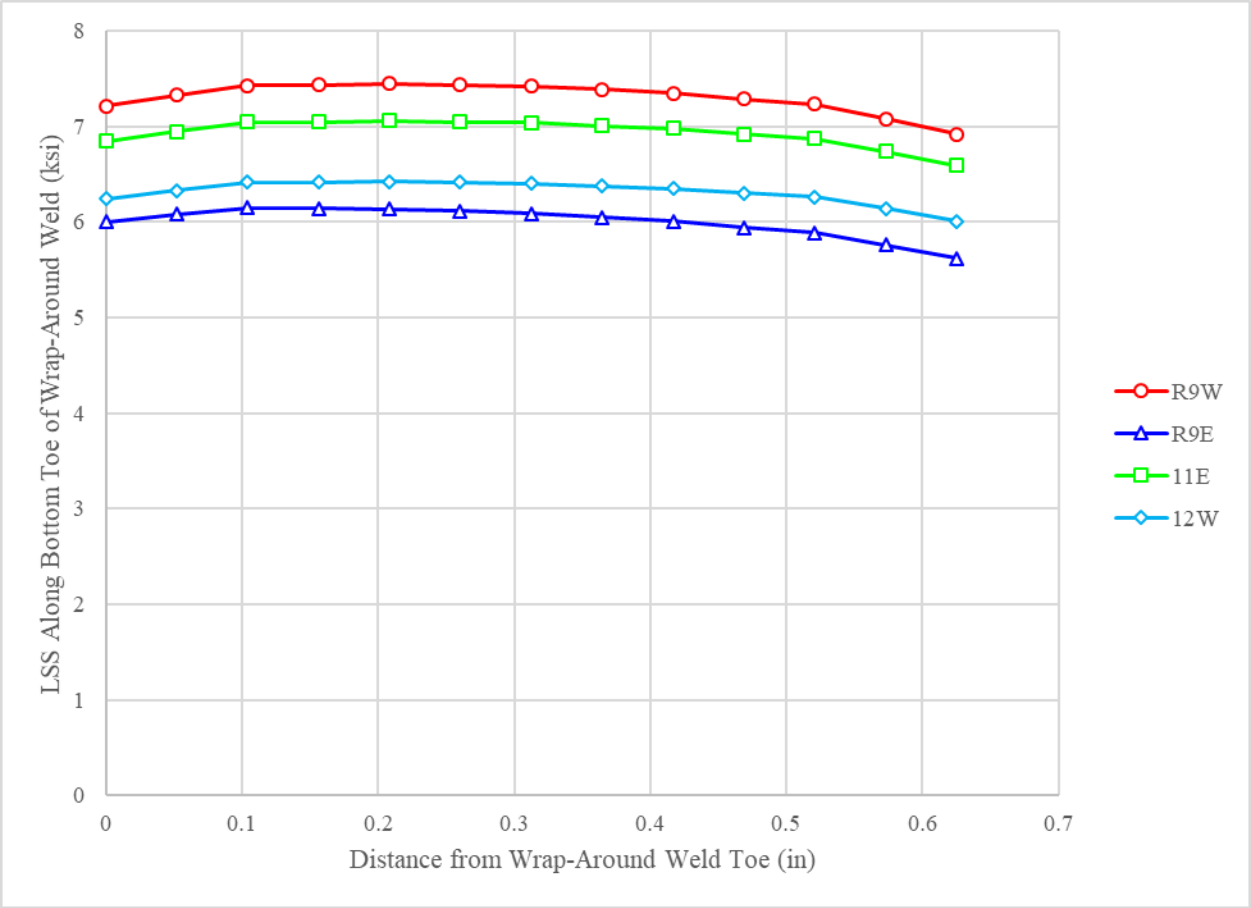

Figure 33. Plot of LSS along wrap-around fillet weld toe at four EC RFB connections under loading applied at Actuator 3

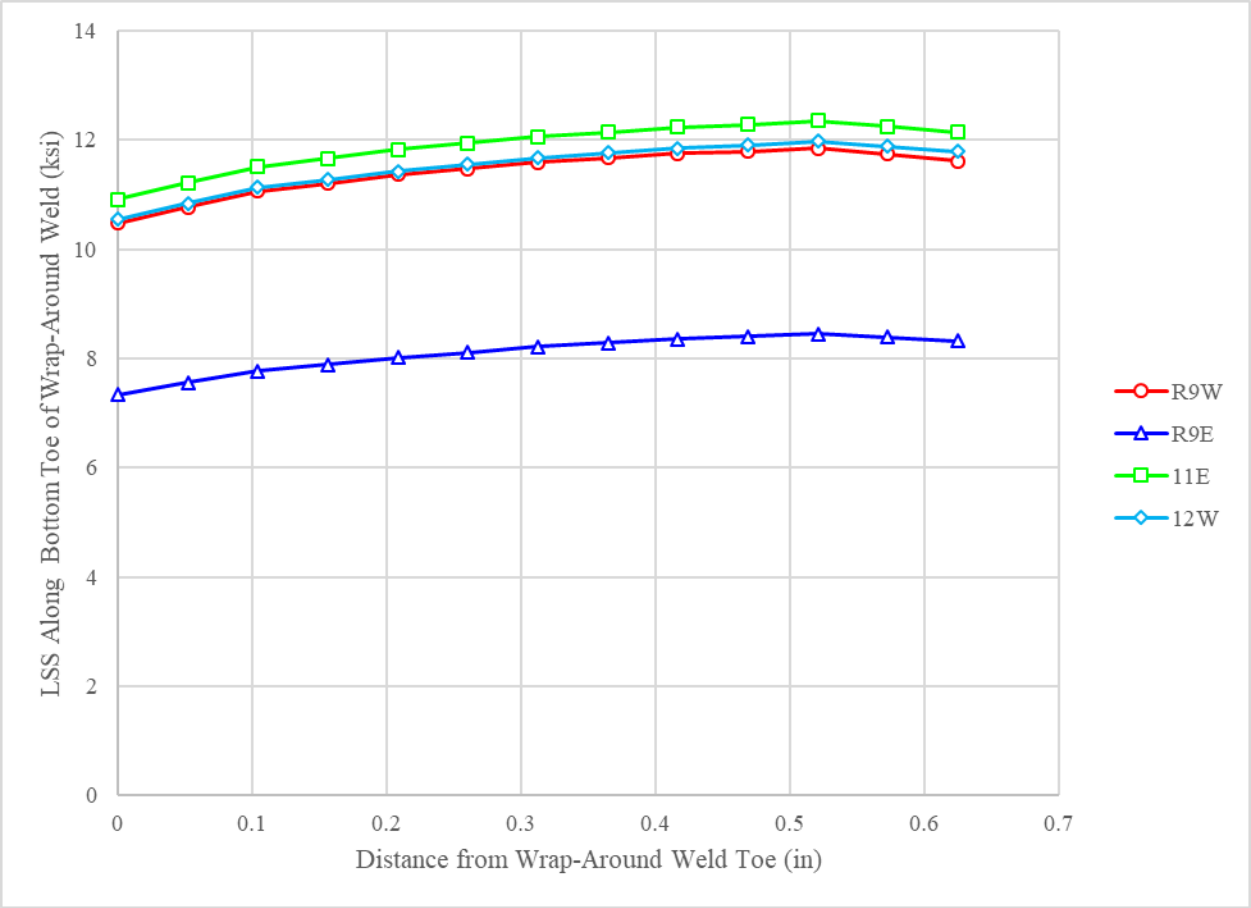

Figure 34. Plot of LSS along wrap-around fillet weld toe at four EC RFB connections under loading applied at Actuator 4

Table 10. Vertical rib wall stresses and LSS from FEA at the weld toe of the wrap-around fillet weld at the most highly stressed EC RFB connections at Floor Beam 2 under loading applied at Actuator 3 and Actuator 4

Rib	Actuator 3 0.4t (ksi)	Actuator 3 1.0t (ksi)	Actuator 3 LSS (ksi)	Actuator 4 0.4t (ksi)	Actuator 4 1.0t (ksi)	Actuator 4 LSS (ksi)
9W	7.42	6.17	8.25	11.59	9.67	12.87
9E	6.09	5.11	6.74	8.21	6.90	9.08
11E	7.04	5.87	7.81	12.06	10.10	13.36
12W	6.40	5.37	7.09	11.67	9.80	12.92

Table 11. Differences in LSS from FEA and LSS from strain measurements at the weld toe of the wrap-around fillet weld at the most highly stressed EC RFB connections at Floor Beam 2 under loading applied at Actuator 3 and Actuator 4: (LSS Diff) = ((LSS from FEA) – (LSS from measurements))/(LSS from measurements)

Rib	LSS Diff for Actuator 3 Loading (%)	LSS Diff for Actuator 4 Loading (%)
9W	18.8	30.1
9E	-22.4	22.4
11E	20.2	-15.5
12W	14.6	-2.6

CHAPTER 5. SENSITIVITY STUDY MATRIX

INTRODUCTION

The results of the literature review and survey of industry practice established a range of parameters typical of OSDs for highway bridges in the United States and worldwide. To study the conditions under which it would be appropriate to use this EC RFB connection with wrap-around reinforcing fillet welds (i.e., conditions when adequate fatigue performance can be expected), a sensitivity study using FEA was performed. In preparation for this study, the critical parameters were identified and are summarized in this section of the report. A number of parameters were deemed to be unimportant and are therefore not included in the study. A summary of the finite element models used to assess the sensitivity of the expected fatigue performance to variations in the key variables of a given OSD configuration is presented.

The OSD variables are categorized as either global or local variables. Global variables are those which concern the large-scale dimensions of the OSD and affect the nominal member responses of the OSD and bridge superstructure. Some examples are rib span (or floor beam spacing) and floor beam stiffness.

Local variables are those which affect the local RFB connection stresses and have limited effect on the nominal member responses of the OSD and bridge superstructure. Some examples are welding detail (e.g., PJP vs. fillet) and cut-out geometry.

It should be noted that variables deemed important are those which significantly affect the behavior of OSDs with closed ribs and EC RFB connections, the focus of this research study.

GLOBAL VARIABLES

The global OSD variables assessed in the sensitivity study are described in this section.

Transverse Support System Stiffness

Previous research found that weld toe stresses would be above allowable limits for an OSD with EC RFB connection in a new-construction application (Saunders, et al., 2019). In this context, a new-construction application refers to an OSD with integral floor beams which are typically comprised of a web and bottom flange. For this application, the researchers suggested using a fully-fitted RFB connection, without the extended cut-out beneath the rib.

The primary purpose of the extended cut-out is to introduce flexibility at the RFB connection when vehicle loads are between floor beams. This loading condition produces rib end rotation at the floor beam, which results in out-of-plane bending of the floor beam web. An EC RFB connection offers reduced restraint to the end rotation of the rib and therefore lower stresses compared to a fully fitted RFB connection.

OSDs used for redecking applications on existing bridges are typically supported on existing deep transverse members (e.g., floor beams or floor trusses) which provide significant restraint to rib end rotation. Additionally, the depth of the OSD floor beam above the existing transverse

member is typically limited to maintain existing roadway elevations (the removed bridge deck is typically a concrete slab on steel stringers). In these redecking applications, OSDs have been commonly detailed with EC RFB connections in order to avoid high out-of-plane stresses resulting from the high degree of restraint from the supporting superstructure and the relatively shallow and stiff OSD floor beam.

As discussed in Chapter 3, the full-scale prototype OSD test specimen replicated a portion of the steel superstructure of a long-span suspension bridge carrying six lanes of traffic. The transverse floor trusses of the bridge span nearly 100 ft. and are spaced at 19 ft. 9 inches, which is the span of the OSD rib (there are intermediate diaphragms but they are unsupported at their ends and therefore do not reduce the rib span). This span is near the suggested limit of 20 ft. for rib span outlined in the FHWA OSD manual (Connor et al., 2012). Considering the good performance of the full-scale prototype OSD test specimen at this long rib span, and that such long rib spans are often needed in redecking applications where the EC RFB connection is most applicable, the rib span is not included as a variable in the sensitivity study. All sensitivity study cases had the rib span of 19 ft. 9 inches used in the full-scale fatigue test program.

It is expected that the stiffness of the transverse floor beam or floor truss may vary from bridge to bridge. Therefore, the stiffness of the transverse floor beam was considered in the sensitivity study. Two cases were considered. The first case is the stiffness of the transverse truss of the full-scale prototype test specimen. The second case represents a transverse truss with the same geometry but half of the stiffness, achieved by reducing the elastic modulus of the transverse truss elements.

Rib Cross-Section

Closed-rib OSDs in the United States have been designed with both trapezoidal and round bottom ribs, though the trapezoidal ribs are more common. The cross-section shape can affect both the global and local OSD stresses under live loading. There may be fabrication considerations in the selection of the rib cross-section. Considering these factors, the rib-cross section geometry was included in the sensitivity study. One trapezoidal rib cross-section and one round bottom rib cross-section were considered.

Deck Plate Thickness

The deck plate thickness is a critical parameter affecting the fatigue performance of the rib-to-deck plate connection. To a lesser degree, the deck plate thickness can also affect the performance of the RFB connection and therefore this variable was included in the sensitivity study.

Attempts to optimize the design of early OSDs led to thin deck plates, but in many cases, this resulted in longitudinal fatigue cracking in the deck plate and overlay at the rib-to-deck welds.

The full-scale prototype OSD test specimen had a deck plate thickness of 3/4 inch. OSDs with a deck plate thickness of 5/8 inch have exhibited good performance in service to date. Additionally, the FHWA OSD manual suggests a minimum deck plate thickness of 5/8 inch. Therefore, the sensitivity study included two deck plate thickness, namely 5/8 inch and 3/4 inch.

Analysis Matrix

A total of three global variables were considered in the sensitivity study. For each combination of variables, a global model (MA) was created encompassing the entire full-scale prototype OSD test specimen (three transverse trusses, two OSD rib spans, and 14 ribs). The local response of each global model at the RFB connections was assessed using local submodels (SMB) at Ribs 9, 11, and 12. Table 12 presents a summary of the 8 cases analyzed for the global variable sensitivity study.

Table 12. List of analysis cases to evaluate sensitivity of global variables for OSDs with EC RFB connections (Note: tested configuration is Case GV1)

Case Name	Rib Cross-Section	Transverse Truss Stiffness (w.r.t. original)	Deck Plate Thickness (inches)	Global Model Name	Submodel Names
GV1	Trapezoidal	x 1.0	3/4	GV1MA	GV1SMBR9 GV1SMBR11 GV1SMBR12
GV2	Trapezoidal	x 1.0	5/8	GV2MA	GV2SMBR9 GV2SMBR11 GV2SMBR12
GV3	Trapezoidal	x 0.5	3/4	GV3MA	GV3SMBR9 GV3SMBR11 GV3SMBR12
GV4	Trapezoidal	x 0.5	5/8	GV4MA	GV4SMBR9 GV4SMBR11 GV4SMBR12
GV5	Round	x 1.0	3/4	GV5MA	GV5SMBR9 GV5SMBR11 GV5SMBR12
GV6	Round	x 1.0	5/8	GV6MA	GV6SMBR9 GV6SMBR11 GV6SMBR12
GV7	Round	x 0.5	3/4	GV7MA	GV7SMBR9 GV7SMBR11 GV7SMBR12
GV8	Round	x 0.5	5/8	GV8MA	GV8SMBR9 GV8SMBR11 GV8SMBR12

LOCAL VARIABLES

The local variables considered in the sensitivity study are described in this section.

RFB Connection Weld Length

The vertical length of the weld on the rib wall can have a significant effect on the stiffness of an EC RFB connection and on the stresses at the weld toes of the wrap-around fillet welds at the cut-out (and weld) termination on the rib wall. Intuitively, as the length of the weld becomes shorter, the vertical shear stress in the weld increases. Decreasing the length of the weld also increases the flexibility of the rib wall which affects the local stress. arious bridge design provisions suggest a minimum ratio of unwelded height of the rib, *c*, to the total rib depth, *h*, though these limitations vary.

In AASHTO LRFD BDS[1] (AASHTO, 2020), the *c*/*h* ratio is suggested to be greater than 1/3 (see Figure 4). In Eurocode 3[2], the *c*/*h* ratio is suggested to be greater than 0.15 for highway bridges (see Figure 5), and 1/3 for railway bridges (see Figure 6) (European Committee for Standardisation, 2006).

The *c*/*h* ratio for the full-scale prototype OSD test specimen was 0.46. EC RFB connections with *c/h* ratios of 0.60, 0.46, and 0.33 were included in the sensitivity study to cover a range of ratios within existing bridge design provisions.

Cut-out Geometry

Three general classes of EC RFB connection were previously identified, namely Type 1, 2, and 3, as shown in Figure 1, Figure 2, and Figure 3, respectively. A Type 2 connection features a CJP weld that is ground smooth. Though such a connection would be expected to exhibit adequate fatigue performance, this detail is not as efficient to fabricate as Types 1 and 3. Therefore, the Type 2 connection was not considered in the sensitivity study.

As shown in Figure 1, a Type 1 EC RFB connection has a cut-out geometry with a cut-out edge that terminates tangentially to the rib wall with a weld tab. The fillet or PJP connection weld wraps around the weld termination (through the cut-out). The full-scale prototype OSD test specimen featured Type 1 EC RFB connections that are the focus of this research.

As shown in Figure 3, a Type 3 EC RFB connection features a cut-out geometry with a cut-out edge which terminates perpendicularly to the rib wall. The fillet or PJP connection weld wraps around the weld termination (through the cut-out).

Analysis Matrix

A total of two local variables were considered in the sensitivity study, namely the RFB connection weld length (3 variations) and the cut-out geometry (2 variations). For each combination of these local variables, two global variables were considered, namely the transverse truss stiffness and rib cross-section. For each combination of local and global variables, a global and corresponding submodels were created.

New global models (MA) and submodels (SMB) were created for each combination of local variables and were analyzed at Ribs 9, 11, and 12, as indicated in Table 13. Analysis cases LV1 through LV4 were previously performed in the global variable sensitivity analyses. The boundary displacements for each case were obtained from global models (MA) and applied to the corresponding submodel (SMB) boundaries at Ribs 9, 11, and 12. As shown, a total of 12 cases were considered.

Two other local variables which are believed to have an important effect on the fatigue performance of the EC RFB connection are the profile of the wrap-around fillet weld, and the depth of penetration along the weld (i.e., PJP vs. fillet welds). These variables were assessed through separate FEA studies as described in the next sections.

Table 13. List of analysis cases to evaluate sensitivity of local variables for OSDs with EC RFB connections (Note: tested configuration is Case LV1; Cases LV2-4 completed in the Global Variable study)

Case Name	RFB Connection Weld Length *c/h*	Cut-Out Geometry	Rib Cross-Section	Transverse Truss Stiffness (w.r.t. original)	Global Model Name	Submodel Names
LV1	0.46	Type 1	Trapezoidal	1.0x	GV1MA	GV1SMBR9 GV1SMBR11 GV1SMBR12
LV2	0.46	Type 1	Trapezoidal	0.5x	GV3MA	GV3SMBR9 GV3SMBR11 GV3SMBR12
LV3	0.46	Type 1	Round	1.0x	GV5MA	GV5SMBR9 GV5SMBR11 GV5SMBR12
LV4	0.46	Type 1	Round	0.5x	GV7MA	GV7SMBR9 GV7SMBR11 GV7SMBR12
LV5	0.46	Type 3	Trapezoidal	1.0x	LV5MA	LV5SMBR9 LV5SMBR11 LV5SMBR12
LV6	0.46	Type 3	Round	1.0x	LV6MA	LV6SMBR9 LV6SMBR11 LV6SMBR12
LV7	0.33	Type 1	Trapezoidal	1.0x	LV7MA	LV7SMBR9 LV7SMBR11 LV7SMBR12
LV8	0.33	Type 1	Round	1.0x	LV8MA	LV8SMBR9 LV8SMBR11 LV8SMBR12
LV9	0.33	Type 3	Trapezoidal	1.0x	LV9MA	LV9SMBR9 LV9SMBR11 LV9SMBR12
LV10	0.33	Type 3	Round	1.0x	LV10MA	LV10SMBR9 LV10SMBR11 LV10SMBR12
LV11	0.6	Type 1	Trapezoidal	1.0x	LV11MA	LV11SMBR9 LV11SMBR11 LV11SMBR12
LV12	0.6	Type 3	Trapezoidal	1.0x	LV12MA	LV12SMBR9 LV12SMBR11 LV12SMBR12

RFB Connection Welds

The RFB connection of the full-scale prototype OSD test specimen had PJP welds with 1/4-inch penetration and 5/16-inch reinforcing fillet welds on both sides of the 5/8-inch floor beam web. Some OSDs with EC RFB connections have been detailed with simple fillet welds (and no PJP welds) such as the Maritime Off-Ramp in Oakland, CA and the Danziger Bridge in Louisiana without any signs of root or throat cracking to date.

A sensitivity study was performed to assess the likelihood of root or throat cracking of the RFB connections weld. Unlike the LSS and effective notch stress methodologies used to evaluate weld toe cracking as described previously, to evaluate root or throat fatigue cracking, a nominal stress approach was utilized. A fillet welded EC RFB connection and a PJP welded EC RFB connection were considered in the sensitivity study. Two different global and local variable combinations were selected from the previous results which produced the highest in-plane normal (perpendicular and parallel to the weld) and shear stress conditions in the floor beam web near the RFB connection weld.

For each of these conditions, submodels were prepared to assess both PJP welds and fillet welds. A SMB-level mesh (which included the unfused strip between the floor beam web and rib wall) were prepared to assess these stress conditions.

Nominal stress fatigue design checks from AASHTO LRFD BDS[1], Eurocode 3[2], and DNV[9] were used to assess the stress conditions on the weld throat for each of the global/local variable combinations. The fatigue provisions of AASHTO LRFD BDS[1] address two modes of weld root or throat cracking. The first is the case of a continuous fillet-welded or PJP-welded connection, with tensile normal stress parallel to the weld. Fatigue cracks can initiate at discontinuities in the weld root and propagate in a plane that is perpendicular to the weld axis. The resistance for this root cracking mode is determined in AASHTO LRFD BDS[1] by Fatigue Category B.

The second mode of weld root or throat cracking in AASHTO LRFD BDS[1] is associated with a discontinuous plate in tension connected by a pair of fillet welds or PJP welds (as in the RFB connection) to a continuous transverse plate and subjected to transverse stresses as shown in Figure 35 (also referred to as a “cruciform connection”). The nominal stress is the normal stress in the discontinuous plate in the direction perpendicular to the weld axis. Fatigue cracks can initiate at the weld root and propagate through the throat to the weld face. The resistance for this throat cracking mode is determined in AASHTO LRFD BDS[1] by Fatigue Category C with a reduction factor that is a function of the geometry of the welds, penetration, and connected plate thickness. Nominal stresses calculated on the loaded plate area are used as the stress index to compare the demand with the resistance.

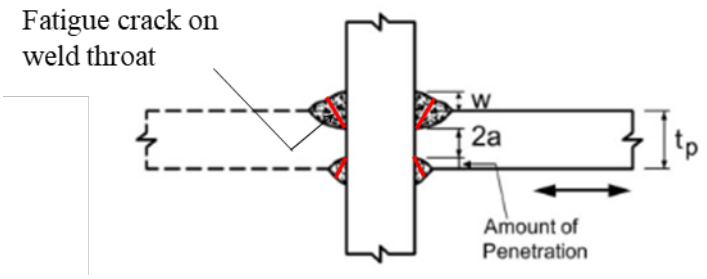

Figure 35. AASHTO LRFD BDS[1] cruciform/tee tension connection and fatigue strength equation (AASHTO, 2020)

In the first edition of the AASHTO LFRD BDS[3] (AASHTO, 1994), a third mode of weld root or throat cracking was considered, namely throat cracking under shear. This fatigue crack was anticipated to initiate and propagate on the weld throat. The fatigue strength of fillet welds in shear was determined by Fatigue Category E with a CAFT of 4.5 ksi and the nominal stress was calculated as the average stress on the weld throat (shear force divided by the weld throat area). The fatigue resistance of fillet welds in shear is no longer included in the latest version AASHTO LRFD BDS[1]. However, provisions for the fatigue strength of fillet welds in shear are currently included in other bridge design provisions around the world, including Japan (Japan Road Association, 2012), Europe (European Committee for Standardisation, 2002), and Great Britain (BSI, 1999).

To assess the EC RFB connection welds, the fatigue design assessment approaches of Eurocode 3[2] (EC3) (European Committee for Standardisation, 2002) and "Fatigue Design of Offshore Steel Structures, RP-C203"[9] (DNV) (DNV, 2011) were considered, as they have been used in previous OSD research (Saunders, et al., 2019) where throat cracking in fitted EC RFB connections was observed. It was found that improved results were obtained when using DNV[9] and EC3[2] since the stress indices in these provisions both account for the combination of shear and normal stresses. The fatigue design assessment procedures in both EC3[2] and DNV[9] employ nominal-stress approaches to assess the likelihood of root or throat fatigue cracking for a combination of shear and normal stresses. Similar to the assessment of fillet welds for the strength limit states, the applied forces (or stresses) on the connection are used to calculate nominal stresses on the effective weld throat using force equilibrium, which are then compared to an *S-N* curve. EC3[2] prescribes the linear combination of fatigue damage indices from these two stresses. DNV[9] prescribes a stress index which is a non-linear function of these two stresses. Neither EC3[2] nor DNV[9] includes the effects of tensile normal stress parallel to the weld in combination with the other stresses (this mode of root cracking is assessed separately in both specifications).

The EC3[2] and DNV[9] fatigue design assessment approaches were used to assess the likelihood of fatigue cracking for two selected EC RFB connection configurations from the FEA study that exhibited high normal and/or shear stresses at in the welds. Each configuration was analyzed once with fillet weld configuration, and once with a PJP configuration matching the full-scale prototype OSD test specimen. Thus, fatigue evaluations of four cases were performed.

[9] DNV-RP-C203 Fatigue design of offshore steel structures is not a Federal requirement.

In each of the four cases, both the combined shear/transverse-normal stress and longitudinal normal stress modes of cracking was assessed at multiple points along the weld. Nominal stresses were obtained from the FEA results at each evaluation point.

A fatigue assessment of the connection welds was also performed per AASHTO LRFD BDS[1], though three modes of cracking were assessed separately since AASHTO LRFD BDS[1] does not specify a methodology for evaluation of a combined mode of cracking. These three modes represent fatigue cracks driven by (1) normal stresses parallel to the weld axis; (2) normal stresses perpendicular to the weld ("cruciform connection stresses"); and (3) shear stresses in the weld (per AASHTO LRFD BDS 1st Edition[3]).

Weld Profile

The fatigue performance of a welded steel bridge detail is typically assessed in design using a nominal stress approach. The effects of stress concentration, local weld geometry, and residual stresses are accounted for by the various fatigue categories (Categories A through E in AASHTO LRFD BDS[1]) which vary based on the configuration of the detail. The resistance is compared to a demand stress, which is the nominal stress index (e.g., Mc/I or P/A) at the location of the detail.

The local structural stress (LSS) approach (also known as the structural hot-spot approach) can be used to assess the fatigue life with more refined analysis of the detail. In this methodology, the local stresses are extrapolated to the weld toe location and compared to a specified resistance (Fatigue Category C is suggested in AASHTO LRFD BDS[1] for OSD details). This method is useful in cases where a nominal stress index cannot be determined, as is often the case for OSD details. Unlike the nominal stress index, the LSS does include the effect of local connection geometry, but does not include the effect of local weld geometry, such as weld toe radius and convexity/concavity of the weld.

To assess the effect of local weld geometry on the fatigue resistance, the effective notch stress approach can be used. This approach utilizes the local stress at the weld toe with models that include the weld geometry, assuming linear elastic material and with a standard weld toe radius to model the theoretical notch-like condition at the weld toe as shown in Figure 36. The approach can also be used to evaluate weld root cracking. The methodology is described in detail in (Fricke, 2010).

It has been found that a weld toe radius of 1 mm produces reasonable results for fatigue assessment of certain welded steel joints. A finely meshed finite element model is needed (much finer than that which is needed for an assessment using the LSS approach). Element lengths along the 1 mm radius of less than 0.25 mm are suggested. Figure 37 shows an example of the necessary mesh density at the weld toe with quadratic elements.

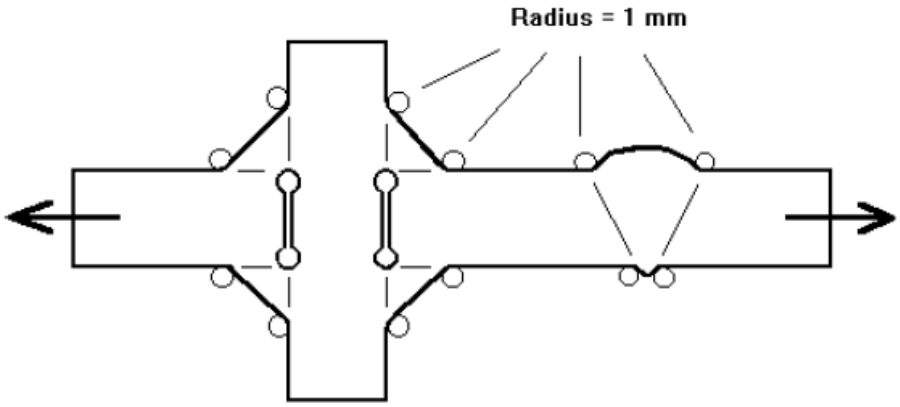

Figure 36. Round conditions at theoretical notches for the assessment of typical welded details using the effective notch stress approach (Hobbacher, 2008)

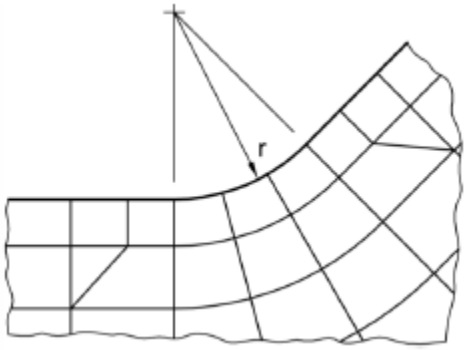

Figure 37. Typical quadratic element mesh at weld toe radius suggested for notch stress analysis (Fricke, 2010)

The maximum principal stresses along the surface of the effective notch are obtained from the finite element analysis results. These maximum stresses are then compared to the applicable *S-N* curve for the material to assess the likelihood of fatigue crack initiation and propagation.

To evaluate the sensitivity of the results to local weld geometry, and third level of submodeling was employed. Three submodel C (SMC) level finite element models were created. Each model encompassed the wrap-around fillet weld at an EC RFB connection identified to have the highest stresses in the previous sensitivity study modelling. The SMC mesh was prepared as needed for the effective notch stress analysis. Each of the models included a weld toe radius of 1 mm, with three different weld face angles. The weld face angle is measured between base metal and the weld face. At each weld toe, a radius of 1 mm is assumed.

Three SMC analyses were performed, featuring weld face angles of 120, 135, and 150 degrees. The results of these analyses were used to assess the sensitivity of the fatigue performance (assessed using effective notch stress) to weld face angle.

CHAPTER 6. SENSITIVITY STUDY RESULTS

INTRODUCTION

The results of the literature review and survey of industry practice established a range of parameters typical of OSDs for highway bridges in the United States and worldwide. A sensitivity study using FEA has been performed to explore the limits at which the economical EC RFB connection detail has a high likelihood of adequate fatigue performance. A finite element model of the full-scale prototype OSD test specimen was prepared and the results were compared to measurements from the test program, as described in Chapter 4. Adjustments were made to the model to improve the agreement.

The key OSD variables were identified and a matrix of analysis cases was developed as described in Chapter 5. The sensitivity study analyses were then performed to assess the sensitivity of the fatigue performance to the key global and local OSD variables.

To evaluate the performance of each connection configuration, the vertical local structural stress (LSS) in the rib wall along the wrap-around fillet weld toe are obtained from each FEA model (i.e., SMB). To evaluate the likelihood of weld toe cracking, the LSS is the stress index that is compared to a fatigue resistance determined by an *S-N* curve (for finite life) and CAFT (for infinite life). In this study, the LSS is the peak stress under any load application and since there was no reversal from the application of the four loads, the LSS also represents the stress range produced by the cycle of four actuator load applications. However, it is known that comparison of LSS to the CAFT is conservative and that a modest exceedance of the CAFT is not necessarily indicative of fatigue cracking. It is also known that the local geometry of the fillet weld (namely weld toe radius and angle) affects the fatigue resistance (ISO, 2014). This is demonstrated by absence of weld toe cracking despite the relatively high stress ranges (over 13 ksi) at the wrap-around fillet weld toe measured during the large-scale OSD fatigue test. Therefore, to evaluate the results of the sensitivity study, it is assumed that so long as the LSS is less than 14 ksi (i.e., an assumed wrap-around fillet weld toe LSS limit), adequate fatigue performance can be expected. To achieve this performance, the profiles of the RFB connection wrap-around fillet welds should meet or exceed the favorable weld profiles of the full-scale prototype OSD test specimen. It should be noted that an LSS a wrap-around fillet weld toe LSS limit of 14 ksi is not currently in any OSD design provision and has been selected by the researchers as a reasonable target LSS value by the researchers that is comparable to the maximum LSS measured at the center of the wrap-around EC RFB connection weld toe on the rib wall in the full-scale prototype OSD test specimen which exhibited good fatigue performance. Additionally, relative comparisons of the LSS from different RFB connection configurations can be made to assess the sensitivity of individual variables, without regard to performance.

To evaluate the likelihood of throat cracking of the fillet or PJP RFB connection welds, a different methodology is used. In this methodology, the stress index is calculated as a combination of nominal shear and normal stresses acting on the weld throat. A number of different fatigue evaluation methodologies were considered, including those from AASHTO LRFD BDS[1], Eurocode 3[2], and DNV[9]. Each combination results in a nominal stress index at a

number of points along the weld length. At each point, the nominal stress index is compared to a resistance determined by an *S-N* curve and CAFT.

Finally, an evaluation of the effect of weld profile was performed using the effective notch stress approach. Three different weld face angles at the toe were considered. In this approach, a finely meshed model of the weld toe region developed with a 1 mm radius transition between base metal and weld metal at the weld toe. In this case, the principal stress on the radiused surface at the weld toe is the stress index which should be compared to an *S-N* curve to assess the likelihood of cracking.

GLOBAL VARIABLE STUDY

Description

Three global OSD variables were assessed in the sensitivity study, namely (1) rib cross-section (round and trapezoidal); (2) transverse truss stiffness (100% and 50% of the full-scale prototype OSD test specimen); and (3) deck plate thickness (3/4 inch and 5/8 inch). A total of eight analysis cases in the global variable study were considered in the global variable study as shown in Table 12. For each configuration shown in Table 12, both a global model and three submodels were prepared. The global model (MA) encompasses the entire full-scale prototype OSD test specimen (three transverse trusses, two OSD rib spans, and 14 ribs) as shown in Figure 23. MA is comprised of a combination of 3D brick elements for the OSD (not including welds) and shell elements for the transverse and longitudinal trusses and support columns. Brick elements were 20 node quadratic formulation with reduced integration (Abaqus element type C3D20R). Shell elements were 8 node quadratic formulation with reduced integration (Abaqus element type S8R). Details including the rib splices, transverse truss batten plates, and transverse truss gusset plates (at FB2 only) were explicitly modeled (see Figure 23 through Figure 25). The geometry of the RFB connections in each global model (MA) match those of the corresponding submodels (SMB) for each global variable analysis case.

It was found from the laboratory testing and previous FEA that for the applied loading pattern, four RFB connection wrap-around fillet welds experienced the highest weld toe stresses. These four critical welds were located directly beneath the loading pads as shown in Figure 38. These locations are denoted by the rib number and side (east or west), namely R9W, R9E, R11E, R12W. These two load pad locations represent the worst-case conditions. At Rib 9, the load pad straddles the rib (both sides are highly stressed). At Ribs 11 and 12, the load pad straddles the space between the rib, producing high stresses in the sides of the ribs closest to the load pad.

Each of the three submodels (SMB) encompasses the RFB connection at one rib (models were created at Ribs 9, 11, and 12) at Floor Beam 2 (FB2), and 1 ft. 6 inch of rib length on either side of FB2 (see Figure 27). The RFB connection welds are included in each SMB. The entirety of each SMB is modeled using 20 node quadratic brick elements with reduced integration (Abaqus element type C3D20R). The boundary displacements of each SMB were obtained from the results of the corresponding global model (MA). Results were extracted from the critical wrap-around fillet weld toes in each model.

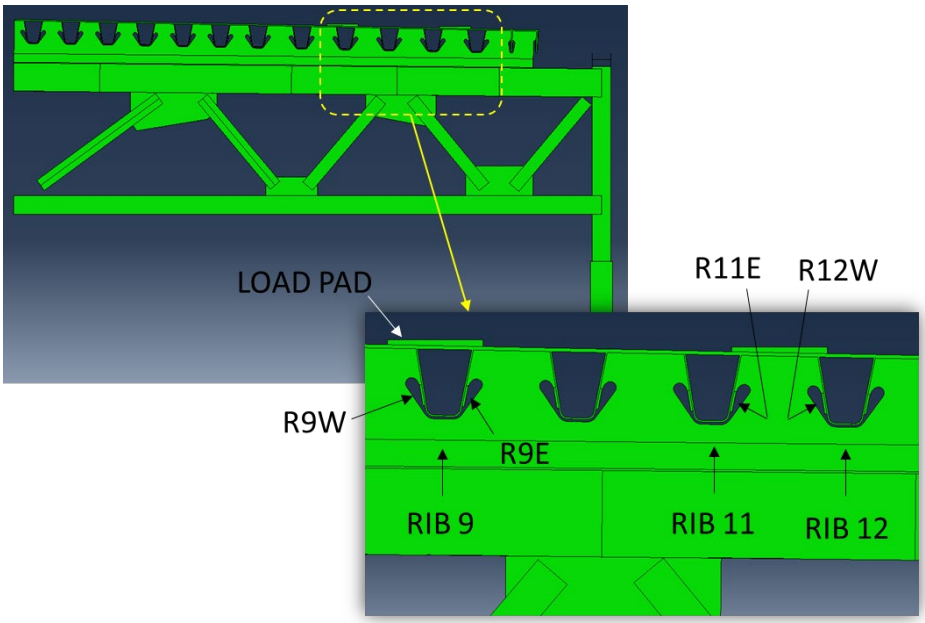

Figure 38. Global Model (MA) showing locations of critical vertical rib wall stress at RFB connection wrap-around fillet weld at Floor Beam 2 (R9W, R9E, R11E, and R12W)

General Behavior

As noted, the stress response at the rib wall at the wrap-around toe was largest at the wrap-around fillet welds at the east and west side of Rib 9 (R9E and R9W), the east side of Rib 11 (R11E), and the west side of Rib 12 (R12W). The response at Rib 9 is representative of a case in which a wheel load patch straddles the rib (both rib walls are loaded). The response at Ribs 11 and 12 is representative of a case in which a wheel load patch is centered between ribs (only one rib wall of each rib is directly loaded).

In each of these cases, the local stress response at the wrap-around fillet weld toe has a similar pattern. Figure 39 presents a contour plot of stress normal to the wrap-around fillet weld toe at the east side of Rib 11 (R11E) under the 82.8 kips tandem axle loading (AASHTO LRFD BDS[1] Fatigue I loading with 15% dynamic impact) at Actuator 4, for the as-tested EC RFB connection configuration (Case GV1). The stresses are tensile, and are slightly higher to the right side of the weld toe. This variation is due to the eccentricity of the load pad for Actuator 4 with respect to Floor Beam 2.

Figure 40 is a contour plot of maximum absolute value principal stress at the same rib for the same loading and OSD configuration (Case GV11), on a section through the mid-thickness plane of the floor beam web. The contour levels were set with a maximum of +5 ksi and minimum of -5 ksi. Regions with maximum tensile principal stress greater than +5 ksi are shown in light grey. Regions with minimum compressive principal stress less than -5 ksi are shown in dark grey. The figure shows that at the wrap-around fillet weld, the response of the rib wall is dominated by out-of-plane bending since there is tension of the exterior face of the rib wall (at the weld toe). This out-of-plane bending is also evident in the exaggerated displaced shape of the rib. For Rib 11, the

loading is centered between Ribs 11 and 12, and therefore only the east side of Rib 11 (side closest to Rib 12) experiences high stresses at the wrap-around fillet weld toe.

Figure 41 shows the same type of plot for Rib 9 for the same loading and OSD configuration. The out-of-plane behavior of both rib walls (9E and 9W) is similar to that shown for Rib 11E in Figure 40. Vertical tensile stresses develop on the outside of the rib wall at the weld toe, and compressive stresses develop directly opposite the weld toe on the inside of the rib.

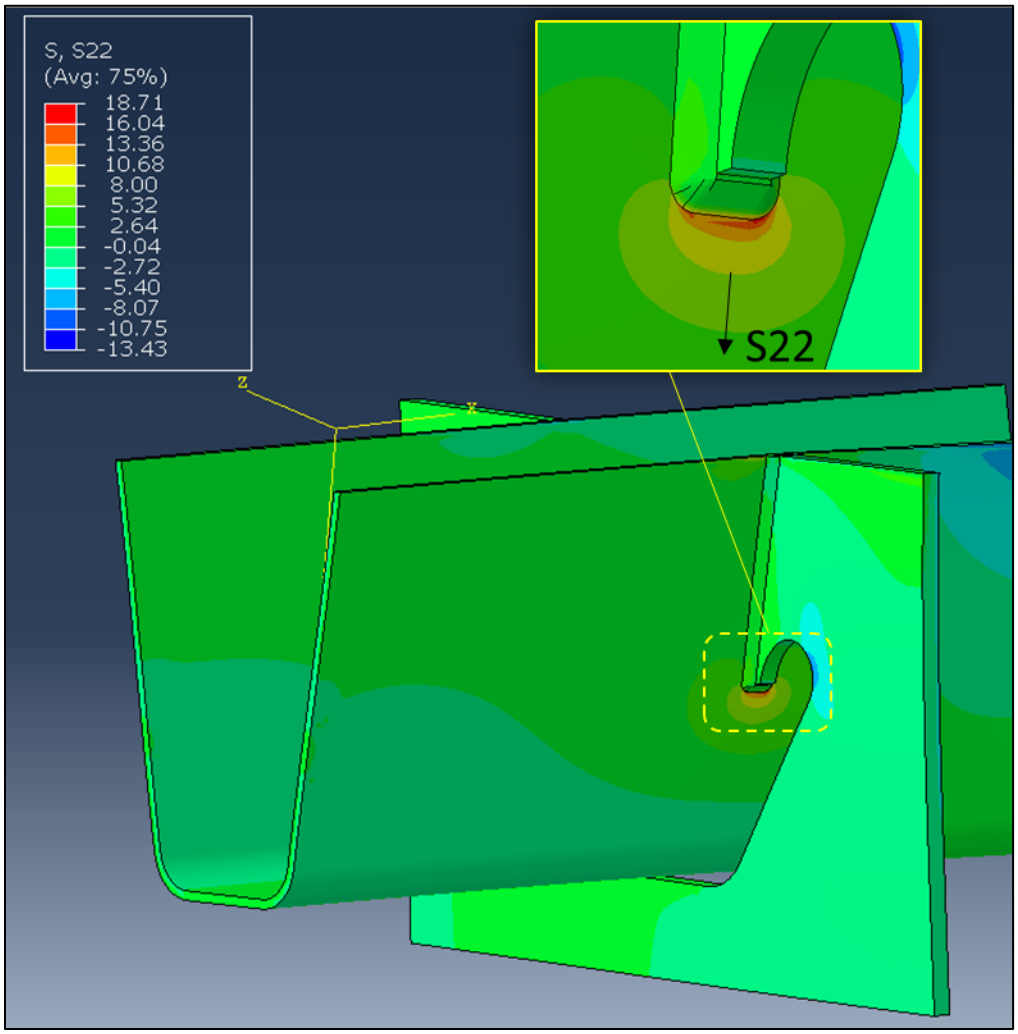

Figure 39. Submodel B (SMB) – FEA contour plot of normal stress perpendicular to the wrap-around fillet weld toe on east rib wall of Rib 11 (R11E) under 82.8 kip loading at Actuator 4 for the as-tested OSD configuration (Case GV1)

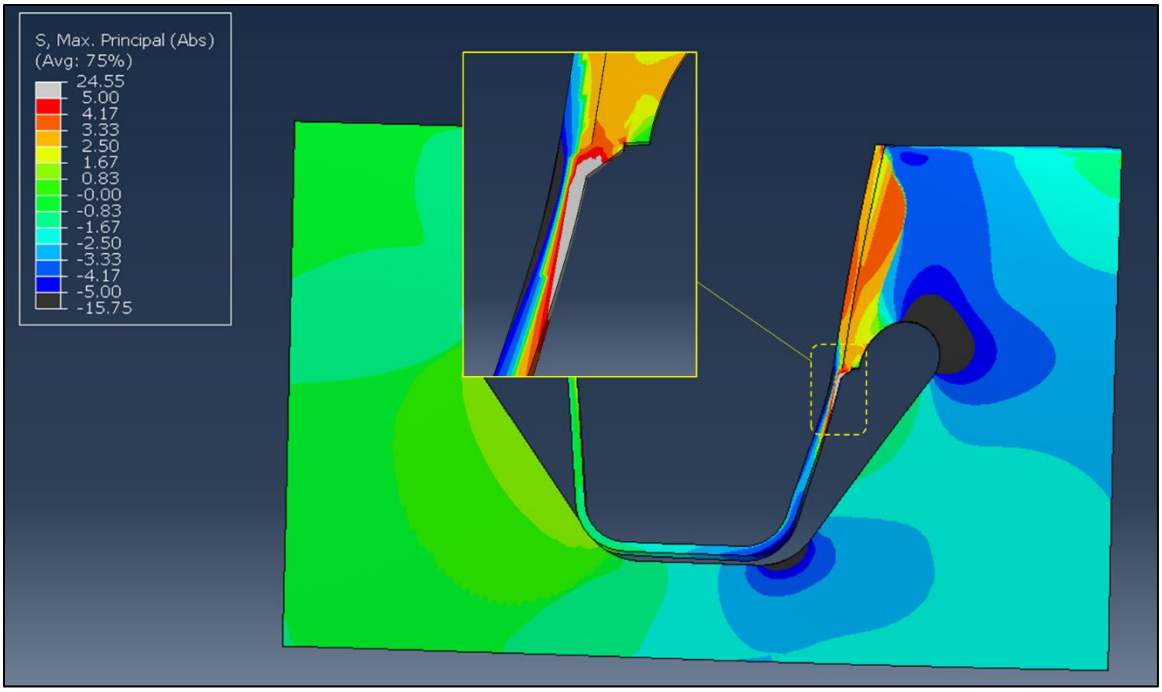

Figure 40. Submodel B (SMB) – FEA contour plot of maximum absolute value principal stress on the mid-thickness plane of the FB2 web at Rib 11 under 82.8 kip loading at Actuator 4 for the as-tested OSD configuration (Case GV1), showing out-of-plane bending of rib wall at wrap-around fillet weld toe.

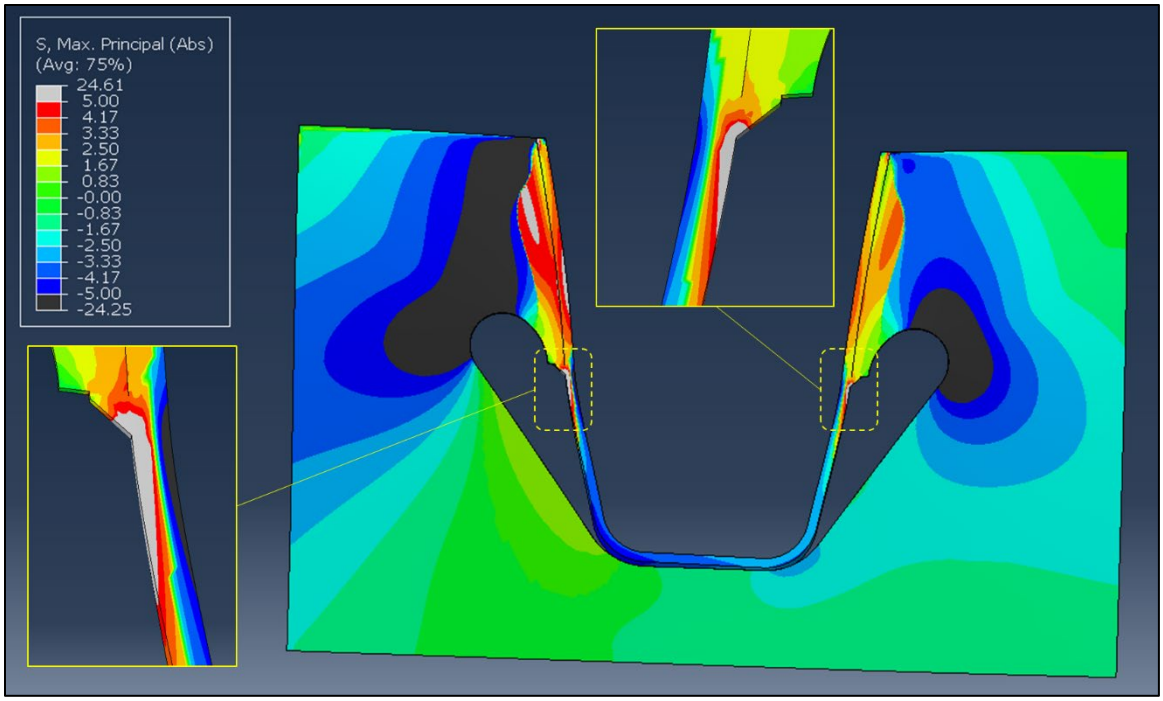

Figure 41. Submodel B (SMB) – FEA contour plot of maximum absolute value principal stress on the mid-thickness plane of the FB2 web at Rib 9 under 82.8 kip loading at Actuator 4 for the as-tested OSD configuration (Case GV1), showing out-of-plane bending of rib wall at wrap-around fillet weld toe.

Results

The following describes the results of the global variable study. The fatigue performance of a given RFB connection detail configuration is assessed by considering the magnitude of the largest LSS with respect to an assumed wrap-around fillet weld toe LSS limit of 14 ksi, selected by the researchers as a benchmark based on the measurements and observed fatigue performance of the full-scale prototype OSD test specimen tested at Lehigh University (this threshold is not included in AASHTO LRFD BDS[1] or any other design provision).

In these fatigue assessments, the LSS is considered as the stress index. At each of the critical locations, the LSS was determined at a number of points along the weld toe by extracting vertical stresses from the SMB finite element models along horizontal paths 0.4 times the rib wall thickness (0.125 inch) and 1.0 times the rib wall thickness (0.3125 inch) away from the weld toe. At each point along these paths, linear extrapolation was used to estimate the LSS at the weld toe at each of the four critical rib locations. For each global variable case (see Table 12), the maximum LSS for each of the four critical locations was obtained. The results are summarized in Table 14. The table shows that the LSS were highest for Cases GV6 and GV8, with round ribs and thinner deck plates (5/8 inch). Case GV8 featured transverse trusses with 50% stiffness. The lowest LSS were observed in Cases GV1 (as-tested condition) and GV3 (as-tested but with 50% transverse truss stiffness).

A comparison of the LSS at each of the four critical locations between corresponding cases with and without the transverse truss stiffness reduction is shown in Table 15. The results show that reducing the transverse truss stiffness by 50% had little effect on the LSS at the critical details. Generally, reducing the transverse stiffness lowers the LSS at the critical details, though this reduction is modest (maximum of 5%).

Performing a similar comparison between models with 3/4 inch and 5/8 inch deck plate showed that the reduction in deck plate thickness increased the LSS by as much as 12%. The results are summarized in Table 16.

It was found that the effect of the rib cross-section varied with other local variables. The sensitivity to rib cross section was also examined in the results of the local variable study. Generally, it was found that the LSS were higher for cases with round ribs compared to trapezoidal ribs.

Table 14. Summary of maximum LSS at the wrap-around fillet weld toes at four critical rib locations (R9W, R9E, R11E, and R12W) – global variable study models

Case Name	Rib R9W	Rib R9E	Rib R11E	Rib R12W
GV1	13.26	9.44	13.82	13.37
GV2	14.07	9.73	15.11	14.98
GV3	13.31	8.96	13.55	13.31
GV4	14.08	9.26	14.80	14.97
GV5	16.12	13.39	14.74	15.63
GV6	17.09	13.97	15.91	17.10
GV7	15.66	12.78	14.10	15.43
GV8	16.59	13.36	15.23	16.97

Table 15. Differences in LSS at critical EC RFB connections between models with original transverse truss and models with transverse trusses with 50% stiffness (+ differences denote higher stress for models with 50% stiffness)

Cases	R9W	R9E	R11E	R12W
GV1-GV3	0.4%	-5.1%	-1.9%	-0.4%
GV2-GV4	0.1%	-4.8%	-2.0%	-0.1%
GV5-GV7	-2.8%	-4.6%	-4.3%	-1.3%
GV6-GV8	-3.0%	-4.4%	-4.2%	-0.8%

Table 16. Differences in LSS at critical EC RFB connections between models with 3/4 inch deck plate and models with 5/8 inch deck plate (+ differences denote higher stress for models with 5/8 inch deck plate)

Cases	R9W	R9E	R11E	R12W
GV1-GV2	6.1%	3.1%	9.3%	12.0%
GV3-GV4	5.8%	3.4%	9.2%	12.5%
GV5-GV6	6.0%	4.3%	7.9%	9.4%
GV7-GV8	5.9%	4.5%	8.0%	10.0%

LOCAL VARIABLE STUDY

Description

Two local variables were considered in the sensitivity study, namely: (1) the RFB connection weld length (*c/h* with three variations); and (2) the cut-out geometry (Type 1 (tangential cut-out termination) and Type 3 (perpendicular cut-out termination)). For a number of combinations of these local variables, two global variables were also considered, namely the transverse truss stiffness and rib cross-section. A deck plate thickness of 3/4 inch was considered for all cases.

Initially during the sensitivity planning, it was assumed that changes in the local variables considered would not affect the global response of the full-scale prototype OSD test specimen and therefore, the reanalysis of the global models would be unnecessary (i.e., a single global model analysis could be used to drive the boundary displacements of multiple submodels with varying connection weld lengths and cut-out geometries. However, this assumption was checked by comparing results with and without reanalysis of the corresponding global model. The differences were found to be significant and therefore, the submodels (SMB) for each local variable analysis case were driven by a global model (MA) with matching RFB connection weld length (i.e., *c/h*), cut-out geometry, and rib cross-section type.

A summary of the analysis cases for the local variable sensitivity study is shown in Table 13. Analysis cases LV1, LV2, LV3, and LV4 correspond to analysis cases GV1, GV3, GV5, and GV7 performed in the global variable sensitivity analyses. For each case, the boundary displacements for the submodels (SMB) were obtained from a corresponding global model (MA). As shown, a total of 12 cases were analyzed. The EC RFB connection geometries for each analysis case are shown in Figure 42 through Figure 47.

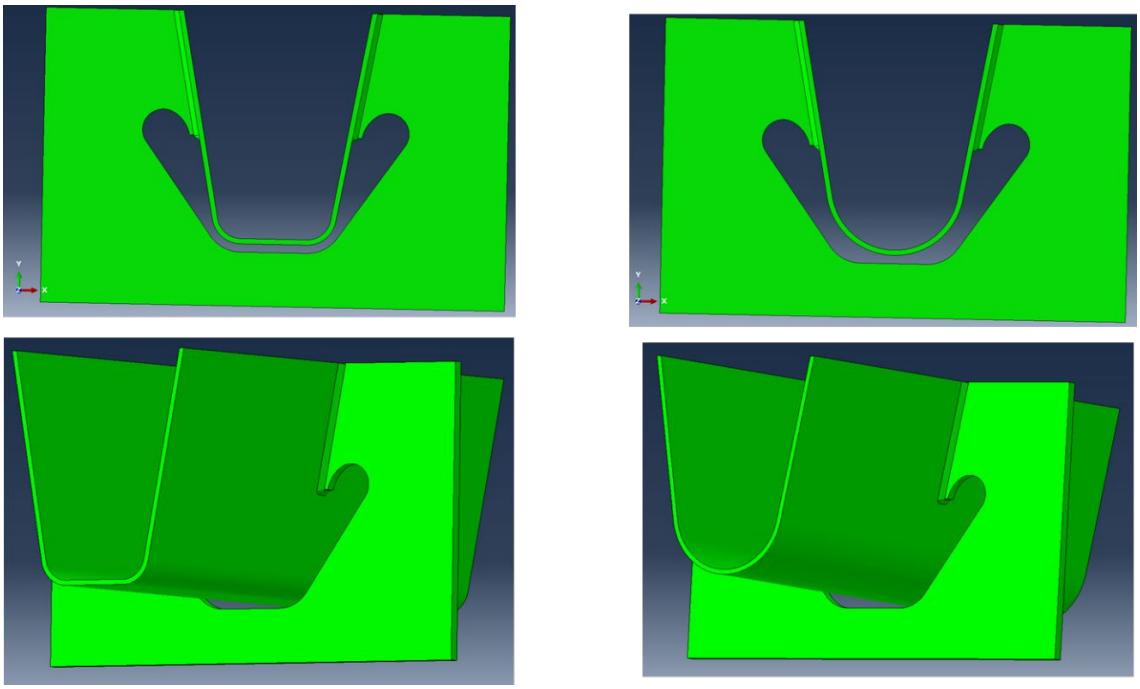

(a) (b)

Figure 42. Submodel geometries for Cases (a) LV1 (trapezoidal rib) and (b) LV3 (round rib), with Type 1 cut-out geometry and *c/h* = 0.46. LV1 represents the geometry of the full-scale prototype OSD test specimen

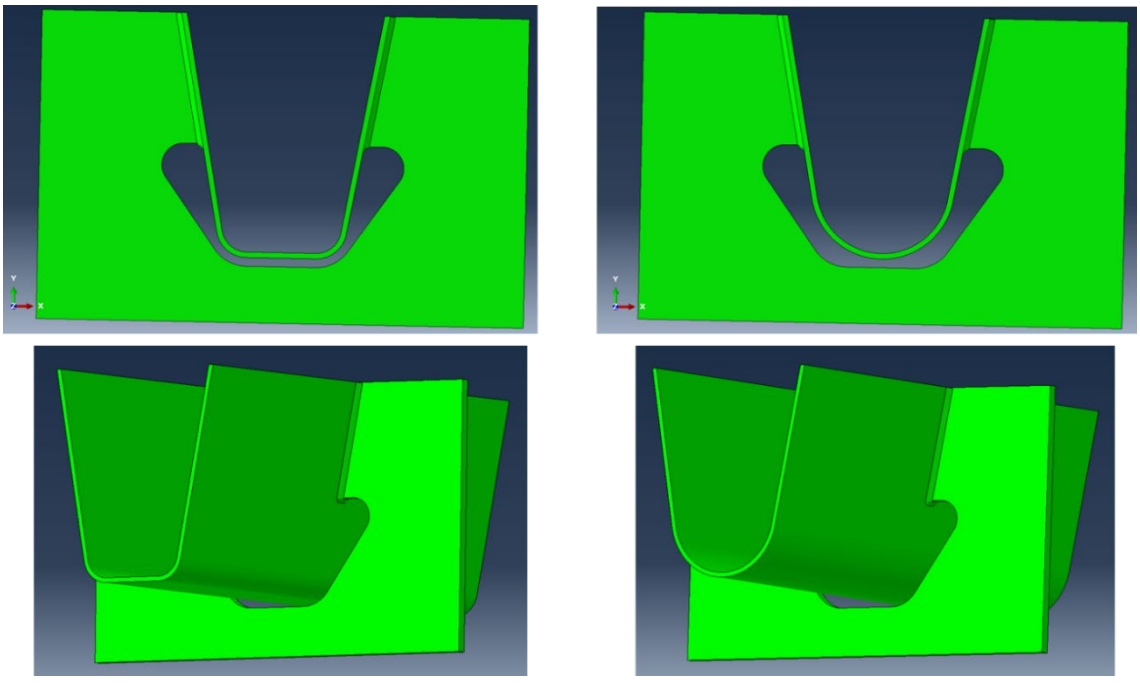

(a) (b)

Figure 43. Submodel geometries for Cases (a) LV5 (trapezoidal rib) and (b) LV6 (round rib), with Type 3 cut-out geometry and *c/h* = 0.46

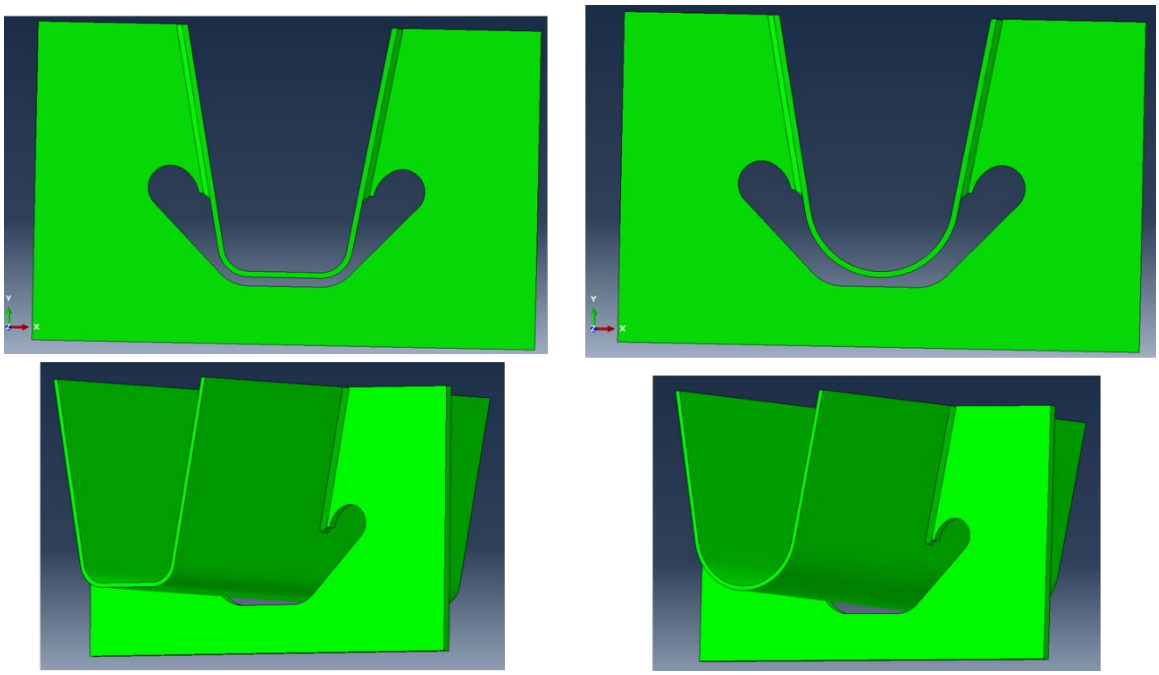

(a) (b)

Figure 44. Submodel geometries for Models (a) LV7 (trapezoidal rib) and (b) LV8 (round rib), with Type 1 cut-out geometry and *c/h* = 0.33

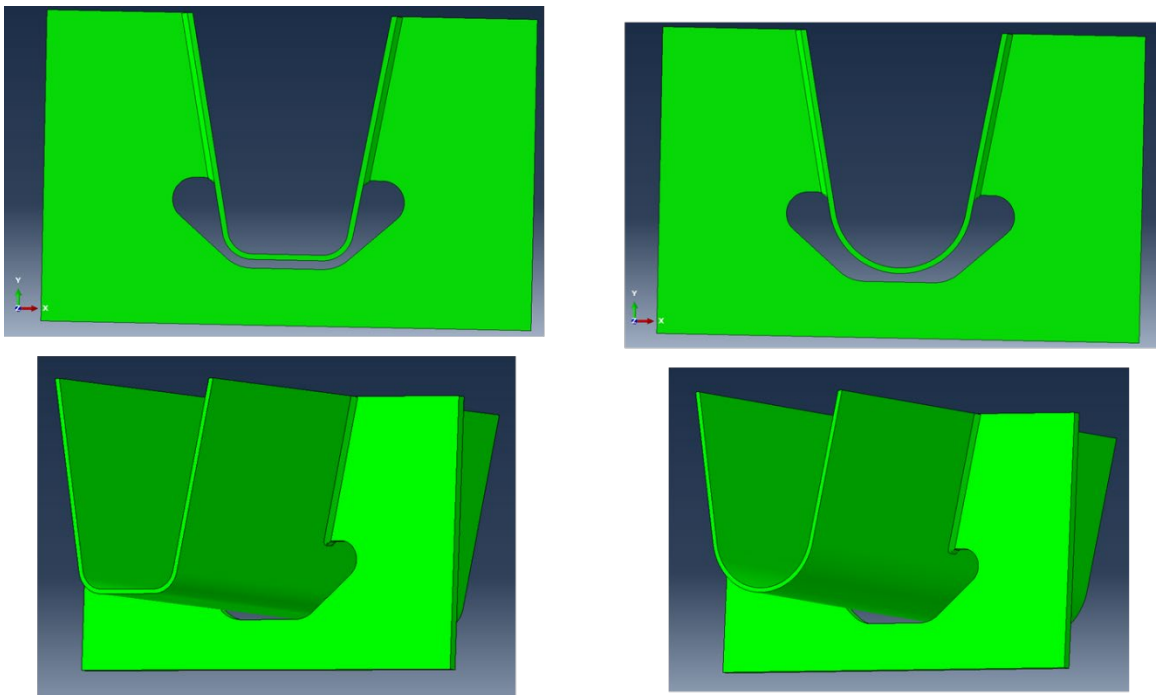

(a) (b)

Figure 45. Submodel geometries for Cases (a) LV9 (trapezoidal rib) and (b) LV10 (round rib), with Type 3 cut-out geometry and *c/h* = 0.33

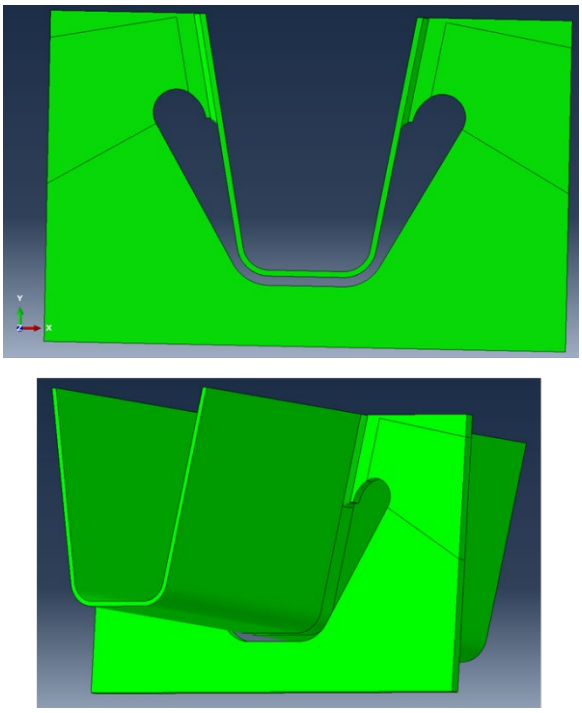

Figure 46. Submodel geometry for Case LV11 with Type 1 cut-out geometry and *c/h* = 0.6

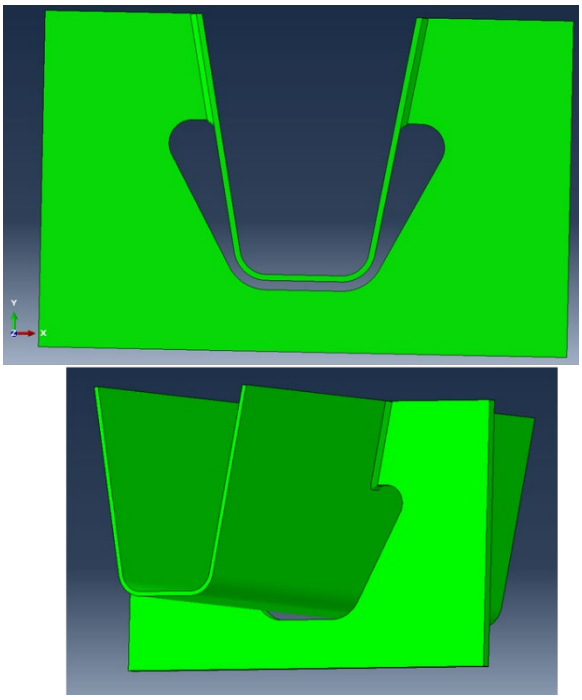

Figure 47. Submodel geometry for Model LV12 with Type 3 cut-out geometry and *c/h* = 0.6

Results

The fatigue performance of a given RFB connection detail configuration is assessed by comparing the magnitude of the largest LSS (the stress index) to a fatigue threshold (i.e., a CAFT) since infinite fatigue life performance is most likely necessary for OSD which may be subjected to many cycles in service. For reasons discussed earlier, a wrap-around fillet weld toe LSS limit of 14 ksi has been considered for this study by the researchers based on the measurements and the observed fatigue performance during the full-scale OSD fatigue test program at Lehigh University. This assessment approach needs weld profiles that meet or exceed the favorable weld profiles observed in the full-scale prototype OSD test specimen.

For each of the local variable cases, comprising a global model (MA) and matching submodel (SMB), data were extracted at the critical locations and LSS were extrapolated along the weld toe. The results are summarized in Table 17. The best performance was observed for Case LV7, which has the same cut-out geometry as the as-tested configuration (Type 1), but a shallower cut-out (*c/h* equal to 0.33). Adequate performance is also expected for Case LV5 (Type 3, *c/h* equal to 0.46). Both of these cases incorporated trapezoidal ribs. The results show that the stresses were generally higher for round ribs. The worst performance observed was for Cases LV8 and LV10, which featured round ribs, shallow cut-outs (*c/h* equal to 0.33), and Type 1 and 3 cut-outs, respectively.

A summary of comparisons between analysis cases to study the sensitivity to rib shape is shown in Table 18. The results show that changing the ribs from trapezoidal to round ribs can increase the LSS by up to 43%.

Table 19 presents the results of comparisons to assess the sensitivity to cut-out shape (Type 1 vs. Type 3) for trapezoidal ribs. The same comparison for round ribs is shown in Table 20. The results show that for larger *c/h* and trapezoidal ribs, the Type 3 connection has lower stresses (up to 16% less). For the case with *c/h* equal to 0.33, the effects are mixed and do not exhibit a clear trend. For the cases with round ribs, the stresses are generally lower for Type 3 connections but not at all locations.

Table 21 presents a comparison between Cases to assess the sensitivity to RFB connection weld length (*c/h*). For trapezoidal ribs, it appears that reducing the *c/h* ratio reduces the LSS in most cases. There is not a clear trend for round ribs.

It should be noted that in these comparison tables, the LSS represents the maximum LSS along the weld toe at a given RFB connection location.

Table 17. Summary of maximum LSS at the wrap-around fillet weld toes at four critical rib locations – local variable study models

Case Name	Rib R9W	Rib R9E	Rib R11E	Rib R12W
LV1	13.26	9.44	13.82	13.37
LV2	13.31	8.96	13.55	13.31
LV3	16.12	13.39	14.74	15.63
LV4	15.66	12.78	14.10	15.43
LV5	11.36	7.91	13.34	13.02
LV6	14.17	10.12	16.17	16.04
LV7	11.38	8.35	12.08	11.90
LV8	13.82	11.06	16.07	17.02
LV9	9.19	6.80	13.18	13.90
LV10	12.22	9.72	16.35	17.57
LV11	15.57	11.23	14.75	13.67
LV12	13.63	9.40	14.05	13.13

Table 18. Local variable study, effect of rib cross-section (trapezoidal vs. round): percent differences between maximum LSS at four critical ribs

Type 1 Cut-Out *c/h* = 0.46	Type 1 Cut-Out *c/h* = 0.33	Type 3 Cut-Out *c/h* = 0.46	Type 3 Cut-Out *c/h* = 0.33
LV3 (Round)	LV8 (Round)	LV6 (Round)	LV10 (Round)
LSS_{LV3}/LSS_{LV1} = min +7% max +42%	LSS_{LV8}/LSS_{LV7} = min +21% max +43%	LSS_{LV6}/LSS_{LV5} = min +21% max +28%	LSS_{LV10}/LSS_{LV9} = min +24% max +43%
LV1 (Trapezoidal)	LV7 (Trapezoidal)	LV5 (Trapezoidal)	LV9 (Trapezoidal)

Table 19. Local variable study, effect of cut-out geometry (Type 1 vs. Type 3): percent differences between maximum LSS at four critical ribs - trapezoidal ribs

c/h = 0.6	*c/h* = 0.46	*c/h* = 0.33
LV12(Type 3 Cut-Out)	LV5 (Type 3 Cut-Out)	LV9 (Type 3 Cut-Out)
LSS_{LV12}/LSS_{LV11} = min -16% max -4%	LSS_{LV5}/LSS_{LV1} = min -16% max -3%	LSS_{LV9}/LSS_{LV7} = min -19% max +17%
LV11 (Type 1 Cut-Out)	LV1 (Type 1 Cut-Out)	LV7 (Type 1 Cut-Out)

Table 20. Local variable study, effect of cut-out geometry (Type 1 vs. Type 3): percent differences between maximum LSS at four critical ribs - round ribs

***c/h* = 0.46**	***c/h* = 0.33**
LV6 (Type 3)	LV10 (Type 3)
$LSS_{LV6}/LSSmax_{LV3}$ = min -24% max +10%	LSS_{LV10}/LSS_{LV8} = min -12% max +3%
LV3 (Type 1)	LV8 (Type 1)

Table 21. Local variable study, effect of RFB connection weld length (*c/h* = 0.33, 0.46, and 0.6): percent differences between maximum LSS at four critical ribs

Trapezoidal Rib	**Trapezoidal Rib**	**Round Rib**	**Round Rib**
Type 1 Cut-Out	Type 3 Cut-Out	Type 1 Cut-Out	Type 3 Cut-Out
LV11 (*c/h* = 0.6)	LV12 (*c/h* = 0.6)	-	-
LSS_{LV11}/LSS_{LV1} = min +2% max +19%	LSS_{LV12}/LSS_{LV5} = min +1% max +20%	-	-
LV1 (*c/h* = 0.46)	LV5 (*c/h* = 0.46)	LV3 (*c/h* = 0.46)	LV6 (*c/h* = 0.46)
LSS_{LV7}/LSS_{LV1} = min -14% max -11%	LSS_{LV9}/LSS_{LV5} = min -19% max +7%	LSS_{LV8}/LSS_{LV3} = min -17% max +9%	LSS_{LV10}/LSS_{LV6} = min -14% max +10%
LV7 (*c/h* = 0.33)	LV 9 (*c/h* = 0.33)	LV8 (*c/h* = 0.33)	LV10 (*c/h* = 0.33)

ASSESSMENT OF WELD ROOT AND THROAT CCACKING OF PJP AND FILLET WELDED RFB CONNECTIONS

The RFB connection of the full-scale prototype OSD test specimen featured PJP double-bevel-grove welds with 1/4-inch penetration on both sides of the 5/8-inch-thick floor beam web as shown in Figure 13. No throat cracks in these welds were observed after 8 million cycles of loading using either visual inspection of the weld face or macro-etch specimens cut transversely through the welds. The cost-effectiveness of the connection would be improved through the use of fillet welds instead of PJP welds, since preparation of the edge of the floor beam web would not be needed.

The PJP welds of an EC RFB connection should be detailed based on the results of FEA for both strength and fatigue limit states, and also meets the minimum size in AASHTO/AWS D1.5[6] (generally 1/4-inch penetration for typical OSD plate thicknesses). To design for strength, nominal stresses on the weld throat from FEA can be compared to the allowable resistance based on the weld metal strength. For fatigue design, design methodology is limited for cases with combined stresses such as the EC RFB connection. In this study, stress indices are calculated using various design approaches. It is believed that if the fatigue damage indices for a proposed EC RFB connection design are similar to those shown in the analysis presented in this report for the PJP-welded (as-tested) case, the fatigue performance will likely be adequate.

In this study, FEA results were used to assess the likelihood of weld throat/root cracking of the RFB connection welds, considering both fillet-welded and PJP welded details. Two OSD connection configurations were considered, namely (1) the as-tested configuration (Case GV1); and (2) an OSD with the same configuration but with a shorter weld length (*c/h* ratio of 0.6) (Case LV11). The RFB connection of Case LV11 minimizes the length of the RFB connection weld and therefore would represent a worst-case configuration for shear (i.e., the minimum effective weld throat area).

For each connection configuration, two weldments were considered, namely (1) 1/4-inch PJP double-bevel-groove weld with 5/16-inch reinforcement (as-tested weld); and (2) two-sided 5/16 inch fillet welds (no bevel preparation on the floor beam web).

A nominal stress approach was used to evaluate root or throat fatigue cracking. Stresses were extracted from the FEA models at a number of points along paths as shown in Figure 48. Normal stresses parallel to the weld axis were extracted on the mid-thickness edge of the floor beam web (where it meets the rib wall) extending from the deck plate at the top to the end of the weld (see Figure 48(a)). Transverse normal and longitudinal shear stresses were extracted in the floor beam web at a distance equal to the floor beam web thickness away from the weld toe, along five paths through the floor beam web thickness (both surfaces, 1/4 thickness points, and mid-thickness). At each point along the path, the average shear and normal stress of the five paths were used for the fatigue evaluation (the average stress is taken as the membrane stress in the floor beam web). It is important to note that weld throat cracking is currently only addressed in AASHTO LRFD BDS[1] through the cruciform connection which is represented by Fatigue Category C, reduced by a factor that is a function of the size of the welds, penetration depth, and connected plate thickness (AASHTO, 2020), with a stress index represented by the membrane stress perpendicular to the weld in the connected plate. There is no consideration of combination of

other stress components such as shear and normal stress parallel to the weld in AASHTO LRFD BDS[1].

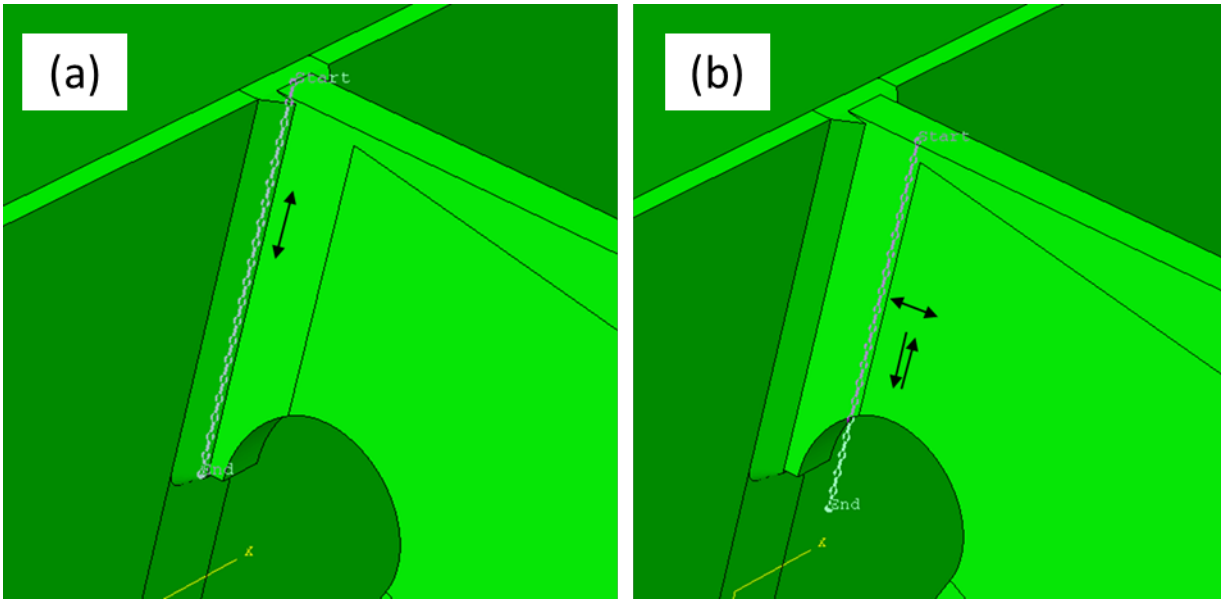

Figure 48. Paths used to extract stresses for fatigue evaluation of RFB connection welds; (a) longitudinal stress at the mid-thickness of the web (single path); (b) transverse normal and shear stresses along five paths through the thickness, at a distance of one floor beam thickness from the weld toe (note only near-surface path shown)

The fatigue performance of each detail configuration is assessed using the mean fatigue life of each detail, determined using the mean *S-N* curve (Keating & Fisher, 1986) from the fatigue test data that had been used to develop the lower bound S-N curve (i.e., the design *S-N* curve, (AASHTO, 2020)). The Palmgren-Miner linear damage model (Miner, 1945) is used to quantify the fatigue damage for each model configuration using a "fatigue damage index," equal to the total number of cycles at a given stress range (n) divided by the fatigue life at that stress range (N). For nominal stress fatigue design approaches, the demand is determined by a stress index which is a combination of nominal shear and normal stresses acting on the effective throat of the weld. The resistance is determined by an *S-N* curve (fatigue life N as a function of stress range S), which varies based on the geometry of a structural detail which are grouped by "fatigue category". For this sensitivity study, the mean *S-N* curve for the appropriate fatigue category is used to estimate the fatigue life. A fatigue damage index of greater than 1.0 indicates that the mean fatigue life is exhausted (and that fatigue cracking is likely).

The approach employed in this sensitivity study is similar to nominal stress fatigue limit state checks from AASHTO LRFD BDS[1], Eurocode 3[2], Part 1.9 (European Committee for Standardisation, 2006), and DNV-RP-C203[9] (DNV, 2011). The limit state checks in these provisions were used to assess the stresses on the weld throat for each of the global/local variable combinations. However, for this study, the mean fatigue resistance was used (instead of the lower bound resistance).

As mentioned in the RFB Connection Welds section in Chapter 5, the fatigue provisions of AASHTO LRFD BDS[1] include two common modes of weld root or throat cracking. The first is the case of a continuous fillet-welded connection, such as a web-to-flange connection of an I-girder, where the nominal stress is the normal stress in and near the weld in the direction along the axis of the weld, due to global flexure of the girder (i.e., longitudinal stresses). Fatigue cracks initiate at discontinuities in the weld, typically at the weld root. These fatigue cracks propagate in a plane that is perpendicular to the weld axis. The resistance for this root cracking mode is determined in AASHTO LRFD BDS[1] by Fatigue Category B (the finite-life fatigue resistance is similar in Eurocode 3[2]).

The second mode of weld root or throat cracking considered in the AASHTO LRFD BDS is associated with a discontinuous plate in tension connected by a pair of fillet or PJP welds (as in the RFB connection) to a continuous transverse plate. This connection detail is also referred to as a "cruciform connection." The nominal stress is the normal stress in the discontinuous plate in the direction perpendicular to the weld axis. Weld throat fatigue cracking can occur and the resistance for this fatigue cracking mode is determined in AASHTO LRFD BDS[1] by Fatigue Category C with a reduction factor that is a function of the geometry of the welds, penetration, and connected plate thickness. The cracks initiate at the weld root and propagate through the throat and eventually to the weld face.

In the first edition of the AASHTO LFRD BDS[3] (AASHTO, 1994) a third mode of weld root or throat cracking was considered, namely throat cracking under shear. The fatigue resistance of fillet welds in shear was determined by Fatigue Category E with a threshold of 4.5 ksi and the nominal stress was calculated as the average stress on the weld throat (shear force divided by the weld throat area). The fatigue crack was expected to propagate on the weld throat. The fatigue resistance of fillet welds in shear is no longer included in the latest version AASHTO LRFD BDS[1]. However, provisions for the fatigue resistance of fillet welds in shear are currently included in other bridge design provisions around the world, including Japan (Japan Road Association, 2012) and Europe (European Committee for Standardisation, 2002). The stress index used for the fatigue evaluation varies among these provisions but is either solely longitudinal shear stress or a combinations of shear stresses and normal stress on the weld throat. Note that there are currently no provisions in AASHTO LRFD BDS[1] to combine fatigue damage from the various types of stress.

Eurocode 3[2] calculates the fatigue resistance of fillet welds for weld throat cracking as a function of both nominal normal and shear stresses which are used to calculate stress indices for fatigue assessment. The transverse normal fatigue stress index, $\sigma_{w,transverse}$, is:

$$\sigma_{w,transverse} = \sqrt{\sigma_{\perp}^2 + \tau_{\perp}^2} \quad \text{(Eq. 3)}$$

where $\sigma_{\perp}$ is the nominal transverse normal stress, and $\tau_{\perp}$ is the nominal transverse shear stress. The longitudinal shear fatigue stress index, τ_w, is equal to $\tau_{\parallel}$ which is the nominal longitudinal shear stress. The stresses $\sigma_{\perp}$, $\tau_{\perp}$, $\tau_{\parallel}$, are all nominal stresses acting on the effective weld throat area (see Figure 49). For the EC RFB connection under investigation, $\tau_{\perp}$, is small (through-thickness shear in the floor beam web) and was assumed to be zero in the following calculations. The fatigue damage indices for transverse normal stress index ($\sigma_{w,transverse}$) and transverse

longitudinal shear stress index (τ_w) are calculated separately and added together to obtain an overall fatigue damage index for the weld.

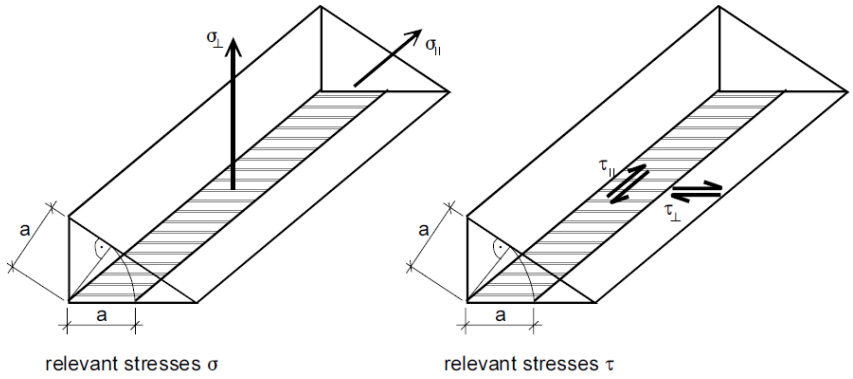

Figure 49. Stress indices for weld fatigue assessment per Eurocode 3[2] (European Committee for Standardisation, 2002)

Section 2.3.5 of DNV[9] calculates the fatigue resistance of fillet welds for weld throat cracking. Unlike Eurocode 3[2], DNV[9] utilizes a single fatigue stress index, σ_w, is calculated as:

$$\sigma_w = \sqrt{\sigma_\perp^2 + \tau_\perp^2 + 0.2\tau_\parallel^2} \quad \text{(Eq. 4)}$$

These assessment approaches were used to evaluate the likelihood of fatigue cracking for the EC RFB connections identified using stress data from FEA. At each location to be evaluated, the FEA stresses are used to calculate a stress index, which is then used to calculate the mean fatigue life and the corresponding fatigue damage index. This fatigue damage index is the basis of the performance assessment. For cases of stress indices less than the CAFT, the corresponding fatigue life, N, is determined by linearly extending the finite life *S-N* curve below the CAFT (i.e., with a slope of -3).

For each case, five damage indices were calculated using the FEA stresses. These include Eurocode 3 (EC3[2]), DNV[9], AASHTO LRFD BDS[1] for longitudinal normal stress (Category B), AAHSTO LRFD BDS for the transverse normal stress (cruciform), and AASHTO LRFD BDS 1st Edition[3] for weld shear.

Figure 50 presents plots of fatigue damage index for the four critical weld locations for Case GV1, considering a two-sided fillet-welded connection. Figure 51 presents the same results for the PJP-welded connection (as tested). In each of these plots the horizontal axis represents the distance along the weld axis starting from the deck plate. Figure 50 shows that the fatigue damage index considering AASHTO[3] Category E for weld shear for the fillet welded condition at Rib 9W is high (equal to 2.0).

Figure 52 presents plots of fatigue damage index for the four critical weld locations for Case LV11 with the shortest weld length, considering a two-sided fillet-welded connection. Figure 53 presents the same results for the PJP-welded connection (as tested).

The plots shown that increasing the EC RFB connection welds from fillet to PJP with fillet reinforcement significantly reduces the fatigue damage indices. The effective throat size for one fillet weld is 0.22 inches (= 0.707 x 5/16 inch). However, for a PJP with 1/4-inch penetration and 5/16-inch fillet reinforcement, the effective throat is 0.40 inches, almost twice the magnitude. This reduces the nominal stresses by 45%. Considering the slope of 3 in the *S*-*N* curve, this results in an increase in the expected fatigue life by a factor of 6 (= $(1/0.55)^3$).

A summary of the maximum throat cracking fatigue damage index for each of the five fatigue assessments performed considering both PJP and fillet-welded connections, for Case GV1 (as-tested configuration) is presented in Table 22. The results summary for Case LV11 are presented in Table 23. The results show that better performance would be expected for the as-tested configuration, i.e., Case GV1 with PJP welding. Changing this configuration to a fillet welded connection results in fatigue damage indices of greater than 1. The results also indicate that the shorter weld length configuration of Case LV11 could also exhibit adequate performance so long as PJP welds are used.

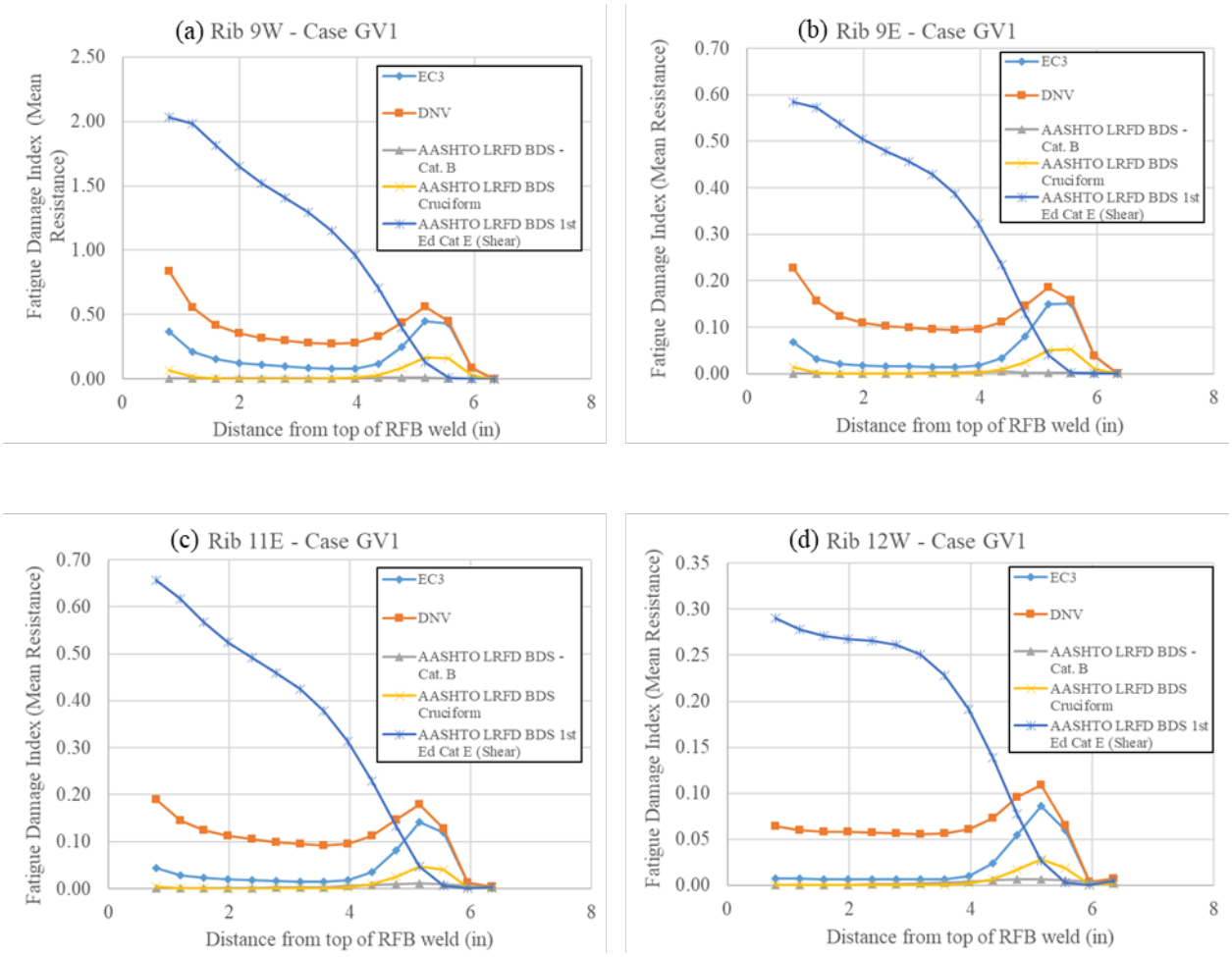

Figure 50. Plots of fatigue damage index for weld cracking versus distance from the deck plate along the weld for fillet-welded (5/16") RFB connection - Case GV1 (Type 1 Cut-out, *c/h* = 0.46)

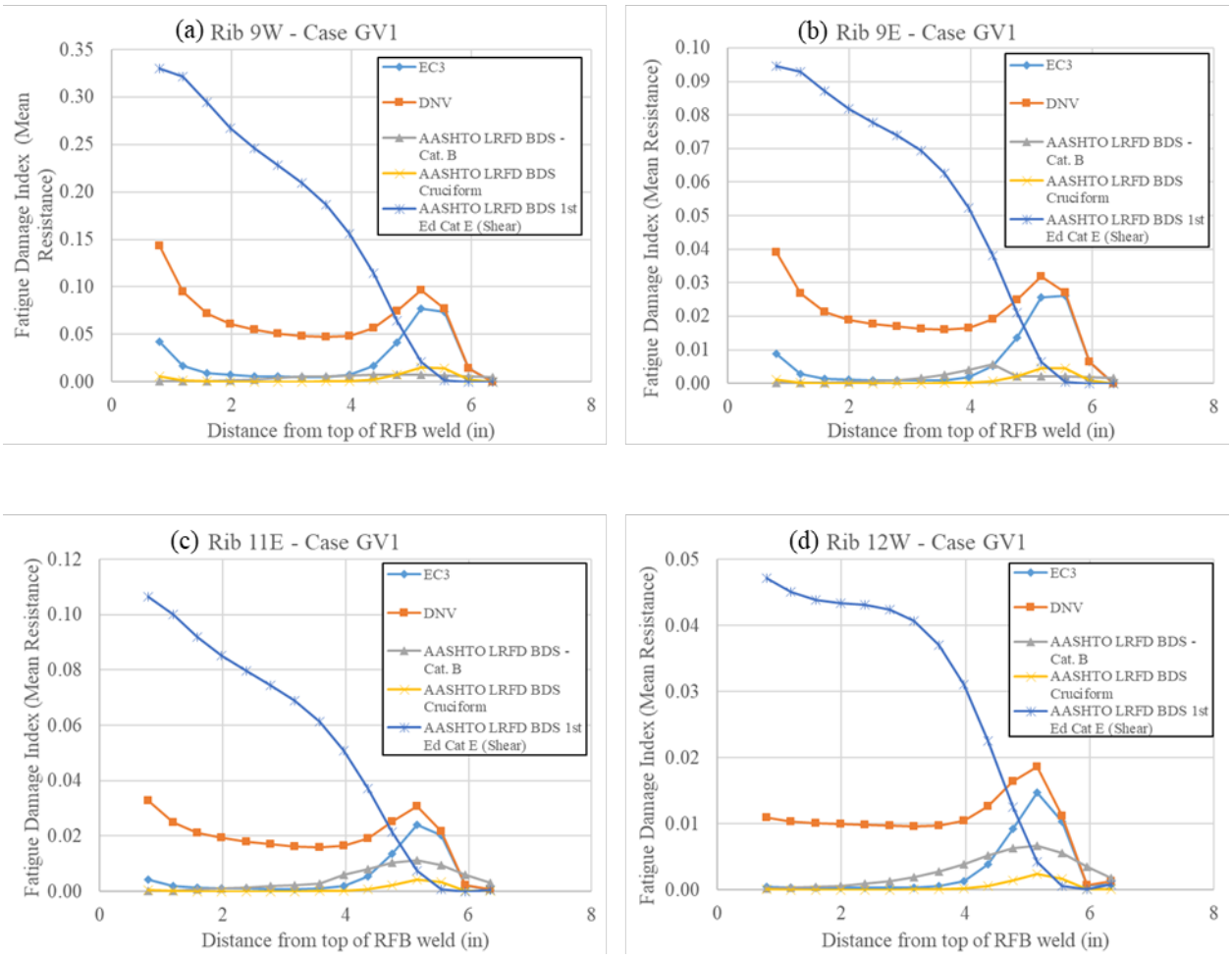

Figure 51. Plots of fatigue damage index for weld cracking versus distance from the deck along weld for PJP-welded (1/4" penetration and 5/16" reinforcement) RFB connection - Case GV1 (Type 1 Cut-out, *c/h* = 0.46)

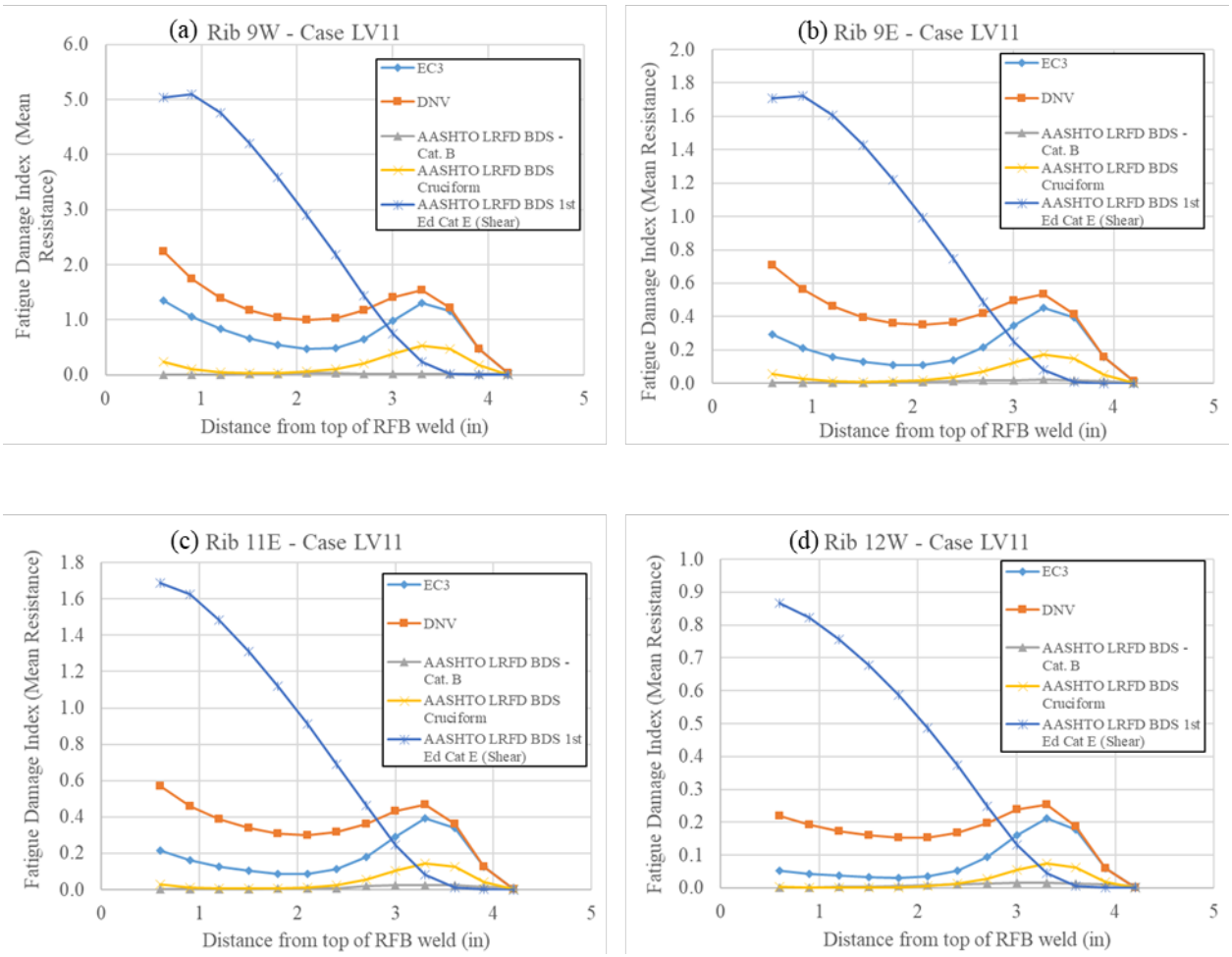

Figure 52. Plots of fatigue damage index versus distance along weld from deck plate for weld throat fatigue for fillet-welded (5/16") RFB connection - Case LV11 (Type 1 Cut-out, *c/h* = 0.6)

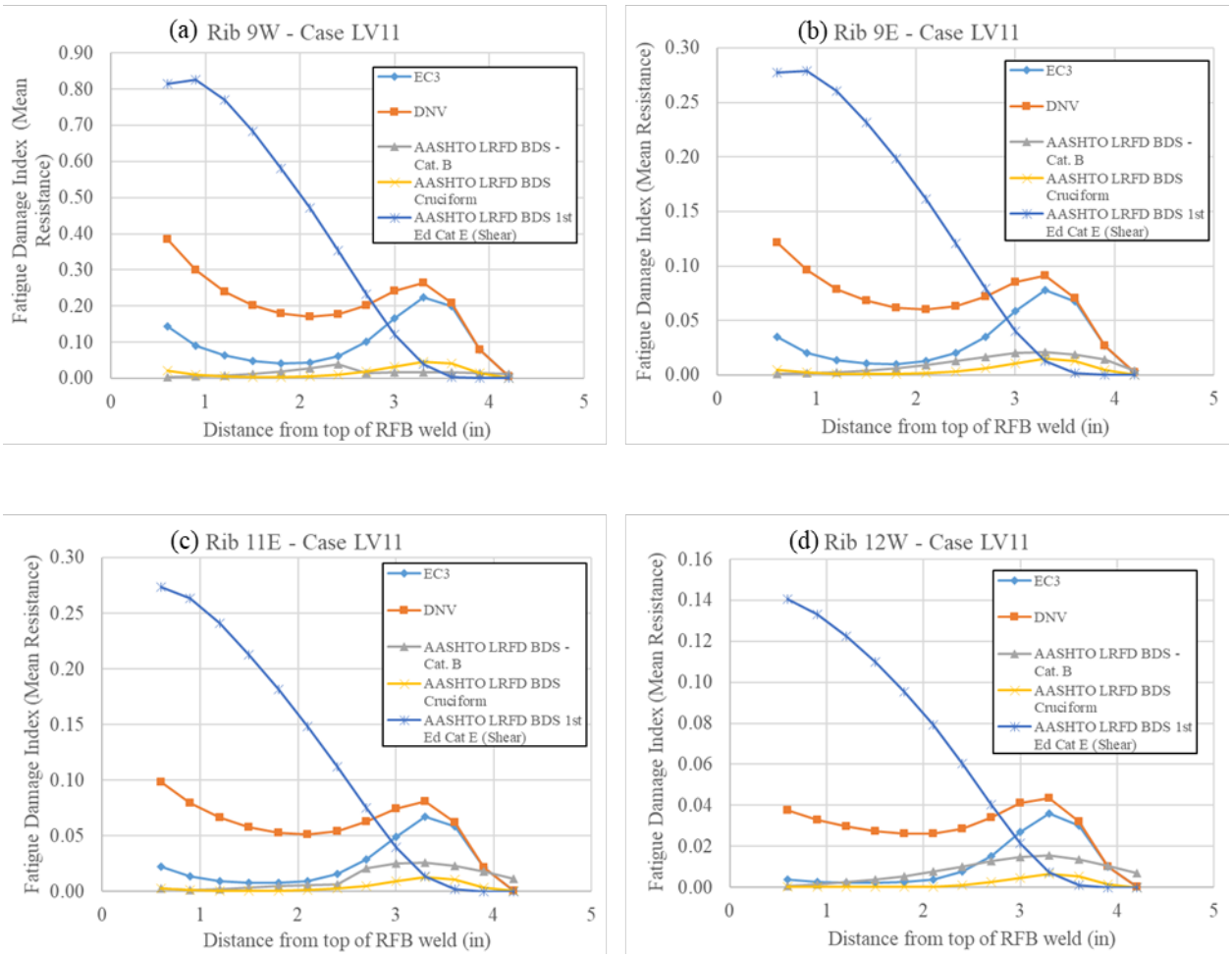

Figure 53. Plots of fatigue damage index versus distance along weld from deck plate for weld throat fatigue for PJP-welded (1/4" penetration and 5/16" reinforcement) RFB connection - Case LV11 (Type 1 Cut-out, *c/h* = 0.6)

Table 22. Summary of maximum fatigue damage index (mean resistance) along the RFB connection weld at Rib 9W for various stress conditions per Eurocode 3[2], DNV[9], and AASHTO[1] – Model GV1 (as-tested RFB connection geometry) with PJP (1/4" penetration with 5/16" reinforcement and fillet welded (5/16") connections, under 8 million applied cycles of AASHTO[1] Fatigue I loading

Mean Fatigue Resistance	Stress Condition	PJP Weld	Fillet Weld
Eurocode 3[2]	Normal/shear	0.08	0.45
DNV[9]	Normal/shear	0.14	0.84
AASHTO[1] Category B	Longitudinal normal	0.01	0.01
AASHTO[1] Cruciform	Transverse normal	0.01	0.17
AASHTO LRFD 1st Ed. [3] Category E (Shear)	Longitudinal shear	0.33	2.04

Table 23. Summary of maximum fatigue damage index (mean resistance) along the RFB connection weld at Rib 9W for various stress indices per Eurocode 3[2], DNV[9], and AASHTO[1] – Model LV11 (Type 1 Cut-out, *c/h* = 0.6) with PJP (1/4" penetration with 5/16" reinforcement and fillet welded (5/16") connections, under 8 million applied cycles of AASHTO[1] Fatigue I loading

Mean Fatigue Resistance	Stress Condition	PJP Weld	Fillet Weld
Eurocode 3[2]	Normal/shear	0.22	1.35
DNV[9]	Normal/shear	0.38	2.24
AASHTO[1] Category B	Longitudinal normal	0.04	0.04
AASHTO[1] Cruciform	Transverse normal	0.05	0.53
AASHTO LRFD 1st Ed. [3] Category E (Shear)	Longitudinal shear	0.83	5.10

SENSITIVITY OF WELD TOE CRACKING TO LOCAL WELD GEOMETRY

This study was undertaken to assess the effect of the local weld geometry on the potential for weld toe fatigue cracking. The effective notch stress approach was used to assess the effect of local weld face angle at the wrap-around fillet weld toe of the RFB connection. It was noted from an assessment of macro-etch specimens from these welds that the weld face angle and weld toe radius were favorable and could be expected to exhibit better fatigue performance than a typical fillet weld. This assessment was performed following the methodology described in (Fricke, 2010).

To evaluate the sensitivity of the results to local weld geometry, a third level of FEA submodeling was employed. Three submodel C (SMC) level finite element models were created. Each SMC encompassed the horizontal portion of the wrap-around fillet weld of the EC RFB connection at the east side of Rib 11 (R11E) at Floor Beam 2, and a full-thickness portion of the rib wall. For each SMC model, the displacements along the boundaries of SMC were obtained from the SMB analysis from the as-tested configuration (Case GV1) in order to assess the observation of no cracking and compare to the measurements during the full-scale test program.

Each SMC mesh was prepared as needed for the effective notch stress analysis, with each model incorporating a weld toe radius of 1 mm at the rib wall weld toe (the critical weld toe). One model featured a concave weld face with a weld face angle of 150 degrees at the weld toe. A second model featured a flat weld face with a weld face angle of 135 degrees at the weld toe. The final model featured a convex weld face with a weld face angle of 120 degrees at the weld toe. The weld face angle is obtuse and measured between base metal and the weld face at the toe.

It was noted in Chapter 3 that acceptable limits for weld toe angle are suggested in ISO 5817[7] (ISO, 2014) and ISO 6520[8] (ISO, 1998). For welds subjected to fatigue stresses, three quality levels are provided, namely C63, B90, and B125, with minimum weld face angles of 90, 100, and 110 degrees, respectively. These levels correspond to lower bound fatigue strength at 2 million cycles of 63 MPa (9.1 ksi), 90 MPa (13.1 ksi), and 125 MPa (18.1 ksi), respectively, however it is noted that fillet welds are excluded from quality level B125 (ISO, 2014). For comparison, the lower bound fatigue strength at 2 million cycles for Fatigue Categories D, C and B in AASHTO LRFD BDS[1] are 71.2 MPa (10.3 ksi), 89.7 MPa (13.0 ksi), and 125 MPa (18.2 ksi), respectively.

It should be noted that AASHTO LRFD BDS[1] and AWS D1.1[5] (AWS, 2015) do not have explicit considerations for weld face angle of fillet welds. AWS D1.1[5] states the "the faces of fillet welds may be slightly convex, flat, or slightly concave." However, it also provides an allowable convexity, which is a limit to the deviation of the weld face from the straight line between the weld toes (i.e., the theoretical weld face), which is denoted by the variable "*C*" which varies by the type of fillet weld joint, and the theoretical weld face width ("*W*"). The larger the value of *C*, the larger the convexity of the weld face. For an inside corner fillet weld, and *W* equal to 0.44 in (for an equal leg 5/16-inch fillet weld used for the EC RFB connection detail of interest), *C* is less than 1/8 in per AWS D1.1[5]. Fitting a circular arc to the two weld toes, and a point 1/8-inch offset from the center of the theoretical weld face, the weld face angle at the toes is 76 degrees (see Figure 54). Therefore, per this limit of *C*, a weld face angle as low as 76 degrees would be permissible by AASHTO/AWS D1.1[5]. This is significantly less than the weld

face angle limit in ISO 5817[7] of 90 degrees for the lowest fatigue performance category (see Table 7).

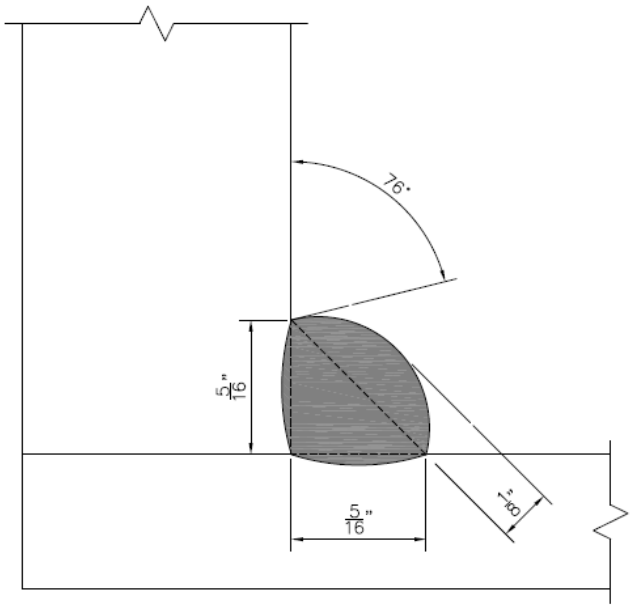

Figure 54. Illustration showing a 5/16 inch fillet weld with allowable convexity, C, equal to 1/8 per AWS D1.1 and the corresponding weld face angle at the weld toe

For Case GV1, the maximum LSS at Rib 11E was 13.82 ksi. At this stress range, the lower bound fatigue life, *N*, (AASHTO Fatigue Category C) is 1.67 million, corresponding to a fatigue damage index (*n/N*) of 4.8 at 8 million cycles. Considering the mean resistance of Fatigue Category C, the fatigue life is 2.14 million cycles, corresponding to a fatigue damage index of 3.7 at 8 million cycles. This shows that the fatigue resistance determined by Category C may not apply to the welds of the full-scale prototype OSD test specimen with favorable profiles. If this calculation was performed assuming B125 quality level (corresponding to AASHTO Category B lower bound resistance), the lower bound and mean fatigue damage indices are 1.8 and 0.8, respectively. This suggests that AASHTO Fatigue Category B may be more representative of the resistance for the welds of the full-scale prototype OSD test specimen with favorable profiles. However, as noted, per ISO 5817[7], fillet welds are excluded from quality level B125 in their as-welded condition.

The maximum principal stresses along the surface of the effective notch are determined from the SMC finite element analysis. Using the effective notch stress approach, these maximum principal stresses are then compared to *S-N* curve appropriate for the effective notch stress approach, regardless of the geometry of the detail. The lower bound *S-N* curve for FAT 225 has a slope of -3, with a resistance of 225 MPa (32.6 ksi) at 2 million cycles (Fricke, 2010). The maximum principal stresses are summarized in Table 24. For each weld face angle case, the maximum principal stress at the center of the weld, and anywhere along the weld toe are presented. The results show that increasing the weld face angle reduces the effective notch stress, as expected.

For the effective notch stress approach, the mean fatigue life is determined from the FAT 309 fatigue category (i.e., resistance of 309 MPa (44.8 ksi) at 2 million cycles) based on statistics provided in (Fricke, 2010) and is used to evaluate the fatigue performance of the selected OSD EC RFB connections. Table 25 shows the calculated mean fatigue life, *N*, based on FAT 309 calculated using the largest maximum principal stress (i.e., largest effective notch stress) from FEA shown in Table 24. The results show that increasing the weld face angle reduces the effective notch stress, and increases the fatigue life, as expected. Except for the 150-degree weld face angle case, the 8 million cycles applied to the full-scale prototype OSD test specimen exceeded these calculated mean fatigue lives. However, the macro-etch specimen removed from Rib 11E at FB2 exhibited a weld toe radius of 2.3 mm which is larger than the 1 mm radius assumed for the SMC analysis, which could improve the fatigue performance.

For 8 million applied loading cycles, the worst-case fatigue damage index for the highest effective notch stress (weld face angle of 120 degrees) is 1.4 (= 8 $x10^6$/5.9 $x10^6$). For comparison, the largest LSS from FEA of the full-scale prototype OSD test specimen was 13.82 ksi at Rib 11E (see Table 14). The LSS is linearly extrapolated to the weld to using the stresses from a coarser SMB mesh and therefore does not include the local effects of the weld face angle. Using a mean resistance determined by AASHTO Fatigue Category C, the mean fatigue life, *N*, determined using the LSS methodology is 2.14 $x10^6$ cycles. The corresponding fatigue damage index is 3.7, significantly higher than that calculated using the effective notch stress method for a weld face angle of 120 degrees, equal to 1.4. Based on these results, it can be concluded that the good performance is likely due to the favorable weld profile.

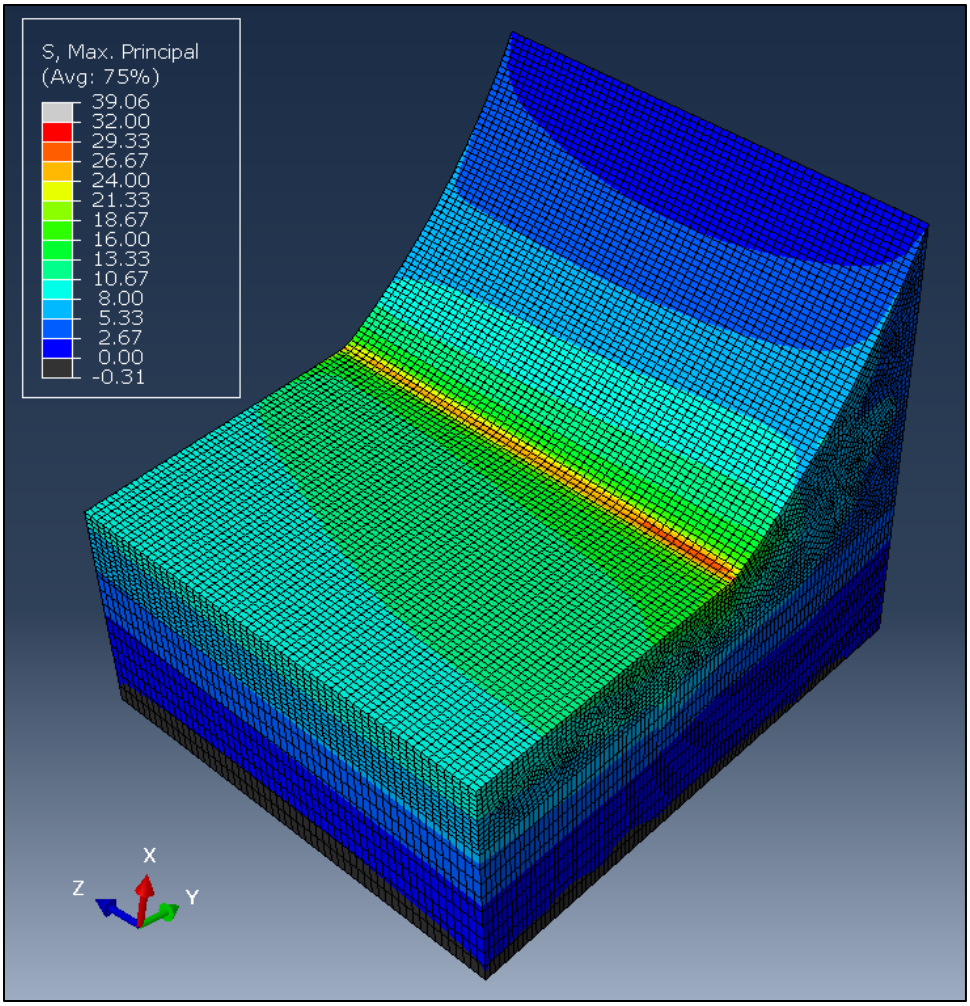

Figure 55. Contour of maximum principal stress (in ksi) for notch stress analysis, SMC, for tested OSD configuration (GV1MA) with load applied at Actuator 4, at Rib 11E (SMB) with 1mm weld toe radius at rib wall and concave weld face (weld face angle of 150 degrees)

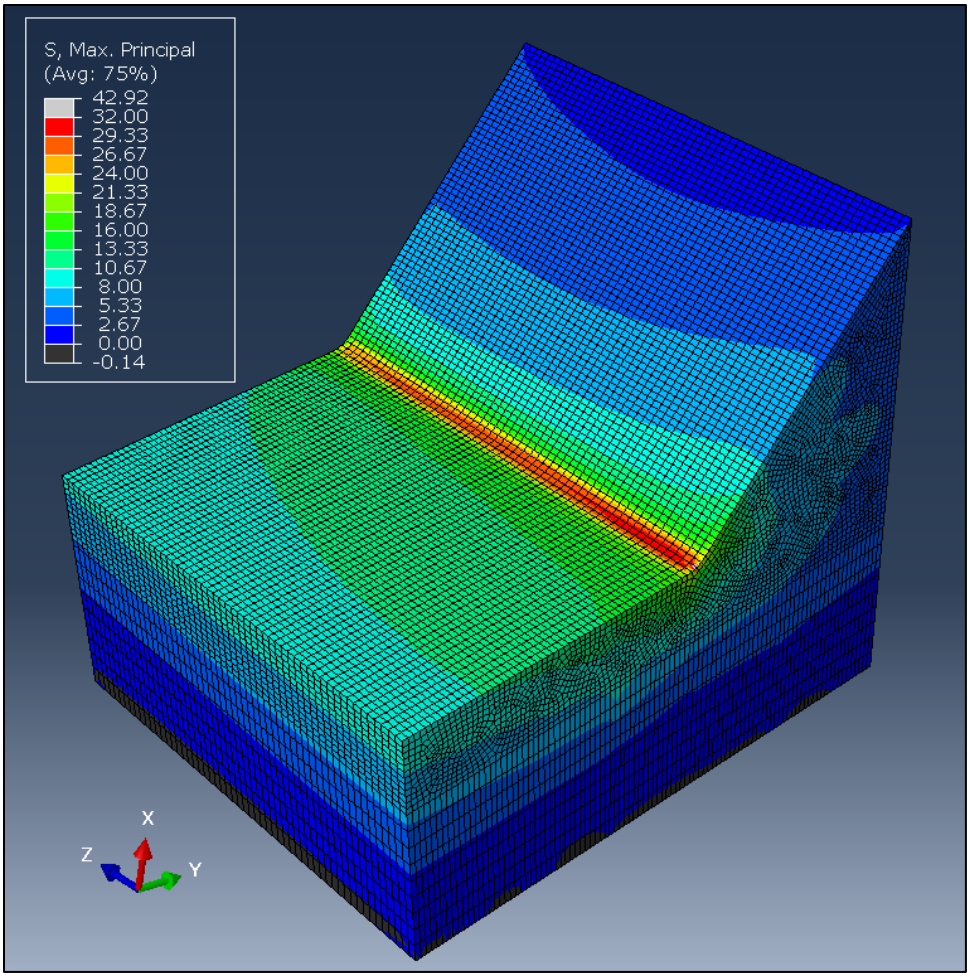

Figure 56. Contour of maximum principal stress (in ksi) for notch stress analysis, SMC, for tested OSD configuration (GV1MA) with load applied at Actuator 4, at Rib 11E (SMB) with 1mm weld toe radius at rib wall and planar weld face (weld face angle of 135 degrees)

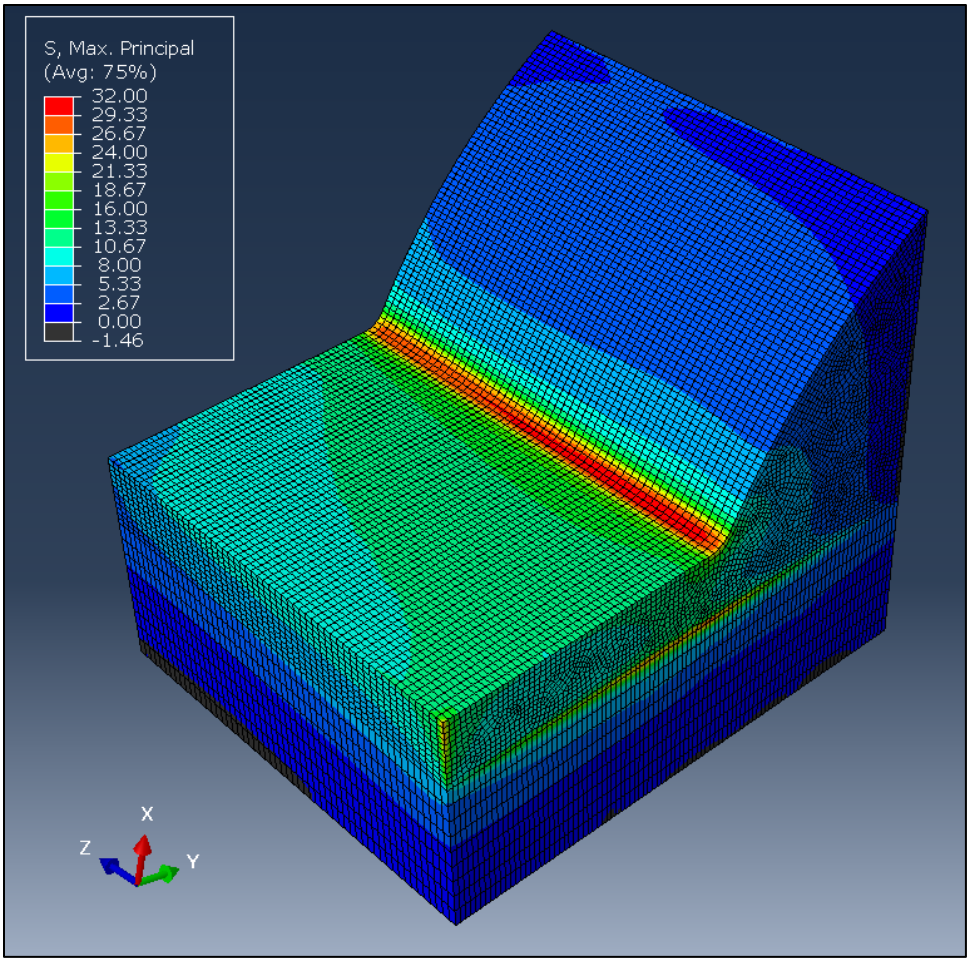

Figure 57. Contour of maximum principal stress (in ksi) for notch stress analysis, SMC, for tested OSD configuration (GV1MA) with load applied at Actuator 4, at Rib 11E (SMB) with 1mm weld toe radius at rib wall and convex weld face (weld face angle of 120 degrees)

Table 24. Effective notch stress at the center of the floor beam web and the maximum value along the weld toe at the wrap around weld of RFB connection 11E in the as-tested configuration (GV1MA)

Weld Face Angle (deg)	Effective Notch Stress at Center of FB Web (ksi)	Maximum Effective Notch Stress Along Entire Weld (ksi)
150	25.5	27.9
135	28.9	31.1
120	30.2	31.3

Table 25. Mean fatigue life, *N*, (FAT290) based on effective notch stress at the center of the floor beam web and at the point of maximum effective notch stress along the weld toe at the wrap around weld of RFB connection 11E in the as-tested configuration (GV1MA)

Weld Face Angle (deg)	N Based on Effective Notch Stress at Center of FB Web	N Based on Maximum Effective Notch Stress
150	10.8×10^6	8.3×10^6
135	7.4×10^6	6.0×10^6
120	6.5×10^6	5.9×10^6

OBSERVATIONS FROM SENSITIVITY STUDY

Based on the results presented above, the following observations are noted.

Global Variable Study

1. Reducing the deck plate thickness from 3/4 inch to 5/8 inch increased the weld toe stresses by as much as 12%.

2. Changing the ribs from trapezoidal to round generally resulted in increased stresses.

3. Reducing the stiffness of the transverse trusses by 50% reduced the weld toe stresses at the key EC RFB connections, though the decrease was modest (maximum of 5%).

Local Variable Study

1. The EC RFB connections with the lowest weld toe stresses were Case LV7 with a Type 1 cut-out and shallow cut-out (*c/h* equal to 0.33). Low weld toe stresses were also observed for Case LV5 (Type 3 cut-out with *c/h* equal to 0.46).

2. Changing from trapezoidal ribs to round ribs generally resulted in increased weld toe stresses (increases of up to 43%).

3. For EC RFB connection with trapezoid ribs with *c/h* greater than or equal to 0.46, the weld toe stresses were lower with a Type 3 cut-out. For the EC RFB connections with *c/h* equal to 0.33, no clear trend was evident with respect to the cut-out type.

4. For EC RFB connection with trapezoid ribs, increasing the EC RFB connection weld length (lower *c/h* ratio) generally results in lower weld toe stresses. This trend is not evident for connections with round ribs.

RFB Connection Weld Study

1. Considering the weld throat cracking of the RFB connections welds, the analyses indicate that adequate performance can be expected from the as-tested configuration (GV1) with PJP welds (1/4-inch penetration) and fillet reinforcement welds (5/16-inch). No throat cracks were observed in any of the RFB connections welds of the full-scale prototype OSD test specimen.

2. Adequate fatigue performance can also be expected for the RFB connection with a deeper cut-out (*c/h* equal to 0.6), Case LV11, so long as the same PJP welding is used.

3. Fillet welds could possibly be successfully used instead of PJP welds, however, a larger weld size may be needed. Such a weld would likely need to be multi-pass fillet weld since the 5/16 inch fillet weld considered in this study is the largest single-pass weld. However, it may be possible to design an OSD with EC RFB connections and single pass fillet welds with adequate fatigue performance. Further study is needed to quantify the fatigue resistance of welds under combined stresses.

Weld Profile Study

1. Increasing the weld face angle at the toe resulted in lower effective notch stress, and therefore a longer expected fatigue life.
2. For the as-tested OSD configuration (Case GV1) and considering an application of 8 million cycles, and the mean fatigue resistance of AASHTO Category C, the largest mean fatigue damage index using LSS is 3.7, which occurs at Rib 11E.
3. Using the results of effective notch stress analyses with weld face angles of 120, 135, and 150 degrees, and considering a mean fatigue resistance determined by FAT309 (309 MPa (44.8 ksi) at 2 million cycles) the mean fatigue damage indices are 1.4, 1.3, and 0.96, respectively, significantly lower than the mean fatigue damage index of 3.7 determined using LSS stresses.

The high fatigue damage index obtained using LSS and the mean fatigue resistance (determined by the large fatigue test dataset used to establish Fatigue Category C resistance in AASHTO LRFD BDS (Keating & Fisher, 1986)) indicates that the full-scale prototype OSD test specimen should be expected to crack under the 8 million applied loading cycles. However, no fatigue cracks were discovered through visual inspection or macro-etch evaluation of the critical wrap-around fillet welds after 8 million applied loading cycles. It is concluded that the excellent fatigue performance observed during the laboratory testing is likely due in part to the favorable weld profile at the wrap-around EC RFB connection welds (see macro-etch specimens in Figure 17 and Figure 18) given the significantly lower fatigue damage indices obtained using effective notch stress analysis which indicates that there is a reasonable probability that the as-tested condition would not crack, consistent with the observed performance of the full-scale prototype OSD test specimen.

CHAPTER 7. CONCLUSIONS

SUMMARY OF WORK AND FINDINGS

Orthotropic steel decks (OSDs) offer potential advantages to bridge owners, in particular for redecking applications. Replacement of an existing concrete deck with an OSD offers a significant reduction in dead load which is advantageous for existing suspension bridges with some degree of main cable deterioration. However, the use of OSDs in the United States has been limited due to the relatively high initial cost of fabrication, due in large part to complex welded details developed to achieve the desired fatigue performance. The rib-to-floor beam (RFB) connection is a major cost-driver for fabricated OSDs, and a major consideration in the design of OSDs. Extended cut-out (EC) RFB connections are commonly used for OSDs in redecking applications since this detail increases the flexibility of the connection at the stiff existing floor beams encountered in a typical redecking application, and this flexibility reduces the stresses produced by rib end rotation. This research was focused on economical EC RFB connections, without costly internal stiffeners/bulkheads, CJP welds and associated NDT/repairs, or manual grinding of critical weld toes, for use in redecking applications (i.e., a new OSD on an existing bridge superstructure).

This research was performed to (1) investigate the range of EC RFB connection details used on existing bridges; (2) assess the performance of the full-scale prototype OSD test specimen tested in the ATLSS Center lab in 2018 and use measured data to calibrate a 3D FEA model; (3) assess the sensitivity of the behavior to various global and local OSD geometries using modifications to the calibrated FEA model; (4) explore the effect of penetration depth of EC RFB connection welds on the fatigue performance; and (5) explore the effect of EC RFB connection wrap-around fillet weld face angle on the fatigue performance. The results of the research indicate that adequate performance of economical EC RFB connections (without bulkheads/stiffeners, CJP welds and associated NDT/repairs, or manual grinding) can be expected under design and fabrication conditions consistent with those of the full-scale prototype OSD test specimen tested in the ATLSS Center lab and described in this report.

CONCLUSIONS

The following conclusions are based on the research presented in this report:

1. Worldwide, many existing OSDs with economical EC RFB connections have performed without fatigue cracking in service. In the United States, at least two bridges have been identified that have OSDs featuring economical EC RFB connections (without bulkheads or internal stiffeners, or CJP welding with manual grinding) that have not developed fatigue cracks after at least 25 years of service.
2. A full-scale prototype OSD test specimen, fatigue tested in 2018, did not develop cracks at fatigue-sensitive wrap-around fillet weld toes at the cut-out termination after application of 8 million cycles at 83 kips (approximately the Fatigue I tandem axle load for OSDs from AASHTO LRFD BDS[1]including dynamic allowance). It is noteworthy that LSS values at the weld toes of the wrap-around fillet welds at the cut-out termination on the rib walls greater than 13 ksi were measured during fatigue testing. However, no

cracking was observed at this location indicating that the actual resistance of these welds (which had favorable profiles) likely exceeds Fatigue Category C with a threshold of only 10 ksi.

3. Sensitivity studies of OSDs detailed with economical EC RFB connections using FEA showed that fatigue stresses at these sensitive wrap-around fillet weld toes are affected by other key design parameters as follows:
    a. Lower stresses can be expected for OSDs with trapezoidal ribs than the same OSD with round ribs.
    b. The stresses were sensitive to the deck plate thickness, with a significant stress reduction observed when the deck plate thickness was increased from 5/8 inch to 3/4 inch.
    c. The stresses were not sensitive to the stiffness of the transverse floor truss (or floor beam).
    d. The stresses were lowest for the case with a Type 1 cut-out, with a shallow opening (*c/h* equal to 0.33).
4. A study of the EC RFB connection welds along the rib walls was performed considering both PJP (with fillet-weld reinforcement) and fillet welds. The results indicate that PJP welds appear to exhibit adequate fatigue strength (for several fatigue cracking modes) evaluated using AASHTO BDS LRFD[1], DNV[9], and Eurocode 3[2] fatigue provisions, in most cases. Though the results indicate that single pass fillet welds may not have adequate fatigue resistance in some cases, it may be possible to achieve adequate fatigue performance with single pass fillet welds given the satisfactory fatigue performance of many real-world bridges (there are no publicly-documented examples of weld throat cracking of EC RFB connections on an in-service bridge). The accuracy of these criteria for evaluation of weld throat cracking is thought to be limited in cases with a combination of types and directions of stresses such as an EC RFB connection. As noted, AASHTO LRFD BDS[1] has no fatigue provisions for welds subjected to combined stresses. Further study is needed to quantify the fatigue resistance of welds under combined stresses. However, no weld throat cracks developed in the EC RFB connections of the full-scale prototype OSD test specimen after 8 million loading cycles. This correlates with the findings of the FEA of the PJP welds.
5. Detailed effective notch-stress analyses of selected EC RFB connection configurations showed that the effective notch stress index is sensitive to the weld face angle. Therefore, a weld with favorable weld profile (shallow weld face angle and large weld toe radius), similar to the favorable weld profiles observed in the full-scale prototype OSD test specimen, is expected to have improved weld toe fatigue performance.

OSDs detailed with economical EC RFB connections can provide the advantages of reduced dead load and long service life (exceeding 100 years) with regular maintenance. Based on the research presented in the report, the following suggestions for design of new OSD with EC RFB connections used for redecking applications are made:

1. The OSD should be detailed with trapezoidal ribs.
2. The OSD should be detailed with a 3/4-inch deck plate.
3. The EC RFB connections of Case LV7 (Type 1 cut-out with *c/h* of 0.33) and Case LV5 (Type 3 cut-out with *c/h* of 0.46) had the lowest stresses in the study, and either could be used as a starting point for design of new OSD. Case LV1/GV1 (Type 1 cut-out and *c/h*

of 0.46), representing the as-tested configuration, could also be considered as a design starting point given the excellent performance during the full-scale laboratory fatigue test program.

4. The RFB connection welds should be detailed as PJP welds with reinforcing fillet welds and wrap-around fillet weld at the weld termination.
5. For a future OSD design, if the selected OSD configuration features the same EC RFB connection detail geometry and welding, a ¾-inch deck plate, the same rib thickness and spacing, and a rib span of 19 ft. 9 inches or less, and the fabrication workmanship of the OSD meets or exceeds that of the full-scale prototype OSD test specimen, and meets the welding and tolerance requirements AASHTO LRFD BDS[1] and AASHTO/AWS D1.5[6], the design engineer may consider using the cost-effective EC RFB connection detail studied herein with a Level 1 design approach per AASHTO LRFD BDS[1]. The design engineer would need to develop project notes and specifications to ensure that the desired weld profile at the wrap-around fillet weld at the cut-out termination is produced consistently during production of the OSD. The weld profile should have a concave shape and a smooth transition at the toe to achieve the necessary face angle. Such specifications could include the use of custom weld profile gauges in production, and qualification of the welding procedure using mock-ups that demonstrate the desired weld profile will be achieved consistently. Additionally, the use of collaborative welding robots (cobots) in fabrication could improve the consistency of these critical welds.
6. It is noted in the commentary of AASHTO LRFD BDS[1] that Level 3 design should always be used in the case of a redecking application (for which OSDs with EC RFB connections are better suited), unless an exception is made by the bridge owner. However, the results of the 2018 fatigue test program demonstrate that the OSD EC RFB connection detail featured in the full-scale prototype OSD test specimen is expected to exhibit adequate fatigue performance in a redecking application. Furthermore, the results of the sensitivity studies presented in this report demonstrate an OSD detailed similarly with key parameters within the suggested ranges, and with fabrication workmanship meeting or exceeding that of the full-scale prototype OSD test specimen, can also be expected to exhibit adequate fatigue performance. The favorable results of full-scale testing and sensitivity studies suggests a reduced need for a Level 3 OSD design in similar applications.

FUTURE WORK

The results of the study are promising and it is expected that a standardized EC RFB connection detail could be included in the FHWA OSD manual for OSD Level 1 Design (Dahlberg, et al., 2022). Further FEA of OSDs featuring economical EC RFB connections should be performed to more fully assess the behavior under additional variations of deck geometry, existing bridge superstructure geometry, and loading models. These results would further the range of applicability of a standardized OSD with EC RFB connections with reliable long-term performance.

Further research on fillet- and PJP-welded EC RFB connections should be performed to understand the stress demands and fatigue resistance for weld throat cracking. It is expected that the fatigue resistance is dependent on the combination of shear stress, longitudinal normal stress, and transverse normal stress. The design of complex connections (such as the EC RFB

connection) could entail use of FEA to estimate stress indices which may be a combination of various stress components. These stress indices would then be compared to an appropriate fatigue resistance (i.e., *S*-*N* curves). The results of this research would help to reduce the likelihood of weld throat cracking in these OSDs.

Additionally, it suggested that additional research into the application of notch-stress analysis to assess the sensitivity of fatigue resistance to weld profile parameters such as weld face angle and weld toe radius be performed. Some international standards presently exist as noted in the report. The findings of this future work would aid in the development of improved welding specifications to ensure OSDs are fabricated with the weld profile needed to achieve the desired fatigue performance.

REFERENCES

AASHTO/AWS, 2015. *AASHTO/AWS D1.5: Bridge Welding Code,* Washington, DC & Miami, FL: American Association of State Highway and Transportation Officials & American Welding Society.

AASHTO, 1994. *AASHTO LRFD Bridge Design Specifications, Customary U.S. Units., 1st Edition,,* Washington, D.C.: American Association of State Highway and Transportation Officials.

AASHTO, 2010. *AASHTO LRFD Bridge Design Specifications, 5th Edition,* Washington, D.C.: American Association of State Highway and Transportation Officials.

AASHTO, 2014. *AASHTO LRFD Bridge Design Specifications, 7th Edition,* Washington, D.C.: American Association of State Highway and Transportation Officials.

AASHTO, 2016. *AASHTO LRFD Bridge Design Specifications, Customary U.S. Units., 7th Edition, with 2015 and 2016 Interim Revisions,* Washington, D.C.: American Association of State Highway and Transportation Officials.

AASHTO, 2017. *AASHTO LRFD Bridge Design Specifications, 8th Edition,* Washington, D.C.: American Association of State Highway and Transportation Officials.

AASHTO, 2020. *AASHTO LRFD Bridge Design Specifications, 9th Edition,* Washington, DC: American Association of State Highway and Transportation Officials.

AWS, 2015. *AWS D1.1; Structural Welding Code - Steel,* s.l.: American Welding Society.

BSI, 1999. *Steel, Concrete, and Composite Bridges - Part 10: Code of Practice for Fatigue; BS5400: Part 10.* s.l.:s.n.

Connor et al., 2012. *FHWA Manual for Design, Construction, and Maintenance of Orthotropic Steel Deck Bridges,* Washington, D.C.: US Department of Transportation Federal Highway Administration.

Connor, R. J., 2002. *A Comparison of the In-service Response of an Orthotropic Steel Deck with Laboratory Studies and Design Assumptions,* s.l.: Lehigh University.

Connor, R. J., 2004. Influence of Cutout Geometry on Stresses at Welded Rib-to-diaphragm Connections in Steel Orthotropic Bridge Decks. *Transportation Research Record,* Volume 1892, pp. 78-87.

Cuninghame, J. R., 1987. *Strengthening Fatigue Prone Details in a Steel Bridge Deck.* s.l., s.n., pp. 127-133.

Dahlberg, J. et al., 2022. *Guide for Orthotropic Steel Deck Level 1 Design,* Washington, D.C.: FHWA.

DNV, 2011. *Fatigue Design of Offshore Stuctures, DNV-RP-C203,* s.l.: s.n.

European Committee for Standardisation, 2002. *Eurocode 3: Design of Steel Structures - Part 1.9: Fatigue Strength of Steel Structures,* Brussels: CEN.

European Committee for Standardisation, 2006. *Eurocode 3: Design of Steel Structures - Part 2: Steel Bridges,* Brussels: CEN.

Fricke, W., 2010. *IIW Recommendations for the Fatigue Assessment of Welded Structures By Notch Stress Analysis, IIW-2006-09.* Hamburg: IIW.

Gill, R. J. & Dozzi, S., 1966. Concordia Orthotropic Bridge: Fabrication and Erection. *Engineering Journal,* May.pp. 10-18.

Haibach, E. & Plasil, I., 1983. Untersuchungen zur betriebsfestigkeit von stahlleichtfahrbahne mit trapezhohlsteifen im eisenbahnbrückenbau. [Studies on the fatigue resistance of lightweight steel decks with trapezoidal hollow stiffeners in Railway Bridge]. *Der Stahlbau,* Issue 9, pp. 269-274.

HNTB, 2015. *Cost-Effective Orthotropic Bridge Decks (An Evaluation of Optional Welding Processes),* New York: HNTB Corporation.

Hobbacher, A., 2008. *Recommendations for Fatigue Design of Welded Components (IIW Doc. IIW-1823-07).* s.l.:IIW.

ISO, 1998. *ISO 6520: Welding and Allied Processes - Classification of Gemetric Imperfections in Metallic Materials - Part 1: Fusion Welding,* s.l.: ISO.

ISO, 1998. *ISO 6520: Welding and Allied Processes - Classification of Geometric Imperfections in Metallic Materials - Part 1: Fusion Welding,* s.l.: ISO.

ISO, 2014. *ISO 5817: Welding - Fusion-welded Joints in Steel, Nickel, Titanium and Their Alloys (beam welding excluded) - Quality Levels for Imperfections,* s.l.: ISO.

Japan Road Association, 2012. *Specifications for Highway Bridges, Part II Steel Bridges.* s.l.:s.n.

Keating, P. B. & Fisher, J. W., 1986. *Review of Fatigue Tests and Design Criteria on Welded Details, Final Report,* Bethlehem, PA: Fritz Laboratory.

Kitner, K., 2016. *A Study of Manufacturable Rib-to-Floor Beam Connections in Steel Orthotropic Bridge Decks,* s.l.: Lehigh University, Bethlehem, PA.

Kolstein, M. H., 2007. *Fatigue Classification of Welded Joints in Orthotropic Steel Bridge Decks,* s.l.: T.U. Delft.

Lehrke, H. P., 1990. Fatigue Tests of Stiffener to Cross Beam Connections. *Structural Engineering International.*

Manniche, K. & Ward-Hall, G., 1975. Mission Bridge - Design and Construction of the Steel Box Girder. *Canadian Journal of Civil Engineering,* Issue 2, pp. 169-192.

Miki, C. & Suganuma, H., 2014. Rehabilitation of Strengthening of Orthotropic Steel Bridge Decks. In: *Bridge Engineering Handbook. Construction and Maintenance.* Boca Raton: CRC Press, Taylor & Francis Group, pp. 491-538.

Miner, M., 1945. Cumulative Damage in Fatigue. *Journal of Applied Mechanics.*

Modjeski and Masters, Inc., 2015. *Bridges for Service Life and Beyond 100 Years: Service Limit State Design - SHRP 2 Report S2-R19B-RW-1,* Washington, D.C.: Transportation Research Board.

Moses, F., Schilling, C. G. & Raju, K. S., 1987. *Fatigue Evaluation Procedure for Steel Bridges, NCHRP Report 299,* Washington, D.C.: Transportation Research Board.

Nunn, D. E., 1974a. *An Investigation into the Fatigue of Welds in an Experimental Orthotropic Bridge Deck Panel,* Crowthorne, Berkshire: Transport and Road Research Laboratory.

Nunn, D. E., 1974b. *Trials of Experimental Orthotropic Bridge Deck Panels Under Traffic Loading,* Crowthorne, Berkshire: Transport and Road Research Laboratory.

Renken, F. et al., 2021. An Algorithm for Statistical Evaluation of Weld Toe Geometries Using Laser Triangulation. *International Journal of Fatigue,* 149(August), pp. 1-14.

Saunders, J. et al., 2019. *Fatigue Resistant Rib-to-Floor Beam Connections for Orthotropic Steel Decks (ATLSS Report No. 19-02),* Bethlehem, PA: ATLSS Engineering Research Center, Lehigh University.

Smylie, R., 1966. *Fabrication of Orthotropic Deck Sections for Port Mann Bridge,* Vancouver, B.C., Canada: Committee on Construction Practices - Structures.

Tsakopoulos, P. A. & Fisher, J. W., 2003. Full-scale Fatigue Tests of Steel Orthotropic Decks for the Williamsburg Bridge. *Journal of Bridge Engineering,* 8(5), pp. 323-333.

Tsakopoulos, P. & Fisher, J., 2005. Full-scale Fatigue Tests of Steel Orthotropic Deck Panel for the Bronx-Whitestone Bridge Rehabilitation. *Bridge Structures,* 1(1), p. 55.